Inaugural-Dissertation zur Erlangung der Doktorwürde der Tierärztlichen Fakultät der Ludwig-Maximilians-Universität München

Of bats and ferrets – in vivo characterization of bat influenza H18N11

Von Marco Joachim Gorka

aus Lauf an der Pegnitz

München 2020

Aus dem Veterinärwissenschaftlichen Department der Tierärztlichen Fakultät der Ludwig-Maximilians-Universität München

Lehrstuhl für Virologie

Arbeit angefertigt unter der Leitung von Univ.-Prof. Dr. Gerd Sutter

Angefertigt am Institut für Virusdiagnostik
des Friedrich-Loeffler-Instituts,
Bundesforschungsinstitut für Tiergesundheit, Insel Riems

Mentor: Prof. Dr. Martin Beer

Gedruckt mit der Genehmigung der Tierärztlichen Fakultät

der Ludwig-Maximilians-Universität München

Dekan: Univ.-Prof. Dr. Reinhard K. Straubinger, Ph.D.

Berichterstatter: Univ.-Prof. Dr. Gerd Sutter

Korreferent/en: Univ.-Prof. Dr. Bernd Kaspers

Tag der Promotion: 25. Juli 2020

Meinen Eltern

und

Geschwistern

Die vorliegende Arbeit wurde gemäß § 6 Abs. 2 der Promotionsordnung für die Tierärztliche Fakultät der Ludwig-Maximilians-Universität München in kumulativer Form verfasst.

Folgende wissenschaftliche Arbeiten sind in dieser Dissertationsschrift enthalten:

Kevin Ciminski, Wei Ran*, Marco Gorka*, Jinhwa Lee, Ashley Malmlov, Jan Schinköthe, Miles Eckley, Reyes A. Murrieta, Tawfik A. Aboellail, Corey L. Campbell, Gregory D. Ebel, Jingjiao Ma, Anne Pohlmann, Kati Franzke, Reiner Ulrich, Donata Hoffmann, Adolfo García-Sastre , Wenjun Ma, Tony Schountz, Martin Beer and Martin Schwemmle. **„Bat influenza viruses transmit among bats but are poorly adapted to non-bat species."**, erschienen in Nature Microbiology 2019, online verfügbar unter doi:10.1038/s41564-019-0556-9
*These authors contributed equally

Marco Gorka, Jan Schinköthe, Reiner Ulrich, Kevin Ciminski, Martin Schwemmle , Martin Beer and Donata Hoffmann. **„Characterization of Experimental Oro-Nasal Inoculation of Seba's Short-Tailed Bats (Carollia perspicillata) with Bat Influenza A Virus H18N11."**, erschienen in Viruses 2020, online zu finden unter doi:10.3390/v12020232

TABLE OF CONTENTS

CHAPTER I: INTRODUCTION

Influenza A viruses (IAV) are able to threaten the health of mammals, avian species and humans. Originating from waterfowl, which represent the natural reservoir of most of the different IAV subtypes, the caused disease can range from mild to very severe. Circulating IAV in poultry as well as in swine and equines can lead to huge economic losses and pose a potential zoonotic threat. Additionally to the zoonotic potential of IAV, annually recurring strains of IAV circulate in the human population and cause seasonal epidemics.

Until 2012, 16 different hemagglutinin (HA) and 9 neuraminidase (NA) subtypes were known, and all of them were found in different kinds of aquatic birds. But the world of IAV was properly shaken up as two novel influenza A-like viruses (IALV) were identified with the help of next-generation sequencing in the feces of the little yellow-shouldered bat (*Sturnira lilium*) in Peru and the flat-faced fruit-eating bat (*Artibeus planirostris*) in Guatemala. Provisionally designated as H17N10 and H18N11, these viruses not only expanded the range of natural reservoirs for IAV, but also showed new extraordinary characteristics in comparison to conventional IAV. Neither the HA nor the NA are able to bind to sialic acid residues, the well-known receptor molecule of “classical” IAV. In fact, MHC-II class proteins function as cell-entry mediators for the novel IALVs. In addition, they lack the ability to reassort with conventional IAV and the function of the NA protein is still unknown. These traits raised questions and challenges concerning the zoonotic potential, but also the route of infection and the pathogenesis within the original bat host species.

Additional evidence was found, that supports the hypothesis of bats playing a major role as either being a natural host species of IAV or potential vessel for reassortmant processes. In 2015, serological evidence of IAV in frugivorous bats from Africa, especially concerning H9 specific antibodies, supported this theory. Four years later, a distinct H9N2 line of IAV was characterized and isolated from Egyptian fruit bats (*Rousettus Aegyptiacus*).

On the one hand, the aim of this work was to investigate the zoonotic potential of the new bat influenza A viruses (batIAV), and on the other hand, to highlight the way of infection and pathogenesis in the natural host species.

CHAPTER II: REVIEW OF LITERATURE

II.1 Influenza A viruses

II.1.1 Definitions and taxonomy

Influenza is a viral infection that occurs worldwide and can lead to epidemics, especially during autumn and winter, or even pandemics.[1, 2] Causative agents are influenza viruses (IV), which are part of the family *Orthomyxoviridae* and are divided into four different genera: *Alphainfluenzavirus, Betainfluenzavirus*, *Gammainfluenzavirus* and *Deltainfluenzavirus*.[3-5] All four genera are represented by only one species each, namely *Influenza A virus* (IAV), *Influenza B virus* (IBV), *Influenza C Virus* (ICV) and *Influenza D virus* (IDV), respectively.[5] The cause of seasonal influenza epidemics of humans are IAV and IBV.[1] The division of the different genera is predicated on antigenic variation of the matrix proteins (M1) and nucleoproteins (NP).[6] *Thogotovirus* (TVs), *Quaranjavirus* (QVs) and *Isavirus* do belong likewise to the virus family and represent further genera.[7-9]

IAV comprise a large diversity in their HA and NA genes. At the moment, 18 different subtypes of HA and 11 subtypes of NA are known.[4] Although IAV play a huge role in seasonal influenza epidemics and are the main cause of severe human pandemics, it comes as a surprise that almost all subtypes originate from waterfowl.[10, 11] Merely H17N10 and H18N11 descend from South American bat species.[12, 13] Beside mammals also birds can develop severe illness in consequence of an infection with IAV, especially from subtype H5 or H7. However, the infection appears to be without clinical signs in aquatic birds most of the time.[10]

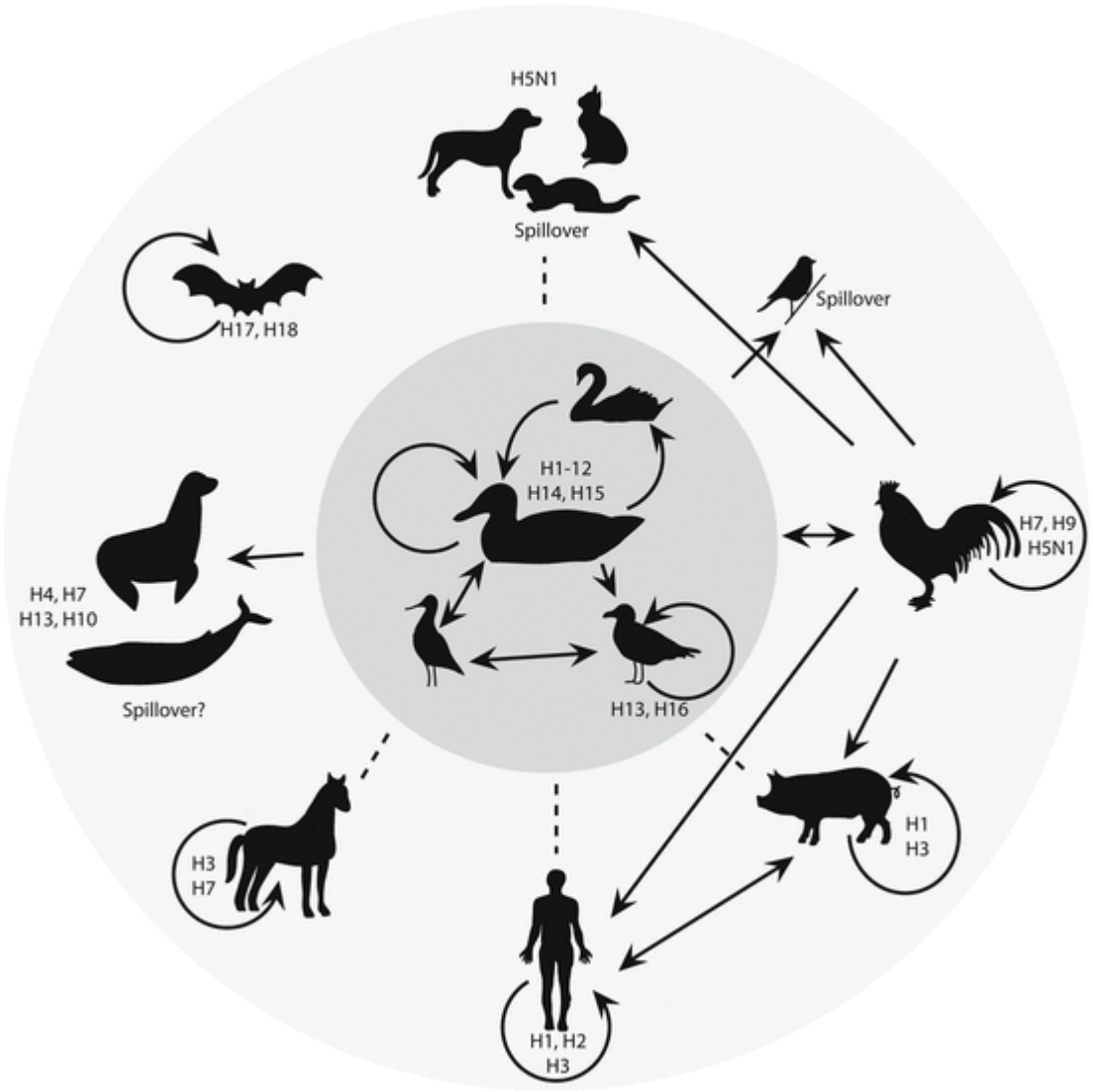

Figure 1. Influenza A subtypes and their hosts

Figure as presented in "Of ducks and Men: Ecology of a Zoonotic Pathogen in a Wild Reservoir Host" by Michelle Wille, Neus Latorre-Margalef, Jonas Waldenström 2017; ISSN: 2366-3324; doi: 10.1007/978-3-319-60616-3_9 [14] *

Waterfowl represent the natural host species of Influenza A viruses. Spillover events to other wild and domestic bird species are demonstrated. Swine take on the role of representing a mixing vessel by being susceptible to avian and human IAV. The role of bats in the ecology of IAV has yet to be determined.[14]

*permission for reproduction in Chapter IX: Supplements

Contrary, there is no classification for IBV based on different types of HA. Two antigenically and genetically distinct lineages are the reason for human influenza B epidemics. The two strains are referred to as yam88-like or vic87-like and are related to either B/Yamagata/16/88 or B/Victoria/2/87, respectively.[15] Both lineages are co-circulating in the human population since 1983, but are fluctuating dependent on the region or time period.[15, 16]

Based on the clinical appearance, a discrimination between IAV and IBV in humans is not possible; however, IBV are allocated with an overall lower clinical attack rate.[17]

The species of ICVs differs from above in public health importance, especially clinical appearance and frequency of occurrence. ICV cause a mild respiratory or even asymptomatic disease in humans. While mainly being encountered and isolated from children below the age of six, the seroprevalance among adults is much higher.[18, 19] Since ICV were isolated from pigs in China in 1981 and in the United States of America in 2011, the topic of a potential species transmission from pigs to humans arouse interest. [20, 21]

The latest introduction to the family of *Orthomyxoviridae* is the genus of *Deltainfluenzavirus* with their species of IDV. They are distinctly related to ICV and are isolated from pigs, which can even develop clinical signs of a respiratory illness, in addition to cattle.[22, 23] There is also evidence of IDV being able to infect ferrets, the surrogate model for human influenza A disease.[3]

II.1.2 Particle structure

IAV are enveloped and polymorphic RNA viruses. Spheroidal forms with an average diameter of 80nm to 120nm prepossess most particles, but filamentous shapes are possible as well.[24-26] The negative-sensed, single-stranded RNA genome comprises eight different segments, that code for at least 11 proteins.[27] RNA segments possess conserved and partially complementary 5′ - and 3′ -end sequences with promoter activity. As depicted in figure 2 the helical, viral RNA is covered by multiple nucleoproteins to form ribonucleocomplexes (RNPs). Associated to each single genome segment are three polypeptides that form the viral RNA dependent RNA polymerase (RdRp). The two glycoproteins, HA and NA as well as the M2-protein, which forms a proton-selective ion-channel within the viral membrane, are part of the lipid bilayer. The HA binds to sialic acid receptors (SRA) and is therefore initiating endocytosis. While human influenza viruses prefer α2,6-linked SRA, the receptor binding cite of the HA of avian species are the α2,3-linked ones.[28] Towards the center of the virion, a protein layer of matrix proteins (M1) succeeds the latter.[29] Other internal proteins are the polymerase basic protein 1 (PB1), polymerase basic protein 2 (PB2), the polymeric acidic protein (PA), the nucleoprotein (NP) and the non-structural protein 2 (NS2).[27]

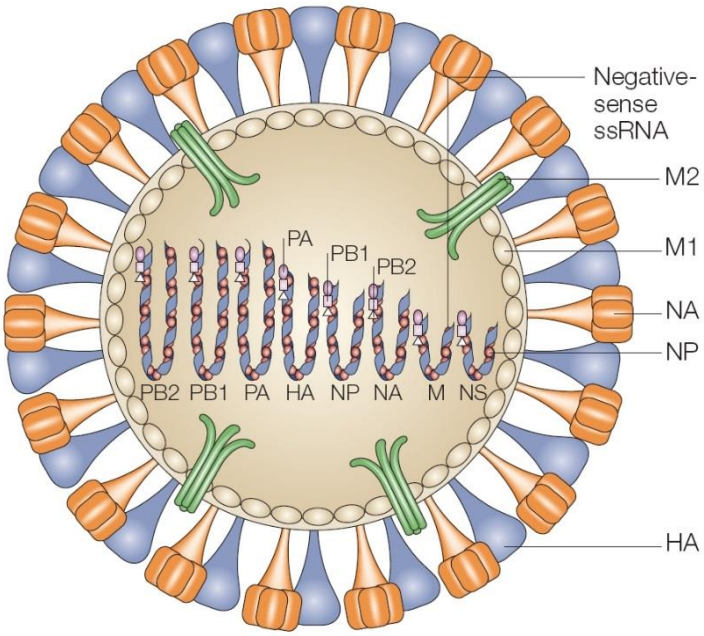

Figure 2. Influenza A virion structure

Figure as presented in "Influenza: lessons from the past pandemics, warnings from current incidents." By Horimoto T. and Kawaoka Y. 2005; PMID: 16064053; doi: 10.1038/nrmicro1208 [30] *

*permission for reproduction in Chapter IX: Supplements

II.1.3 Influenza A – a zoonosis

II.1.3.1 Mechanisms of variation of IAV

As already mentioned beforehand, the natural reservoir host species of IAV are aquatic birds.[10] At the moment, more than 10.000 bird species are known in general and estimations even suggest more than double that number, based on phylogenetic research.[31] Hence, IAV are globally spread and circulate in avian species as well as mammals, like swine and equines. In cases of spill over infections from their animal hosts to humans, IAV can lead to epidemics and even pandemics. IAV-infected humans can develop a respiratory, potentially fatal disease.[1, 2] The direct crossover of an avian influenza virus from e.g. birds to humans, however, is an exceedingly rare event, that requires the virus to adapt and is essentially induced by two mechanisms, called *antigenic drift* and *antigenic shift*.

Antigenic drift occurs through a long-term congregation of point mutations in the RNA, which finally can lead to changes in the amino acid (aa) composition.[4, 10, 32] It is the result of the proofreading deficiency of the RdRp.[4] Since the HA and the NA are the main immunogenic compartments of IAV, changes in the aa compound of these proteins can lead to the ability of evading the responses of the immune system.[33] These rapid occurring changes regularly confront vaccination programs with the challenge to adapt continuously to new IAV variants, which can cause seasonal influenza epidemics. Even though evading virus strains only arise every two to five years, it is important to constantly surveil new occurring IAV strains and adjust vaccine composition accordingly.[34]

Since IAV contain eight different gene segments, reassortment events can take place in case of a coinfection in one host cell with two different IAV strains.[4, 35] As long as this process involves the HA and/or the NA gene segment, it is named *antigenic shift*.[36, 37] The progeny viruses might be able to evade the human immune system, due to their newly obtained features concerning their antigenic makeup.[33] In the event of a coinfection with two different IAV, there are mathematically 256 (2^8) different gene segment combinations and therefore progeny IAV possible.[37] Antigenic shifts represent an important part of IAV evolution and are the main reason for the repeated occurrence of influenza pandemics.[36]

II.1.3.2 Avian influenza viruses

Avian influenza viruses (AIVs) are important pathogens in the poultry industry, circulating for decades and causing devastating outbreaks.[4, 38, 39] AIV can be divided into two phenotypes based on their pathogenicity in chickens: low pathogenic (LP) and highly pathogenic (HP). One of the main virulence determinants of HPAIV is the multi basic cleavage site (MBCS) in the HA of the influenza A subtypes of H5 and H7.[40] In order to be infectious, the original HA0 from virus particles has to be cleaved into two parts, called HA1 and HA2.[40] The monobasic cleavage site of LPAIV can only be split by trypsin-like proteases, which are present in the upper respiratory tract and/or intestinal tract of birds, strictly limiting the infection likewise.[40-42] The MBCS of HPAIV however, can be cleaved by furin-like proteases, which appear to be pervasive, and therefore enable a systemic infection.[41, 42]

Besides the presence of a MBCS in the HA of H5 or H7 viruses, the World Organization for Animal Health (OIE) also determines the pathogenicity of AIV by in vivo testing in chickens. AIV, which surpass an intravenous pathogenicity index (IVPI) of 1.2 or higher, in either 6-weeks old chickens, or cause at least a fatality in 75% of four-to-eight-week-old chickens are identified as being highly pathogenic.[43] Besides the HA subtypes of H5 and H7, H9 viruses are also able to threat human public health, even though transmissions from birds to humans are exceedingly rare.[4, 38, 44] The following part highlights exemplarily four of the most important AIV concerning human health: H5N1, H7N7, H7N9 and H9N2.

H5N1

In 1997, the first cases of fatal human H5N1 infections were reported from Hong Kong. Overall, 18 patients were infected, with six of them being lethal.[44-48] The origin of all genes of the causative virus appeared to be from AIV sources.[4, 44] After the recurrence of the virus in 2003, a further spread from Asia to Europe, the Middle East and Africa started.[38, 44] For the first time, the crossing of the animal-to-human barrier was accomplished for H5N1 [4] and, despite of it being a very rare event, the number of fatal cases of AIV H5N1 in humans in percentage is quite high. Up to date (March 2020), the World Health Organization (WHO) reports a total of 861 cases and 455 deaths.[44, 49] The high percentage of fatal cases is the result of H5N1 being able to overcome the restriction to the respiratory tract and occasionally lead to systemic infections.[44, 50-54] Experiments in ferrets, which are the gold standard of human IAV research about virulence and transmission, showed, that human-to-human transmission of viruses with H5 HA is in the realms of possibility. In addition, H5N1 distinguishes from other AIV by being able to kill high numbers of wild aquatic birds, which was first observed at the Lake Qinghai, in western China in 2005.[38, 55]

H7N7

It was 1996, when a 43-year-old woman in England, who was the owner of pet ducks, was first infected by an AIV of subtype H7, developing a right eye conjunctivitis. Subsequently, the virus was isolated and identified as A/England/268/96.[56, 57] Seven years later, a large outbreak of AIV of subtype H7N7 occurred in poultry in the Netherlands.[58]

Overall, during the outbreak also 86 poultry farm workers and three of their family members were infected, with 78 of them developing a conjunctivitis and even one fatal case.[58, 59] All internal genes of the H7N7 HPAIV in the Netherlands were descendants from a close-by circulating H7N7 LPAIV.[4, 59] Another case of transmission of H7N7 HPAIV from birds to humans happened in August 2013 in Italy, when three breeding and cleaning workers of a poultry farm developed conjunctivitis after an animal culling procedure.[60]

H7N9

In spring 2013, three Chinese citizens, who had contact to birds in variable ways, showed an infection of the lower respiratory tract, which was caused by the novel IAV H7N9.[61] While the low pathogenic H7N9 virus of avian origin did only cause mild or even no illness in poultry, it appears to symbolize a major threat to humans, which was certified by the death of all three above mentioned patients.[61, 62] The low pathogenicity in poultry leads to a major problem in detection and is only to be overcome by active virological surveillance programs.[62] In humans however, the virus can lead to a severe and fatal illness, comprising cough, high fever and pneumonia.[61, 62] Studies with ferrets further revealed transmission via direct contact.[62-64] Since February of 2013, the virus spread in China with overall 1568 confirmed cases, 616 of them being fatal.[65] Luckily, the H7N9-epidemic in China was successfully stopped after the introduction of a H5/H7 bivalent vaccine for chickens.[66]

H9N2

Unlike the above-mentioned HPAIV, LPAIV of subtype H9N2 are not able to attract much awareness concerning public health control and disease management.[67, 68] Not only are they present since the 1980s and have been isolated from terrestrial poultry worldwide, but also AIV of subtype H9N2 are endemic in several Eurasian and African countries.[4, 67-77] While threatening global poultry health, H9N2 and especially its reassortants are able to menace human health likewise.[78-80] The first ever isolation of H9N2 from two children in Hong Kong was published in 1999 and raised a special level of interest, regarding the fact of H9N2 being a LPAIV.[81]

The certainty that some LPAIV of subtype H9N2 prefer the human-type sialic acid receptor and are able to be transferred between ferrets via respiratory droplets emphasizes their zoonotic and pandemic potential.[67, 68] H9N2 viruses have changed significantly during the last decade, leading to an increase of laboratory confirmed cases in China between 2010 and 2013.[68] Since 2015, 26 cases of confirmed human infections have been reported.[82] Based on phylogenetical analysis of the HA gene, LPAIV of subtype H9N2 are divided into two different lineages: the Eurasian and the American. The Eurasian lineage is furthermore split into three sublineages: while A/duck/Hong Kong/Y280/97 (Y280-like), A/Chicken/Beijing/1/94 (BJ94-like) and A/Chicken/Hong Kong /G9/97 (G9-like) represent the Y280-like lineage, A/quail/Hong Kong/G1/97-like (G1-like) represents the G1-lineage and A/Duck/Kong Kong/Y439 (Y439-like) and A/chicken/Korea/38349-p98323/96 (Korean-like) are the representatives of the Korean lineage.[4, 68, 83] Right now, H9N2 viruses are in the center of attention, especially highlighting their contribution of gene segments to different zoonotic AIV in the past due to their reassortment potential.[4, 80, 84-86]

II.1.3.3 Swine influenza and the mixing vessel theory

As already described in chapter II.1.3.2, most of the potential pandemic IAV arise from reassortment between avian and human IAV strains. In terms of representing the mixing vessel for reassortment events, swine stepped into the center of attention.[87, 88] The base of this theory is formed by two major factors, the antigenetic and genetic similarities between some avian, human and swine IAV strains and the susceptibility of pigs to avian and human IAV strains likewise.[87] While the majority of AIVs favors α2,3-linked (avian-receptor) sialic acid residues, most of the human IAV prefer α2,6-linked (mammalian-receptor) ones.[89, 90] Swine are featured with both receptor types in their respiratory tract, leading to their susceptibility for avian and human IAV strains and building up the molecular foundation of the mixing vessel theory.[91] There is plenty of evidence, ranging from in vitro and in vivo experiments to natural occurring IAV reassortants, supporting and proving the role of swine in the creation of new potential pandemic virus strains.[92] The generation of “new” viruses was accomplished by infecting pigs with IAV of humans and swine simultaneously.[93-95]

Kida et al. furthermore proved, that pigs are susceptible to some AIV strains, too, and so potential triple-reassortants between human, swine and avian IAV are feasible.[92] The most noteworthy triple-reassortant was H1N1pdm09, representing the causative agent of the first and only influenza pandemic in the 21th century. In this case, avian-like swine viruses provided the NA and M gene segments, classical swine viruses the NP, NS, HA genes while the PB2, PB1, and PA originated from North American AIV.[4, 44, 96-98] In addition, natural genetic reassortants could be found in swine as well as in humans, respectively.[99, 100]

Despite swine influenza viruses being important pathogens in the pig industry, human cases of infections with swine origin viruses are rare, with only 27 confirmed cases between 1990 and 2010 in the USA.[101] Since 2010, a total of 430 cases of human infection with swine-origin influenza A(H3N2) variant viruses (H3N2v) have been detected in the United States.[102] One of the main factors for transmission of IAV from pigs to humans and vice versa are farm workers that are frequently exposed to swine. They may serve as a bridging population for interspecies transmission.[103, 104]

II.1.3.4 Risk factors of human infections with zoonotic influenza viruses

In the last part of chapter II.1.3, Influenza A – a zoonosis, the sources and routes of human infections with zoonotic IV are highlighted. Although zoonotic infections are rare in comparison to seasonal IAV, the viruses might be able to mutate or reassort in animals or humans and develop the ability for an animal-to-human or even human-to-human transmission.[4] In general, IAV can be transmitted to humans via inhaling of dust or respiratory droplets, but also the conjunctiva appear to be an open door for some AIV, in particular ones of the subtype H7.[105, 106] It seems to be obvious, that the work, contact and handling of swine and essentially poultry, like purchasing on live bird markets (LBM), slaughtering, defeathering, cleaning, cooking and boiling of meat, demonstrate one of the main risk factors for humans to be committed to animal origin IAV.[105, 107] In Asia, the epicenter and source of three of the five pandemics in the last 100 years, and Egypt, live bird markets turn up to be one of the main risk factors for zoonotic transmissions of AIV.[4, 107]

The congregation of different bird species like chickens, ducks or geese from different sources, lead to the continuously circulating and disposition of AIV.[4, 107] Another example from Van Kerkhove et al. shows multiple variating risk factors for an AIV infection, depending on the region and the general customariness regarding poultry treatment. Even though most of the population in rural Cambodia had frequent contact to poultry, performing potential transmission risk activities, the overall number of H5N1 infections in this case was lower, than in comparable studies from Thailand and Vietnam.[108-110] Difference in poultry density per km^2, a lower probability of handling ill chicken and barriers in successful AIV transmission can lead to variations.[108] For the latter one, food preparation and hygiene practices determine a major influence on AIV transmission to humans, e.g. boiling or heating up poultry before defeathering, like it is the habit in Cambodia.[108] Food hygiene procedures furthermore could lead into the risk of transmission being negligible.[111]

II.2 The relevance of bats in virology

Around 20% of all mammal species, overall more than 1300, are bats.[112, 113] A closer look on bats, or to be more precise, on the order Chiroptera, that is furthermore divided into Megachiroptera (megabats) and Microchiroptera (microbats), reveals, that at the moment (March 2020) 30 bat species worldwide are even entitled critically endangered.[114, 115] Bats are the only mammals that own the power to fly and often use echolocation in order to orientate themselves.[116] The main problems bats have to face are from anthropogenic activities, like deforestation, habitat loss, destruction of roosts or even simple hunting and killing. It does not come as a surprise, that all of the 52 European bat species and their roosts are legally protected.[117] In 2008, Jones at al. published, that the majority of Emerging infectious diseases (EIDs, 71,8%) is derived from wildlife.[118] Not only are EIDs threatening global economy and human health, they are also on a significant rise.[118, 119] The intensive contact and harassment of wildlife, and in this case especially bats, menaces the life and health of bats and humans likewise. Bats are described as one of the main sources and risks for zoonotic diseases, even harboring more zoonoses per species than rodents altogether.[120]

In addition, they merge several characteristics, which turn bats into perfect reservoirs for pathogens. Besides the already mentioned increasing contact through anthropogenic activities, bats live in very large colonies, they are able to travel and disseminate viruses over a quite large distance in a comparable short amount of time and are pleased with a long life for their relatively small body size.[115, 121] The differences between the immune systems of bats and humans are also worth to mention. A bunch of highly pathogenic viruses, comprising filoviruses, coronaviruses, lyssa- and henipaviruses, are proved being transmissible from bats to humans.[115, 116] It is demonstrated, that several bat species contain a constrictive viraemia towards some of these viruses, which is probably the result of an overall different immune response.[122-128] The diverse antiviral response probably raised from a long coevolution of bats with their viruses, but was also influenced by factors like the evolution of flight.[123] Since bats are difficult to obtain, house and taken care of, not much about the differences in comparison to humans or rodents is known.

II.3 Discovery and characteristics of bat influenza A-like viruses

As already mentioned beforehand, bats are able to harbor a huge variety of potential zoonotic viruses. Recently, bats were identified to be also hosts to different subtypes of influenza A viruses, respectively.[12, 13, 129, 130] Here, the two influenza A-like viruses H17N10 and H18N11, which played the leading role in this work, are further described.

H17N10

In 2013, Tong et al. described the discovery and identification of an influenza A-like virus from bats. Of the overall 316 tested bats, the rectal swabs of three individuals from the little yellow-shouldered bat (*Sturnira lilium*, family Phyllostomidae) were tested positive via pan-influenza quantitative reverse transcription PCR (RT-qPCR). Since additional specimens of one bat (liver, intestine, lung and kidney tissue) were also tested positive, an infectious process was estimated rather than the digestion of infected food.[12] Genome analysis with the use of next-generation sequencing (Illumina GAIIx and 454 pyrosequencing) and the Sanger-method revealed that the bat virus is more related to influenza A than influenza B or C viruses and was from now on called A/little-shouldered bat/Guatemala/164/2009 (A/bat/Guat/09).

The phylogenetic analysis led to the estimation, that the HA of A/bat/Guat/09 is closer related to the group 1 HAs (subtypes H1, 2, 5, 6, 8, 9, 11, 12, 13, and 16) than to the group 2 HAs (H3, 4, 7, 10, 14, and 15).[12] Therefore, the HA diverged after the split of influenza A HA subtypes into group 1 and 2. On the other side, the NA of A/bat/Guat/09 is neither in a close relationship to influenza A nor to influenza B viruses. This indicates, that the NA of the bat virus probably shares an older ancestral with known influenza viruses.[12]

H18N11

In a second study, 116 bats were captured in the Peruvian Amazonian rainforest. Overall, 18 different bat species were sampled and screened with a pan influenza RT-PCR. The rectal swab and the intestine of one flat-faced fruit-eating bat (*Artibeus planirostris,* family Phyllostomidae) was tested positive. Deep sequencing and Sanger analysis led to the whole-genome information and designation of this virus as A/flat-faced bat/Peru/033/2010 (A/bat/Peru/10).[13] The phylogenetic analysis revealed, that A/bat/Peru/10 is most closely related to A/bat/Guat/09, the virus found in bats from Guatemala a year before.[12, 13] Even though the relation between the two batIAV is the closest, in comparison to other influenza A viruses, there is still a huge evolutionary difference, that it is adequate to designate A/bat/Peru 10 as H18N11.[13]

In order to investigate the spread and circulation of batIAV among bats, a panel of sera was analyzed with an indirect enzyme-linked immunosorbent assay (ELISA) to identify IgG antibodies. Specific IgG antibodies against either the HA or the NA of H18N11 were found in 55 of the 110 Peruvian bats. Furthermore, the positive sera were also tested for antibodies against H17, H1 and H5, but none of the sera showed any kind of cross reactivity, indicating the designation of A/bat/Peru/10 as H18N11 once again. Five additional species were found to be seropositive as well.[13] The serological analysis of the Peruvian bats initiated a similar study, with the goal to examine the seroprevalence of antibodies against H17 or N10 among bats in Guatemala. Here, the ELISA detected specific antibodies against H17, indicating a widespread circulation of bat-influenza A-like viruses in New World bats.[13]

Besides the influenza A viruses H17N10 and H18N11, that were found in the Little yellow-shouldered fruit bat (*Sturnira lilium*) in Peru and the Flat-faced fruit-eating bat (*Artibeus planirostris)* in Guatemala, respectively, bats are hosts to other influenza A viruses as well.[12, 13]

In 2015, Freidl et al. described the serological evidence regarding antibodies against H9 in the straw-colored fruit bat (*Eidolon helvum*) in Ghana.[130] Furthermore, a new Influenza A virus of subtype H9N2 was detected and isolated from Egyptian fruit bats (*Rousettus Aegyptiacus*) from the Nile delta.[129]

Characteristics of bat influenza A viruses

Two studies investigated the function of the glycoproteins by using the expression with vesicular stomatitis virus (VSV) based vector systems. In the first study, Hoffmann et al. found no susceptibility of frequently used human, monkey or canine cell lines in IAV research. However, three different kinds of bat-derived cell lines appeared to be susceptible to bat HA and NA carrying vector particles.[131] However, for a successful infection, pre-treatment of the pseudotypes with trypsin for the activation of the HA was necessary. The type II transmembrane serine protease TMPRSS2 was able to trigger the entry into cells, not only leading to the conclusion of bat HAs accommodating a monobasic cleavage site but also emphasizing the need of studies concerning the zoonotic potential of batIAV, since TMPRSS2 is also available in humans.[131] Further experiments revealed the independency of bat HAs from sialic acid receptors, because no increase in cell entry was found upon treatment of the cells with a sialidase.[131] The study of Maruyama et al. also confirmed these findings with the help of VSVs pseudotyped with the HAs and NAs from batIAV.[132]

One of the main attributes of IAV is the ability to reassort their gene segments and expand their genome variation in the case of a coinfection with another IAV. (Chapter II.1.3.1) Nevertheless, the generation of reassortants, consisting of genes from bat flu H17N10 and IAV SC35M, with the help of reverse genetics, failed, even using only a single bat segment.[133] Therefore, a general incompatibility of batIAV to reassort with conventional IAV could be demonstrated.[133]

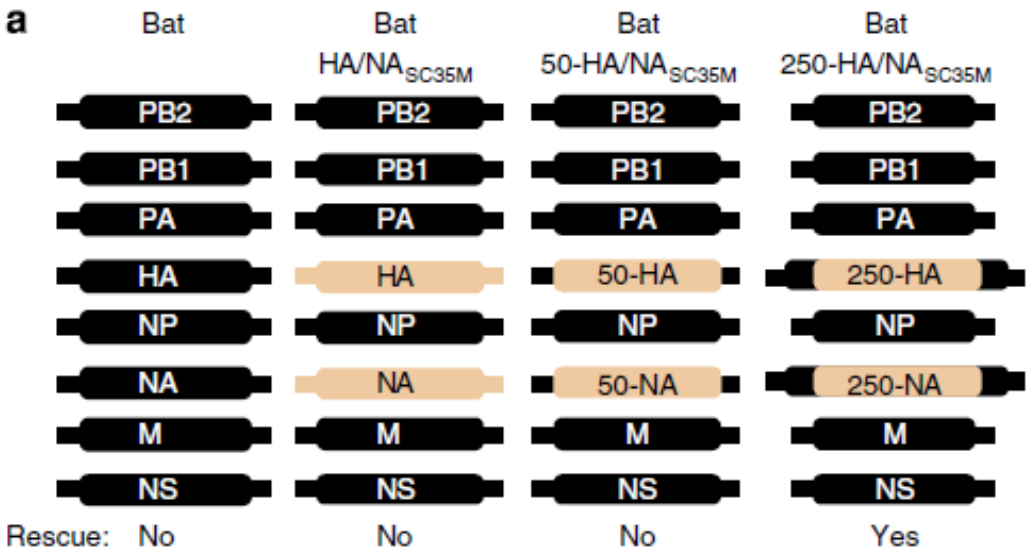

Figure 3. Rescue trials using different combinations of batIAV H17N10 and SC35M segments

Partial figure as presented in: "An infectious bat-derived chimeric influenza virus harbouring the entry machinery of an influenza A virus." By Mindaugas Juozapaitis and Étori Aguiar Moreira 2014; PMID: 25055345; doi: 10.1038/ncomms5448 [133] *

Juozapaitis et al. 2014: "All genomic segments of the H17N10 (Bat), the authentic SC35M HA and NA segments combined with the internal segments of H17N10 (Bat-HA/NASC35M), ORF of HA/NASC35M with the non-coding regions of H17N10 (Bat-50 HA/NASC35M)or ORF of HA/NASC35M with noncoding region and about 100 nt of the 50 and 30 coding sequences of H17N10 (Bat-250 HA/NASC35M)."[133]

*permission for reproduction in Chapter IX: Supplements

The analysis of the crystal structure from the N10 revealed that it shares the same structural properties with the NA proteins of conventional IAV. Nevertheless, it misses conserved amino acids being responsible for sialic acid binding and cleaving. Therefore, N10 is not able to bind to sialic acids and does not have any kind of sialidase activity, which leads to the question, whether bat influenza NAs show any kind of enzymatic activity. Also, the mechanisms of interaction between bat influenza HA and NA has yet not been discovered.[134-136] Despite bat influenza HAs possess a similar overall structure with a conserved putative receptor-binding site, compared to the HAs of conventional IAV, they are neither able to bind to the canonical human α2,6 sialic acid linked, nor to the avian α2,3 linked receptor. Hence, another unique mechanism has to form the basis of cell entry.[13, 137, 138] In fact, Karakus and Thamamongood et al. provided the evidence of major histocompatibility complex class II (MHC-II) human leukocyte antigen DR isotypes (HLA-DR) playing an important role in the cell entry process of batIAV.[139]

Thus, they linked the results of a transcriptomic analysis of susceptible and non-susceptible cell lines with a CRISPR-Cas9 screening. The expression of MHC-II of different species, comprising mice, chicken, bats or pigs, lead to the susceptibility of cells towards batIAV and the idea of a potentially broad host spectrum.[139] Since MHC-II represents ubiquitous proteins of the immune system in many species, including humans, the question if batIAV representing a potential zoonotic risk rose and put itself into an important subject of this work.[140]

CHAPTER III: OBJECTIVES

The recent discovery of two influenza A-like virus sequences in South American bat species raised awareness, especially concerning the replication of these viruses within species, which are known to harbor zoonotic and health threatening viral agents. Up to this date, there were no studies available describing and characterizing the bat influenza A-like viruses in different kinds of animal models, in order to investigate their way of infection, pathogenesis, genetic stability and zoonotic potential, respectively. Both publications further highlight the potential importance of bats regarding virus reservoirs and virus distribution.

1. **Transmission experiments – Characterizing H18N11 and its variant rP11**

   (Chapter IV.1)

   Little is known about the characteristics of both newly discovered batIAV up to this date. In order to understand the features regarding genetic plasticity, intraspecies transmission or zoonotic potential, in vitro analyses and in vivo transmission experiments in mice, ferrets and Jamaican fruit bats shall help to elucidate the yet unknown world of bat flu viruses of subtype H18N11.

2. **Inoculation of Carollia perspicillata with H18N11**

   (Chapter IV.2)

   Seba's short-tailed bats (*Carollia perspicillata*) combine the two features of representing an H18N11 antibody positive South American bat species with excellent characteristics regarding animal experiments. Therefore, the route of infection, the pathogenesis and the not yet determined role as a major virus distributor should be investigated in this bat animal experiment.

CHAPTER IV: RESULTS

Publication I

IV.1 Bat influenza viruses transmit among bats but are poorly adapted to non-bat species

Kevin Ciminski, Wei Ran, Marco Gorka, Jinhwa Lee, Ashley Malmlov, Jan Schinköthe,Miles Eckley, Reyes A. Murrieta, Tawfik A. Aboellail, Corey L. Campbell, Gregory D. Ebel, Jingjiao Ma, Anne Pohlmann, Kati Franzke, Reiner Ulrich, Donata Hoffmann, Adolfo García-Sastre , Wenjun Ma, Tony Schountz, Martin Beer and Martin Schwemmle

Nature Microbiology 2019

doi: 10.1038/s41564-019-0556-9
PMID: 31527796

ARTICLES
https://doi.org/10.1038/s41564-019-0556-9
nature microbiology

Bat influenza viruses transmit among bats but are poorly adapted to non-bat species

Kevin Ciminski[1,2], Wei Ran[1,2,11], Marco Gorka[3,11], Jinhwa Lee[4], Ashley Malmlov[5], Jan Schinköthe[6], Miles Eckley[5], Reyes A. Murrieta[5], Tawfik A. Aboellail[5], Corey L. Campbell[5], Gregory D. Ebel[5], Jingjiao Ma[4], Anne Pohlmann[3], Kati Franzke[7], Reiner Ulrich[6], Donata Hoffmann[3], Adolfo García-Sastre[8,9,10], Wenjun Ma[4]*, Tony Schountz[5]*, Martin Beer[3]* and Martin Schwemmle[1,2]*

Major histocompatibility complex class II (MHC-II) molecules of multiple species function as cell-entry receptors for the haemagglutinin-like H18 protein of the bat H18N11 influenza A virus, enabling tropism of the viruses in a potentially broad range of vertebrates. However, the function of the neuraminidase-like N11 protein is unknown because it is dispensable for viral infection or the release of H18-pseudotyped viruses. Here, we show that infection of mammalian cells with wild-type H18N11 leads to the emergence of mutant viruses that lack the N11 ectodomain and acquired mutations in H18. An infectious clone of one such mutant virus, designated rP11, appeared to be genetically stable in mice and replicated to higher titres in mice and cell culture compared with wild-type H18N11. In ferrets, rP11 antigen and RNA were detected at low levels in various tissues, including the tonsils, whereas the wild-type virus was not. In Neotropical Jamaican fruit bats, wild-type H18N11 was found in intestinal Peyer's patches and was shed to high concentrations in rectal samples, resulting in viral transmission to naive contact bats. Notably, rP11 also replicated efficiently in bats; however, only restored full-length N11 viruses were transmissible. Our findings suggest that wild-type H18N11 replicates poorly in mice and ferrets and that N11 is a determinant for viral transmission in bats.

Originating from aquatic waterfowl, influenza A viruses (IAVs) are zoonotic pathogens that are able to cross species barriers and establish distinct lineages within a broad range of different avian and mammalian hosts[1]. Although cross-species transmissions from animal reservoirs to the human population are usually dead-end infections, in rare cases the acquisition of new genome segment variants through genomic reassortment and adaptive mutations can lead to the emergence of pandemic viruses[2–5]. During 2012 and 2013 and recently in 2018, the complete genome sequences of two previously undescribed IAV subtypes, classified as H17N10 and H18N11, were identified in rectal swab samples from New World fruit bats, which are previously unknown influenza virus reservoirs[6–8]. Although most of the bat-derived genome segments were found to resemble those of conventional IAVs[6,7], structural and biochemical data demonstrated that the surface glycoproteins of H17N10 and H18N11, despite structural similarities, lack the canonical α2,3 or α2,6 sialic acid binding and destroying activities of their conventional haemagglutinin (HA) and neuraminidase (NA) counterparts, respectively[7,9–12]. Instead, H17 HA and H18 HA alone were shown to be sufficient for mediating host cell entry[13,14] by utilizing MHC-II molecules as cell-entry receptors[15]. Interestingly, MHC-II molecules from various vertebrate species, including bats, swine, chicken, mice and humans, support H18-mediated cell entry, permitting potentially broad host tropism[15]. Moreover, the NA-like proteins N10 and N11 seem to be dispensable for viral entry and budding in the context of both H17 and H18-pseudotyped vesicular stomatitis virus (VSV)[13–15], suggesting that authentic H18N11 may replicate independently of N11. Here we studied the genetic stability and replication potential of H18N11 in cells, mice, ferrets and bats.

Results

H18N11 acquires mutations in H18 and N11 after cell culture passaging to increase viral replication. Evidence is lacking about the replication properties and the genetic stability of H18N11 in cell culture. We therefore performed serial in vitro passaging of wild-type (WT) H18N11 in RIE1495 cells in the presence or absence of sialidase pretreatment, which was shown to increase viral yield[13]. After passaging, we observed a successive increase in viral titres for viruses derived from both cells that were pretreated or untreated with sialidase and that were accompanied by amino acid substitutions in the H18 head domain at S235Y or V254F (Fig. 1a,b, Supplementary Fig. 1a,b) and various concurrent deletions in the N11 viral RNA segment ($N11_{del}$; Fig. 1a,b). All of the identified $N11_{del}$ viral RNAs had a single large internal deletion in the coding region with asymmetrical nucleotide contributions at the 3′- and 5′-terminal ends (Supplementary Table 1). Although the 3′ genome

[1]Institute of Virology, Medical Center University of Freiburg, Freiburg, Germany. [2]Faculty of Medicine, University of Freiburg, Freiburg, Germany. [3]Institute of Diagnostic Virology, Friedrich-Loeffler-Institut, Greifswald, Germany. [4]Department of Diagnostic Medicine/Pathobiology, College of Veterinary Medicine, Kansas State University, Manhattan, KS, USA. [5]Arthropod Borne and Infectious Diseases Laboratory, Department of Microbiology, Immunology and Pathology, College of Veterinary Medicine and Biomedical Sciences, Colorado State University, Fort Collins, CO, USA. [6]Department of Experimental Animal Facilities and Biorisk Management, Friedrich-Loeffler-Institut, Greifswald, Germany. [7]Institute of Infectology, Friedrich-Loeffler-Institut, Greifswald, Germany. [8]Global Health and Emerging Pathogens Institute, Icahn School of Medicine at Mount Sinai, New York, NY, USA. [9]Department of Microbiology, Icahn School of Medicine at Mount Sinai, New York, NY, USA. [10]Department of Medicine, Division of Infectious Diseases, Icahn School of Medicine at Mount Sinai, New York, NY, USA. [11]These authors contributed equally: Wei Ran, Marco Gorka. *e-mail: wma@vet.k-state.edu; Tony.Schountz@colostate.edu; Martin.Beer@fli.de; martin.schwemmle@uniklinik-freiburg.de

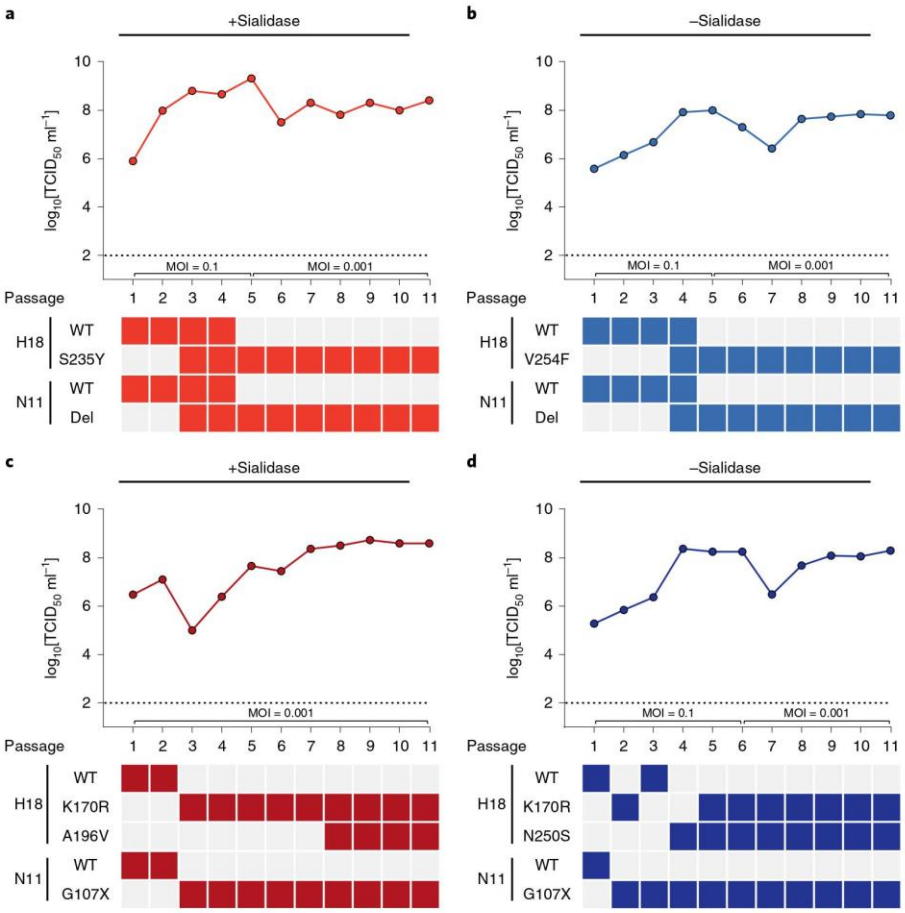

Fig. 1 | Mutations in H18 and N11 enhance replication of H18N11 in vitro. a–d, After recovering the WT H18N11 virus by reverse genetics using HEK293T cells, viruses were serially passaged in canine RIE1495 cells. Before infection, cells were either treated with sialidase or left untreated. Sialidase pretreated (**a,c**) or untreated (**b,d**) cells were infected with H18N11 at the indicated multiplicity of infection (MOI) for 48 h. After each passage, the virus-containing cell supernatant was collected and used for the determination of viral titres by endpoint titration in MDCKII cells. The products of RT-PCR amplification of genomic H18 or N11 sequences were analysed by Sanger sequencing. Corresponding $H18_{WT}$ and $N11_{WT}$ sequences or identified mutations at each passage are highlighted with coloured squares. The dashed lines indicate the detection limit. Each passaging experiment was performed once.

ends were rather short, comprising 101–163 nucleotides, the retained 5′ genome ends were longer and varied between 204–474 nucleotides (Supplementary Table 1). Overall, around 60–80% of the genomic sequence was deleted among the different $N11_{del}$ viral RNA variants. All of the identified viral RNA deletions were out-of-frame deletions, which result in mRNAs that encode C-terminal-truncated N11 proteins. Depending on the specific $N11_{del}$ viral RNA variant, the encoded N11 proteins were 30–70 amino acids in length and comprised only the short cytoplasmic tail, the transmembrane domain and parts of the stalk region (Fig. 2a, Supplementary Table 1).

Repetition of the passaging experiment with a second independent WT H18N11 preparation resulted in similar increasing viral titres together with mutations in both H18 and N11 (Fig. 1c,d). We observed an immediate selection of the K170R substitution in H18 and a nonsense mutation (X) in N11 at G107 ($N11_{G107X}$) caused by the single-nucleotide point mutation at G342U (Fig. 1c,d). The premature stop codon at G107X resulted in a protein truncation, whereby the N11 head domain was lost and only the cytoplasmic tail, the transmembrane domain and a part of the stalk region were retained (Fig. 2a). In subsequent passages, additional mutations in the H18 head domain at either A196V or N250S were acquired (Fig. 1c,d, Supplementary Fig. 1a,b). Sequencing of the viral-particle genome obtained after eleven passages in untreated cells (P11) confirmed the acquisition and fixation of the two mutations in the H18 head domain at K170R and N250S ($H18_{K170R,N250S}$) and the premature stop codon in N11, whereas all of the other genomic segments remained unchanged (Supplementary Table 2).

Next, we generated recombinant viruses on the basis of the in vitro selected H18N11 variant P11 (Fig. 1d), designated rP11, that encode $H18_{K170R,N250S}$ and $N11_{G107X}$. We further generated rP11 variants that either harboured a double stop codon at the positions G107 and T108 ($N11_{G107X,T108X}$), designated $rP11_{N11\ G107X,T108X}$, or a variant encoding the V5 epitope ahead of the two stop codons ($N11_{V5\_G107X,T108X}$), designated $rP11_{N11\_V5\_G107X,T108X}$ (Fig. 2b). All of the recombinant viruses were viable and maintained the introduced mutations, indicating that the head domain of N11 is not required for efficient replication in RIE1495 cells. After infection of RIE1495 cells, we detected a specific V5 signal of 25 kDa only in the lysate of cells infected with $rP11_{N11\_V5\_G107X,T108X}$, corresponding to the

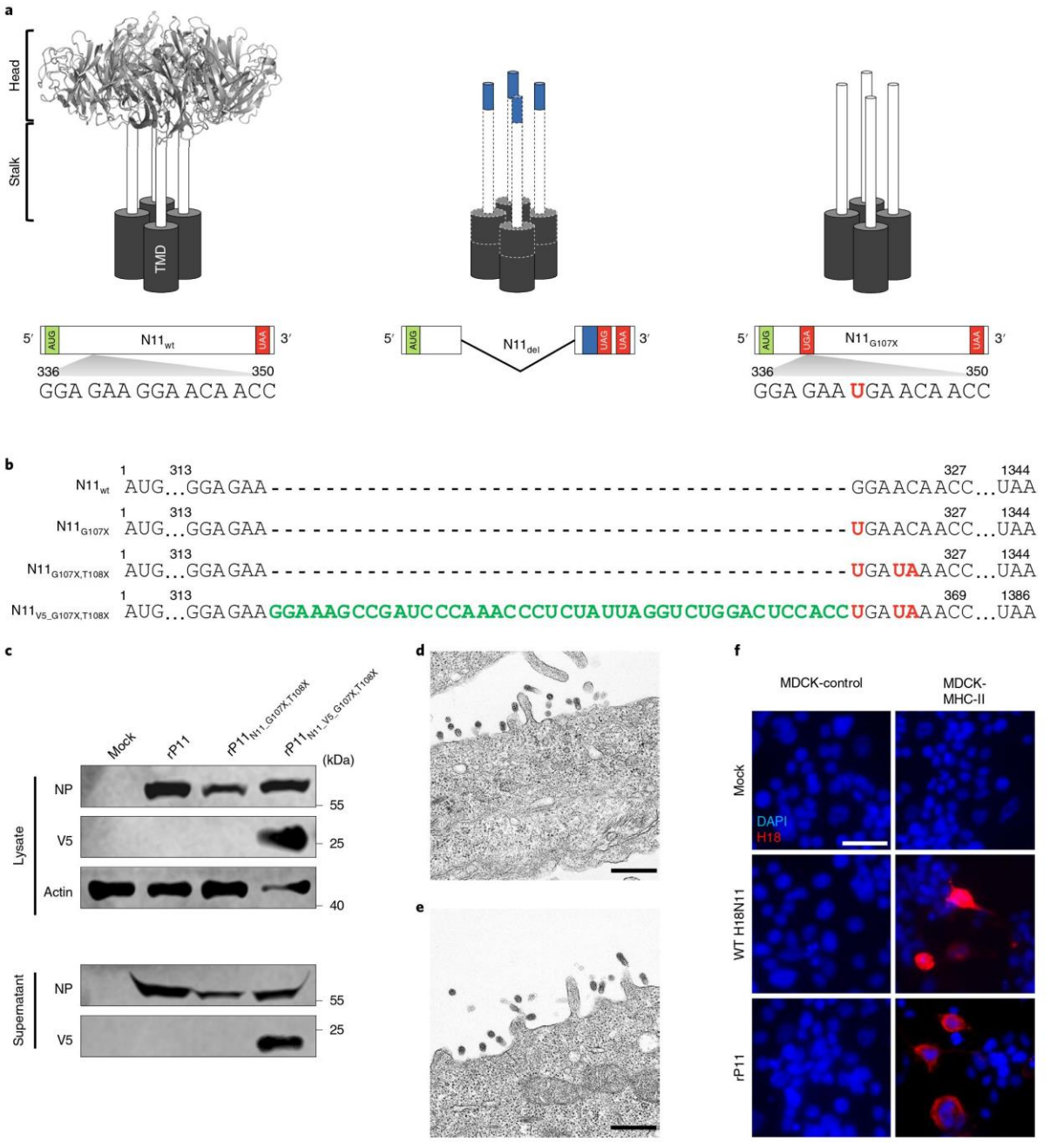

Fig. 2 | H18N11 replicates in the absence of the N11 head domain in vitro. a, Images of the different N11 homotetrameric complex variants found in this study. $N11_{WT}$ monomers comprise a transmembrane domain (TMD), a stalk and head domain. By contrast, $N11_{del}$ and $N11_{G107X}$ lack the functional head domain either because of deletions of the viral RNA genome sequence or the insertion of a point mutation (G342U; highlighted in red), which results in a premature stop codon. Owing to different frame-shift mutations, the C terminus of $N11_{del}$ varies (indicated by dotted lines; Supplementary Table 1) and contains a short unrelated C-terminal peptide (blue). The head domain was created using PyMOL on the basis of the available crystal structure (Protein Data Bank (PDB): 4K3Y). **b**, Alignment of the H18N11 $N11_{WT}$ and N11 mutant nucleotide sequences. Inserted point mutations in the sequences of $N11_{G107X}$, $N11_{G107X,T108X}$ and $N11_{V5\_G107X,T108X}$ that result in a premature stop codon at position G107 and/or T108 are highlighted in red. The introduced V5 amino acid coding sequence in $N11_{V5\_G107X,T108X}$ is indicated in green. **c**, RIE1495 cells were infected with the indicated viruses at an MOI of 10 for 24 h. Subsequently, cell lysate or virus-containing cell supernatant was analysed using western blot to determine the protein levels of NP, V5 and actin ($n=1$). **d**,**e**, RIE1495 cells infected at an MOI of 1 of either WT H18N11 (**d**) or rP11 (**e**) were fixed at 48 h.p.i. and analysed using electron microscopy. Representative micrographs of viral particles released from infected cells of $n=3$ experiments. Scale bars, 500 nm. **f**, MDCK cells expressing human MHC-II (MDCK-MHC-II) or control cells (MDCK-control) were infected with the indicated viruses at an MOI of 5. Successful infection was monitored by immunofluorescence (IF) using H18-specific antibodies. Representative images of $n=3$ independent experiments. Scale bar, 25 μm.

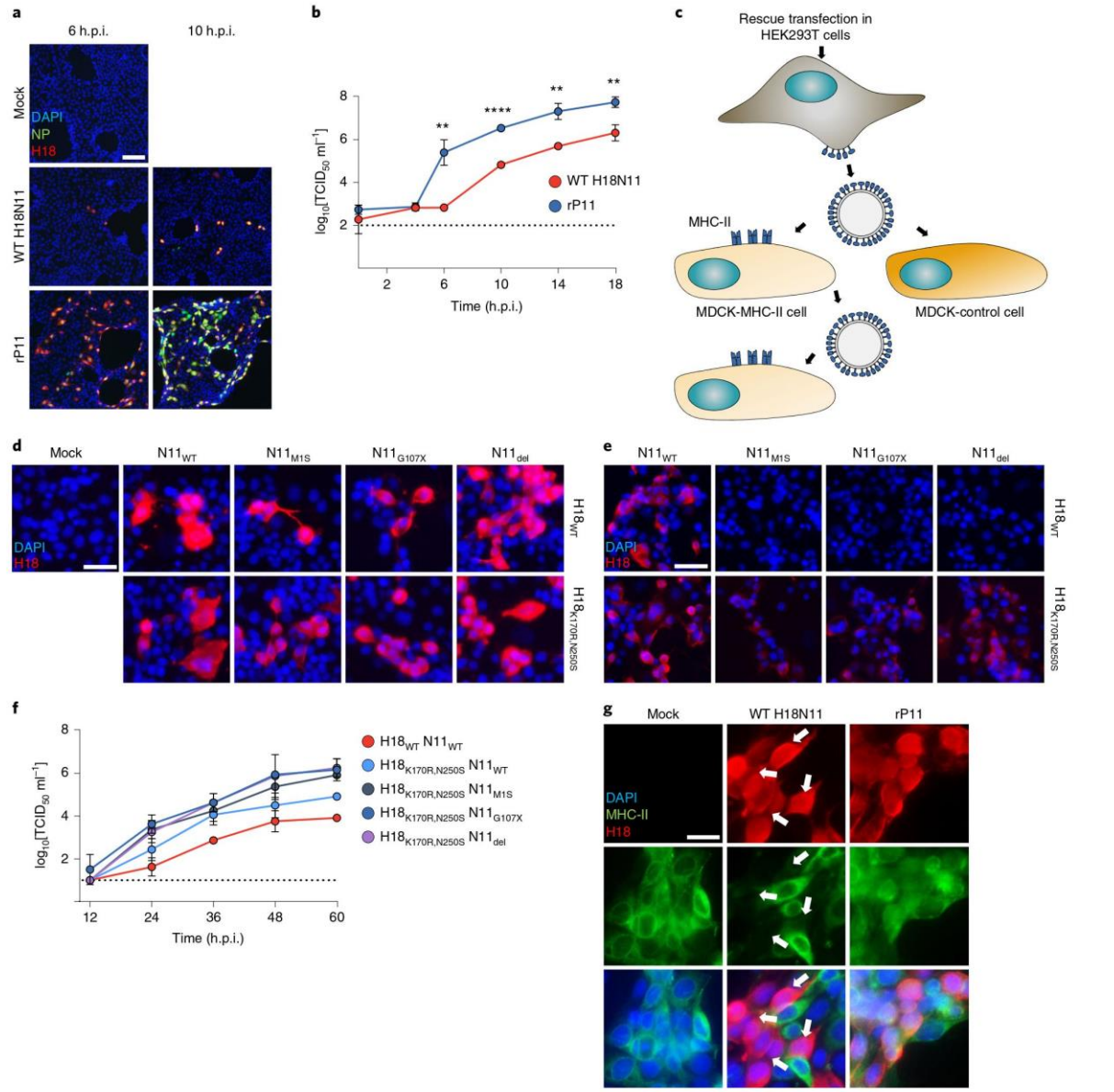

Fig. 3 | $H18_{K170R,N250S}$, rather than N11 truncation, enhances infectivity in vitro. a–**g**, Synchronized infection of RIE1495 cells with WT H18N11 and rP11 at an input multiplicity of 5. **a**, Subcellular localization of H18N11 antigens was monitored over time by IF using NP- and H18-specific antibodies. Representative images of $n=3$ independent experiments. Scale bar, 100 µm. **b**, Viral titres in the supernatant of infected cells were determined by endpoint titration in MDCKII cells at the indicated time points. The dashed line indicates the detection limit. Data are mean ± s.d. of $n=3$ independent experiments; statistical analysis was performed using two-tailed *t*-tests; $^{**}P=0.01$; $^{****}P=0.0001$. **c**, Schematic highlighting the experimental setup that is described below. HEK293T cells were transfected for rescuing different H18N11 virus variants coding for $H18_{WT}$ or $H18_{K170R,N250S}$ together with $N11_{WT}$, $N11_{M1S}$, $N11_{G107X}$ or $N11_{del}$. The $N11_{M1S}$ variant encodes a mutated ATG start codon to prevent translation initiation and protein synthesis. Recovered viruses were propagated in MDCK-MHC-II or MDCK-control cells for 48 h. Newly released viruses from MDCK-MHC-II cells were used to infect other MDCK-MHC-II cells at an MOI of 0.001 for 60 h. **d**,**e**, After infection, cells were fixed and H18 antigen was visualized using IF. Representative images of $n=3$ independent experiments. Scale bars, 50 µm. **f**, Viral titres of infected cells from **e** at different time points after infection. Data are mean ± s.d. of $n=3$ independent experiments. **g**, MDCK-MHC-II cells were infected with the indicated virus at an MOI of 0.5. At 48 h.p.i., samples were fixed, permeabilized and probed with H18- and MHC-II-specific antibodies. White arrows indicate MHC-II-negative infected cells. Representative images of $n=3$ independent experiments. Scale bar, 20 µm.

predicted size of the truncated N11–V5 fusion protein (Fig. 2c). This N11–V5 fusion protein was also observed in viral particle preparations of $rP11_{N11\_V5\_G107X,T108X}$, demonstrating that the truncated N11 protein is incorporated into the viral particle (Fig. 2c). Importantly, loss of the N11 head domain had no influence on the particle structure; released WT H18N11 and rP11 particles

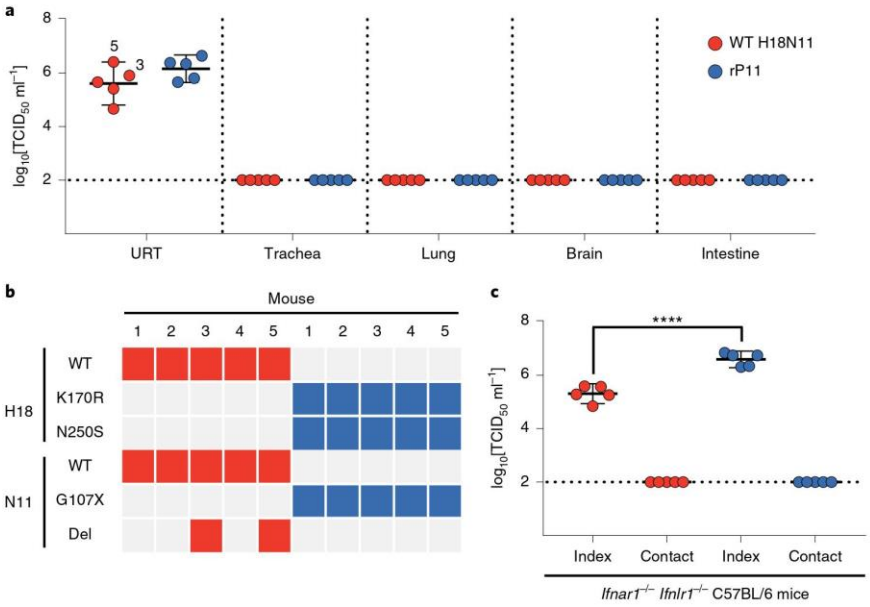

Fig. 4 | Viral replication of WT H18N11 and rP11 is constrained to the URT of infected mice. a, C57BL/6 mice ($n = 5$) were intranasally inoculated with the indicated H18N11 variant (1×10^5 $TCID_{50}$ in 40 µl) and viral organ titres were determined at 4 d.p.i. by endpoint titration in MDCKII cells. Virus isolates 3 and 5 from WT H18N11-infected mice are indicated. Data are mean ± 95% confidence interval. **b**, Viral RNA was isolated from each mouse, reverse transcribed, amplified with H18 and N11 segment-specific primers and analysed using Sanger sequencing. Mutations resulting in amino acid changes in H18 or N11 are indicated with colour-coded squares for each virus. **c**, *Ifnar1*$^{-/-}$ *Ifnlr1*$^{-/-}$ C57BL/6 mice ($n = 5$) were inoculated through the intranasal route with the indicated H18N11 variant (1×10^5 $TCID_{50}$ in 40 µl). At 1 d.p.i., each infected index mouse was separated and co-housed with a naive contact *Ifnar1*$^{-/-}$ *Ifnlr1*$^{-/-}$ C57BL/6 mouse. Viral titres in the URT of index and contact mice were determined at 4 d.p.i. by endpoint titration in MDCKII cells. The dashed line indicates the detection limit. Data are mean ± 95% confidence interval; the statistical analysis was performed using a two-tailed *t*-test, $^{****}P = 0.0001$.

showed a similar spherical morphology (Fig. 2d,e). Furthermore, $H18_{K170R,N250S}$ interacted in a similar manner to $H18_{WT}$ with human MHC-II in a cell-based fusion assay (Supplementary Fig. 1c), and host cell entry of rP11 was still MHC-II dependent as MDCK cells stably overexpressing human MHC-II (MDCK-MHC-II), but not control cells (MDCK-control), were susceptible to infection (Fig. 2f). Together, these findings demonstrate that H18N11 can markedly increase its viral growth properties in vitro by acquiring amino acid mutations in H18 and a truncation of the N11 head domain.

$H18_{K170R,N250S}$ enables viral replication independent of N11. To gain further insights into the selection advantage of the mutant virus rP11 compared with WT H18N11, we performed a synchronized infection of RIE1495 cells. Immunostaining of H18 and viral nucleoprotein (NP) revealed differences in the number of infected cells at early time points (Fig. 3a). Although rP11-infected cells demonstrated pronounced immunostaining signals for NP and H18 as early as 6 h post infection (h.p.i.), low numbers of NP- and H18-positive cells were observed in WT H18N11-infected cells at 6 h.p.i. and 10 h.p.i. Consistently, at 6 h.p.i., we detected newly released infectious particles in the supernatant of rP11-infected cells, whereas infectious WT H18N11 particles were not observed until 10 h.p.i. (Fig. 3b). Together, this suggests that the selection advantage of rP11 over WT H18N11 in vitro is caused by enhanced infectivity. To evaluate the contribution of $H18_{K170R,N250S}$ and truncated N11 to viral replication, we next generated recombinant viruses that encoded different combinations of H18 ($H18_{WT}$ or $H18_{K170R,N250S}$) together with $N11_{WT}$, a start-codon-mutated form of N11 ($N11_{M1S}$) or a truncated version of N11 ($N11_{G107X}$ or $N11_{del}$), and propagated them in either MDCK-control or MDCK-MHC-II cells for 48 h (Fig. 3c). The presence of H18 antigen in infected cells indicated that all of the virus variants released from HEK293T cells were infectious (Fig. 3d) and relied on MHC-II expression (Supplementary Fig. 1d). Viruses coding for $H18_{WT}$ together with $N11_{M1S}$, $N11_{G107X}$ or $N11_{del}$ could not be further propagated after subsequent infection of MDCK-MHC-II cells (Fig. 3e), suggesting that full-length N11 is required in combination with $H18_{WT}$. By contrast, all of the viruses carrying $H18_{K170R,N250S}$ were infectious and replicated to comparable titres regardless of the respective N11 variant (Fig. 3e,f), demonstrating that $H18_{K170R,N250S}$ enables N11-independent viral replication. Finally, immunostaining of MDCK-MHC-II cells showed a reduction in MHC-II signals following infection with WT H18N11 compared with cells infected with rP11 (Fig. 3g), suggesting a role of functional full-length N11 in the regulation of MHC-II expression.

rP11, but not WT, H18N11 is genetically stable in mice. To investigate the viral-replication properties of rP11 compared with WT H18N11 in vivo, C57BL/6 mice were intranasally inoculated with a 10^5 50% tissue culture infective dose ($TCID_{50}$) of either rP11 or WT H18N11, and viral loads of different organs were determined at 4 d post infection (d.p.i.) at the time of peaking titres (Supplementary Fig. 2a). As expected from previous results[15], viral titres in WT H18N11-infected mice were only detected in the upper respiratory tract (URT) and varied between approximately 4.7 and 6.4 $log_{10}[TCID_{50}\,ml^{-1}]$ (Fig. 4a). Similarly, replication of rP11 was confined to the URT, but viral titres consistently reached around 6 $log_{10}[TCID_{50}\,ml^{-1}]$ (Fig. 4a). Sanger sequencing of the H18 and N11 genomic sequences confirmed that virus isolates from

C57BL/6 mice infected with WT H18N11 harboured $H18_{WT}$ and $N11_{WT}$ sequences with the exception of two different isolates (3 and 5) that carried deletions in the N11 viral RNA to different degrees (Fig. 4a,b, Supplementary Table 1). By contrast, rP11 appeared to be genetically stable as none of the five rP11 virus isolates showed any nucleotide exchanges other than the introduced substitutions K170R and N250S in H18 as well as the premature stop codon in $N11_{G107X}$.

Next, to determine whether H18N11 is horizontally transmitted, we intranasally inoculated innate immune-deficient C57BL/6 mice lacking functional type I and III IFN receptor (*Ifnar1*$^{-/-}$ *Ifnlr1*$^{-/-}$) with either WT H18N11 or rP11 and then co-housed these mice with naive contact *Ifnar1*$^{-/-}$ *Ifnlr1*$^{-/-}$ C57BL/6 mice for 4 d. Intranasal inoculation with WT H18N11 and rP11 resulted in robust viral replication in the URT of inoculated index mice (Fig. 4c) but not in any other organ examined, including trachea, lung or brain (Supplementary Fig. 2b), and did not cause weight loss or mortality (Supplementary Fig. 2c). Importantly, none of the contact mice acquired a viral infection from the inoculated donors.

rP11, but not WT H18N11, replicates to detectable levels in various ferret organs but fails to transmit to contact animals. Ferrets mirror the transmissibility and pathogenicity of conventional IAV infections in humans most closely[16–18]. Therefore, to determine H18N11 growth and horizontal transmission in ferrets, we inoculated 12 index ferrets with 10^7 $TCID_{50}$ of the cell-culture-adapted rP11 virus and co-housed four naive contact animals after 1 d for further 20 d (Fig. 5a). All of the nasal washes taken from both index and contact animals were found to be negative throughout the course of experiment with the exception of a weakly positive sample obtained from index ferret 10 at 3 d.p.i. (Fig. 5a). At 4 d.p.i., four index ferrets were necropsied and multifocal atelectasis was detected within the right lung of ferret 10 (Supplementary Fig. 3a). Histopathological analysis of ferrets at 4 d.p.i. revealed moderate pneumonia and rhinitis with multifocal H18 RNA and weak immunoreactivity of viral matrix protein (Fig. 5b, Supplementary Fig. 3c,d, Supplementary Table 3). The pharyngeal and palatine tonsils showed variable follicular hyperplasia and immunoreactivity of H18 RNA and matrix protein in the follicle-associated epithelium (FAE; Supplementary Fig. 3e–g). Furthermore, moderate RNA levels were measured by quantitative PCR with reverse transcription (RT–qPCR) in the trachea, lungs and brain of some of the animals (Fig. 5c, Supplementary Table 4). All of the ferrets appeared to be clinically healthy throughout the course of the study and showed no differences in body weight and body temperature compared with the uninfected animals (Fig. 5d,e). All of the index ferrets examined after 7 d.p.i. seroconverted with detectable NP-specific antibody titres and neutralizing antibodies against the H18 protein (Fig. 5f,g). Sequencing of the reverse-transcribed viral RNA extracted from infected lungs (9 and 10) or nasal conchae (11 and 12) revealed that the K170R and N250S substitutions in H18 were retained, whereas a single nucleotide mutation at U342G in N11 emerged, restoring the $N11_{WT}$ open-reading frame (ORF; Fig. 5h,i). We therefore speculated that full-length N11 might be of functional relevance in ferrets and, accordingly, inoculated 12 index ferrets with the highest possible dose of 10^6 $TCID_{50}$ of WT H18N11 (Supplementary Fig. 4a). However, no viral transcripts were detected in nasal lavage samples nor in any organ, and all of the animals appeared to be clinically healthy (Supplementary Fig. 4b,c); nevertheless, two of the four index ferrets tested after 7 d.p.i. and all of the index ferrets tested at 21 d.p.i. seroconverted with NP-specific antibodies (Supplementary Fig. 4d). Moreover, all of the index ferrets examined after 7 d.p.i. possessed neutralizing antibodies against H18 (Supplementary Fig. 4e). Overall these results suggest that both WT H18N11 and rP11 are only poorly adapted to ferrets.

Full-length N11 is required for efficient transmission of H18N11 in Neotropical Jamaican fruit bats. To determine the replication properties and transmissibility of H18N11 in a putative natural-host reservoir, we infected the Neotropical Jamaican fruit bat (*Artibeus jamaicensis*), which is a close relative of the flat-faced fruit-eating bat (*Artibeus planirostris*) from which the H18N11 sequence was initially isolated[7]. A group of 10 bats was intranasally inoculated with 5×10^5 $TCID_{50}$ of WT H18N11. At 2 d.p.i., two naive contact bats were co-housed with the infected index bats to monitor potential viral transmission (Fig. 6a). As high levels of viral genome were observed in the faeces of naturally infected bats[6,7], rectal swabs taken at the indicated time points were used to surveil and calculate viral shedding by an NP-based RT–qPCR analysis as $\log_{10}$[$TCID_{50}$ equivalents ml^{-1}] (Fig. 6b). At 3 d.p.i., viral RNA was detected in rectal swabs in eight out of ten index bats with an average titre of around 3.6 $\log_{10}$[$TCID_{50}$ equivalents ml^{-1}], whereas both contact bats were found to be virus negative at 1 d post exposure (d.p.e.). Interestingly, from 4 to 8 d.p.e., viral RNA was detectable in rectal swabs of both naive contact bats reaching viral titres of approximately 7 and 5 $\log_{10}$[$TCID_{50}$ equivalents ml^{-1}], respectively (Fig. 6b). From 4 d.p.e., both contact bats also developed mild signs of disease, characterized by nasal and ocular discharge (Supplementary Fig. 5a) that lasted until 8 d.p.e. By contrast, although all eight remaining index bats were found to be virus positive with peaking titres of around 6.4 $\log_{10}$[$TCID_{50}$ equivalents ml^{-1}] (Fig. 6b), at 6 d.p.i., they appeared to be clinically healthy without any signs of disease during the entire experiment. Importantly, although oral swab samples collected from index and contact bats were found to be negative throughout the course of the experiment, we were able to isolate infectious virus from faecal specimens of bats that were found to be H18N11 positive by RT–qPCR analysis (Supplementary Fig. 5b). Subsequent sequencing of viral RNA isolated from rectal swab

Fig. 5 | rP11 exhibits only limited replication ability in ferrets. a, Index ferrets (1–12) were inoculated with 10^7 $TCID_{50}$ of rP11 oronasally. At 1 d.p.i., naive contact ferrets (1–4) were co-housed. Nasal washes were taken at the indicated time points. White and black squares indicate absence and presence of viral RNA in nasal washes, respectively. Grey and red squares indicate the absence and presence of H18N11 RNA in at least one organ, respectively. Asterisks indicate seroconversion. **b**, Histologic findings with detection of viral antigen and RNA in paraffin-embedded tissue of rP11-infected index animals ($n = 4$) at 4 d.p.i. Moderate, subacute, suppurative rhinitis with oedema and infiltrating neutrophils (arrows) (i). Multifocal H18 RNA in the respiratory epithelium (arrow) and in submucosal round cells (arrowhead) (ii). Faintly intracytoplasmic and intranuclear matrix-protein antigen in the respiratory epithelium (arrow) (iii). Moderate, subacute, suppurative and necrotizing bronchiolointerstitial pneumonia with luminal debris (asterisk) (iv). Multifocal H18 RNA in intrabronchial debris and within alveolar macrophages (arrow) (v). Scale bars, i, 50 µm; ii and v, 20 µm; iii, 10 µm; iv, 100 µm. **c**, Organs collected from $n = 4$ euthanized ferrets at 4 d.p.i. (9–12) were tested by RT–qPCR using pan-IAV PB1 primers to determine viral titres as RT–qPCR-derived $\log_{10}$[copies ml^{-1}]. **d**,**e**, Changes in body weight (**d**) and body temperature (**e**) of rP11-infected ($n = 12$), contact ($n = 4$) and control ferrets ($n = 2$) were monitored throughout the course of the experiment. Data are mean ± s.d. **f**,**g**, NP-specific antibody titres (**f**) and serum neutralizing antibodies to H18 (**g**) of index ($n = 12$) and contact ferrets ($n = 4$) were determined. The dashed lines indicate cut-off points. OD_{550}, optical density at 550 nm. Data are mean ± s.d. **h**, Isolated viral RNA from lungs (9 and 10) or nasal conchae (11 and 12) was studied using Sanger sequencing to analyse H18 and N11 genomic sequences. The presence or absence of mutations is indicated by black squares. **i**, N11 sequence extract isolated from ferret 11 (top panel) and 12 (bottom panel). Sequencing was performed once ($n = 1$).

samples that were obtained from index and contact bats at 6 d.p.i. or 4 d.p.e. revealed $H18_{WT}$ and $N11_{WT}$ genomic sequences (Fig. 6c). Furthermore, a serological response with H18N11 NP-specific antibodies was detected in index bats examined at 17 d.p.i. and 28 d.p.i. as well as in both contact animals at 26 d.p.e. (Fig. 6d). Immunoreactivity of H18 RNA and matrix protein was detected in the FAE of jejunal Peyer's patches, in enterocytes and lamina propria-associated round cells interpreted as macrophages and also in

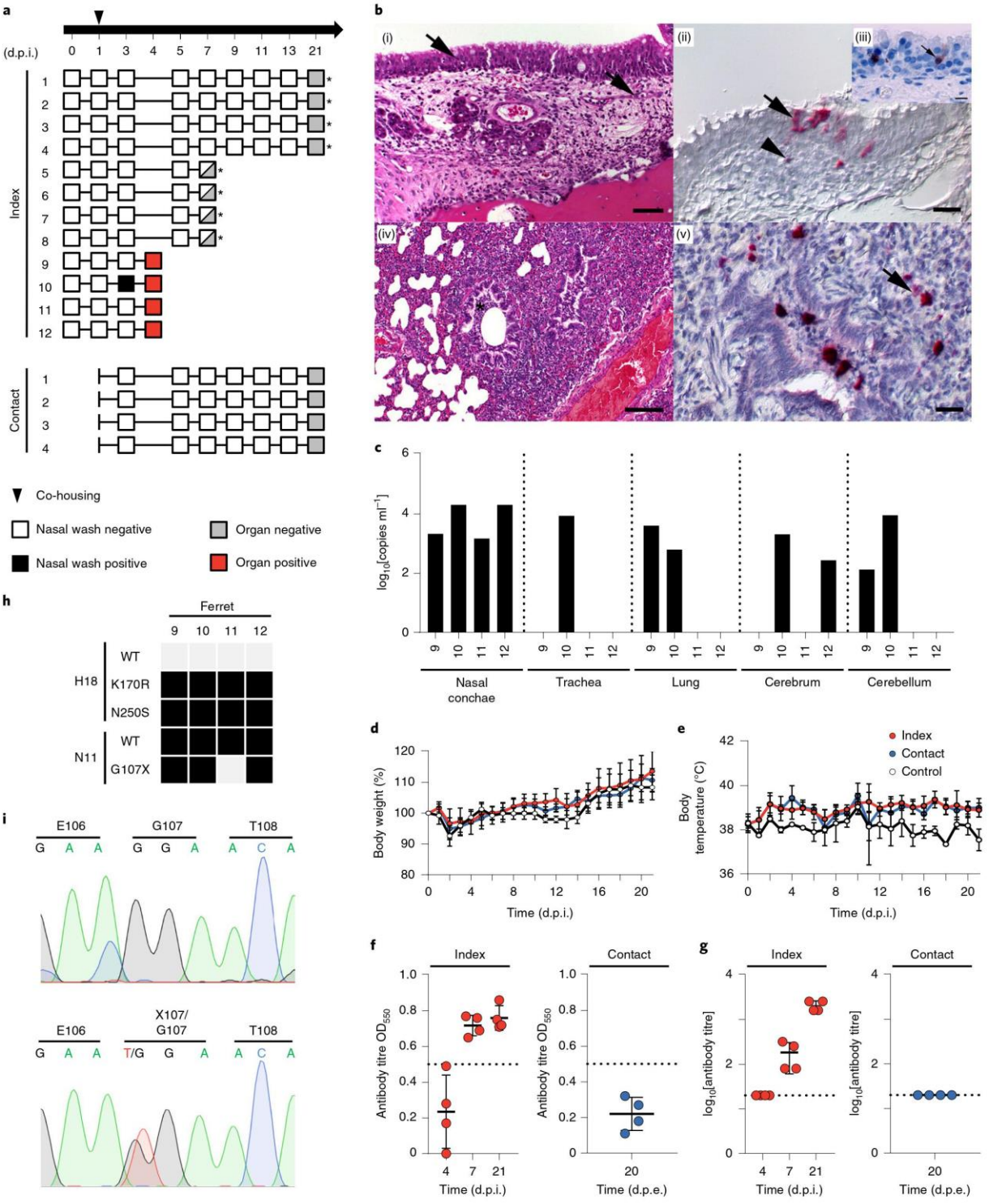

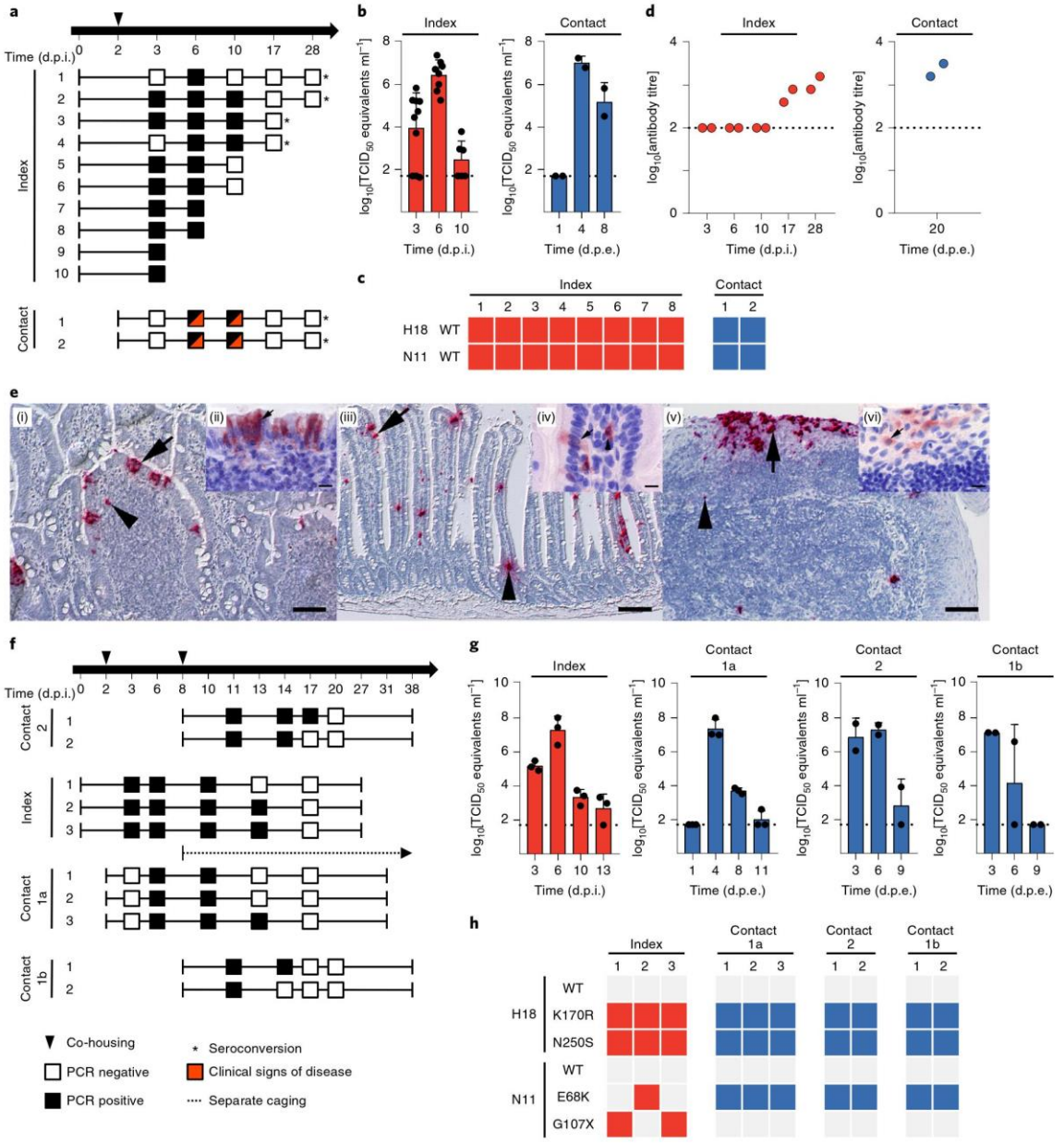

Fig. 6 | Bat IAVs that encode full-length N11 are spread among bats. a, Index bats (1–10) were infected with 5×10^5 $TCID_{50}$ of WT H18N11 intranasally. At 2 d.p.i., naive contact bats (1–2) were co-housed. **b**, Viral titres of rectal swabs from index ($n=10$) and contact bats ($n=2$) were determined by RT–qPCR. Data are mean ± s.d. **c**, Isolated viral RNA from faecal samples of index (red squares) and contact bats (blue squares) was subjected to Sanger sequencing at 6 d.p.i. **d**, NP-specific antibody titres of index and contact bats. The dashed lines indicate the cut-off point. **e**, Viral antigen and RNA in the tissue of WT H18N11-infected index bats ($n=4$). Multifocal H18 RNA in FAE (arrow) and submucosal round cells (arrowhead) of a jejunal Peyer's patch (i). Strong matrix-protein immunoreactivity in FAE (arrow) (ii). Jejunal villi with multifocal H18 RNA in enterocytes (arrow) and in lamina propria-associated round cells (arrowhead) (iii). Matrix-protein immunoreactivity in enterocytes (arrow) and in round cells (arrowhead) interpreted as macrophages or dendritic cells (iv). Multifocal H18 RNA in squamous epithelium (arrow) and scattered in submucosa (arrowhead) of a palatine tonsil (v). Moderately strong matrix-protein immunoreactivity in squamous epithelium (arrow) (vi). Scale bars, i, 50 µm; ii, iv and vi, 10 µm; iii, 100 µm; v, 20 µm. **f**, Index bats (1–3) were infected with 5×10^5 $TCID_{50}$ of rP11 intranasally. Naive contact bats (1–3), designated contact 1a, were co-housed at 2 d.p.i. At 8 d.p.i., index and contact 1a bats were separated. Other naive contact bats (1–2), designated contact 2, were co-housed with the index animals starting at 8 d.p.i. Two other naive contact bats (1–2), designated contact 1b, were co-housed with the contact 1a group from 8 to 31 d.p.i. **g**, Viral titres of rectal swabs as in **b**. **h**, Next-generation sequencing (NGS) of viral RNA isolated from index (red squares) and contact bats (blue squares) at 3 d.p.i. (that is, contact 1a) or 4 d.p.i. (that is, contact 2 and contact 1b). The cut-off was set at 50% frequency. The white and black squares indicate the absence and presence of H18N11 RNA in rectal swab samples, respectively. Orange squares indicate signs of disease. Asterisks indicate seroconversion. Data are mean ± s.d.

the squamous epithelium covering the palatine tonsils of index bats 7–9 (Fig. 6e, Supplementary Table 5). Importantly, no necrotizing or inflammatory lesions were seen in any of the investigated organs.

To evaluate whether rP11 can also replicate and transmit in bats, three Neotropical Jamaican fruit bats were inoculated with 5×10^5 $TCID_{50}$ through the intranasal route. At 2 d.p.i., three naive contact bats, designated contact group 1a, were co-housed with the infected index animals (Fig. 6f). RT–qPCR analysis of rectal swabs taken from index bats revealed that all three index bats were virus positive between 3 and 10 d.p.i. and two bats shed viral RNA until 13 d.p.i., with peak titres of around 7.3 log_{10}[$TCID_{50}$ equivalents ml^{-1}] at 6 d.p.i. (Fig. 6g). Sequencing of viral RNA isolated from rectal swab samples of index bats at 3 d.p.i. revealed that the amino acid substitutions in H18 were maintained in all three isolates, whereas the full N11 coding sequence was restored by a nucleotide point mutation at U342G accompanied by an additional mutation at E68K in index bat 2 and also to a lesser extent in the other index animals (Fig. 6h, Supplementary Table 6). From 4 to 8 d.p.e., all three contact 1a bats were found to be H18N11 RNA positive with average viral titres of around 7.3 and 3.7 log_{10}[$TCID_{50}$ equivalents ml^{-1}]. At 6 d.p.e., bats in the index and contact 1a group were split into separate cages and again co-housed with two naive contact bats each, designated contact group 2 and contact group 1b, respectively. We were thus able to monitor the duration of the rP11 infection in index bats and the transmissibility of the acquired virus in the contact 1a bats (Fig. 6f). H18N11 RNA was identified in rectal samples obtained from bats in contact group 2 from 3 to 6 d.p.e. and one bat shed viral RNA until 9 d.p.e., corresponding with peak titres of around 7.3 log_{10}[$TCID_{50}$ equivalents ml^{-1}] at 6 d.p.e. Notably, both of the contact bats of the contact group 1b started to shed virus at 3 d.p.e. with an average titre of around 7 log_{10}[$TCID_{50}$ equivalents ml^{-1}] (Fig. 6g). After sequencing viral RNA obtained from contact bats at 3 d.p.e. (contact 1a group) or 4 d.p.e. (contact 2 and contact 1b group), we still detected the introduced mutations at K170R and N250S in H18, but all of the isolates harboured a full-length N11 ORF with an amino acid substitution at E68K (Fig. 6h). Taken together, our data strongly suggest that N11 is not required for replication and shedding of H18N11 in its bat host, but rather it is a prerequisite for efficient transmission.

Discussion

Here we demonstrate that bat IAV H18N11 transmits efficiently among Neotropical Jamaican fruit bats, a putative natural-host reservoir[7]. On the basis of high loads of viral transcripts in rectal swabs and the detection of infectious virus in rectal excretions, we assume that H18N11 is spread through virus-containing faeces. Consistent with this, histopathological analysis indicates that viral replication proceeds in the FAE of gut-associated lymphoid tissue, suggesting virus uptake from the gastrointestinal lumen[19]. In a similar manner, low pathogenic avian IAVs replicate in the intestine of ducks and are excreted at high concentrations in faeces[20]. Thus, although the route of IAV transmission might be similar in bat and avian species, it is clearly different to the spread of IAV in humans. Importantly, the function of N11 seems to be particularly related to viral transmission, as viruses encoding full-length N11 showed a growth advantage over those that encode a truncated N11 together with $H18_{WT}$. Although the precise role of N11 remains unclear, it is tempting to speculate that N11 might be involved in the downregulation of MHC-II expression, thereby facilitating virion release. Whether the N11 mutation E68K plays an additional role in this context remains to be determined.

The recent discovery of MHC-II molecules in bats and various other species as cell-entry mediators for the bat IAV subtypes H17N10 and H18N11[15] raised concerns of their epizootic and zoonotic potential[21]. Indeed, our data highlight that—owing to its genetic plasticity—H18N11 becomes rapidly adapted in vitro by acquiring mutations in H18 and by the removal of the N11 head domain. As shown for rP11, such mutant viruses efficiently replicate in mice, suggesting that its rapid adaptability might increase the spill-over potential to other non-bat species. However, the adaptation to new hosts seems to be species-dependent, as infections of bats and ferrets with rP11 resulted in the immediate selection of novel virus mutants coding for a restored N11 ORF while simultaneously maintaining the two amino acid mutations in H18. On the basis of the relatively low replication capacity of H18N11 in ferrets, we speculate that the zoonotic potential is rather low, provided that ferrets are an appropriate animal model to study bat IAV infections of humans. However, viral replication in ferrets was similar to bats primarily detected in the FAE. In ferrets, it was found that the FAE of the pharyngeal and palatine tonsils were strongly positive for H18 RNA and viral antigen, whereas viral replication in bats occurred in the FAE of the gut-associated lymphoid tissue and also partially in palatine tonsils. This preference for the FAE in both animals might be related to the high number of MHC-II-expressing cells that are in close proximity to this type of epithelium.

Infection experiments with rP11 in vitro, in mice and in bats revealed that efficient replication without the help of the NA-like protein N11 is most likely due to two amino acid substitutions in the H18 head domain. Interestingly, HA-autonomous replication has also been shown for classical IAVs in previous studies[22–25]. Those sialidase-independent mutants were generated artificially by consecutive cell culture or in ovo passaging in the presence of neutralizing antibodies or neuraminidase inhibitors. As a result, some NA-negative mutants almost completely lost their affinity to host-cell sialic acids and all of the described NA deletion mutants were attenuated in vitro and in vivo. This emphasizes the need of conventional IAVs for a balanced interplay of the HA-mediated receptor binding and NA-facilitated receptor-destroying function, a cooperation that might be comparably relevant in the context of bat IAVs encoding $H18_{WT}$. Although H18N11 variants that encode $H18_{WT}$ together with a truncated form of N11 failed to spread in vitro, $H18_{K170R,N250S}$ alone facilitated viral replication in cell culture.

Collectively, our study reveals that H18N11 replicates and spreads among bats but is poorly adapted to non-bat host species such as ferrets and mice. The genetic plasticity of H18N11, which allows it to adapt quickly to non-bat species, highlights that closer monitoring of the epizootic and zoonotic potential of these bat-derived viruses is required.

Methods

Cell lines. HEK293T cells were obtained from the American Type Culture Collection (ATCC; CRL-3216). RIE1495 and MDCKII cells were obtained from G. Herrler (University of Veterinary Medicine Hannover) and were described previously[13]. MDCK cells stably overexpressing human MHC-II (MDCK-MHC-II) and control cells (MDCK-control) were generated previously[13]. All cells were cultured in Dulbecco's modified Eagle's medium (DMEM; Gibco, Thermo Fisher Scientific) containing 10% fetal calf serum (FCS), 100 U ml^{-1} penicillin and 100 mg ml^{-1} streptomycin at 37 °C with 5% CO_2. MDCK-MHC-II and MDCK-control were selected using 2.5 µg ml^{-1} puromycin and 300 µg ml^{-1} hygromycin.

Generation of recombinant bat influenza H18N11 viruses. The pHW2000-based rescue system was used to generate recombinant WT H18N11 and H18N11 mutant virus variants as described previously[13]. pHW2000 plasmids encoding $H18_{K170R,N250S}$, $N11_{del}$, $N11_{G107X}$, $N11_{G107X,T108X}$ or $N11_{V5\_G107X,T108X}$ were generated using site-specific mutagenesis primers. To prevent the initiation of translation and protein synthesis of N11, we also generated a pHW2000 rescue plasmid encoding an $N11_{M1S}$ variant, in which the first ATG codon in the 5′ coding sequence of the N11 ORF was mutated to TCC. Furthermore, we generated a pHW2000 plasmid encoding $N11_{del}$ on the basis of the 546-nucleotide viral-RNA deletion variant found in vitro and in vivo. The presence of the introduced mutations was confirmed by sequencing with H18-specific primers (forward, 5′-GCAGGGTGATTATTATTCAGAATGATTACAATAC-3′; reverse, 5′-GCAATAATAGATTGACATTAGCTAACACCAC-3′) and N11-specific primers (forward, 5′- AATAATCGCGGCCGCACCATGTCGTTTCAAACATC GACATGTCTGTTG-3′; reverse, 5′-AATAATCCTCGAGTTACCCCCAGTTGA

CATCTGGCAT-3′). All of the recombinant viruses were passaged twice in RIE1495 cells for stock generation unless otherwise stated.

NGS. Infectious cell culture supernatant was subjected to NGS as described previously[26].

Viral RNA was obtained from bat tissue using TRIzol LS Reagent (Thermo Fisher Scientific) and chloroform (Thermo Fisher Scientific) to achieve phase separation followed by RNA extraction using the NucleoMag VET Kit (Macherey-Nagel) according to the manufacturer's instructions. Viral RNA was subsequently subjected to DNase treatment using ezDNase enzyme (Thermo Fisher Scientific) followed by cDNA synthesis using the SuperScript IV reverse transcriptase enzyme (Thermo Fisher Scientific) with the 3′ loci-specific primer H18_823 (5′-ATCCGTATTCTGGCCAGATGA-3′) and N11_484 (5′-TGTTCTGACACAATTAGGTCTGCAT-3′). cDNA products were amplified incorporating Nextera transposase adapters (italics) using Q5 High-Fidelity DNA Polymerase (New England BioLabs) according to the manufacturer's instructions with approximately 20 cycles of amplification with H18 loci-specific primers (bold) (forward, 5′- *TCGTCGGCAGCGTCAGATGTGTATAAGAGACAG***AATG-TAGACAGTGCATGCCCA**-3′; reverse, 5′-*GTCTCGTGGGCTCGGAGATGT-GTATAAGAGACAG***ATCCGTATTCTGGCCAGATGA**-3′) and N11 loci-specific (bold) (forward, 5′-*TCGTCGGCAGCGTCAGATGTGTATAAGAGACAG***AA-TTATTCCTGTGAGTGTCCAGCT**-3′; reverse, 5′-*GTCTCGTGGGCTCGGA GATGTGTATAAGAGACAG***TGTTCTGACACAATTAGGTCTGCA**-3′). The PCR-amplification products were bead purified using AMPure XP (Beckman Coulter), quantified with Qubit 3.0 (Thermo Fisher Scientific) and dual-indexed using in-house-generated Illumina Nextera Index primers with the Q5 High-Fidelity DNA Polymerase and approximately 10 cycles of amplification. Complete amplicon libraries were bead purified using AMPure XP (Beckman Coulter), quantified with HS D1000 Screen Tape (Agilent Technologies) and a NEBNext Library Quant Kit for Illumina (New England BioLabs) and sequenced with a 2 × 250 bp paired-end V2 kit using an Illumina MiSeq. For sequencing analyses, the amplicon data were processed using an in-house processing workflow. In brief, R1 and R2 .fastq files from paired-end reads generated using an Illumina MiSeq were trimmed for Illumina adapter sequences and reads with phred quality scores of less than 30 using Cutadapt[27]. The trimmed reads were then mapped to the available H18 gene sequence (GenBank: KR077932.1) and N11 gene sequence (GenBank: CY125947.1)[7] using Bowtie2[28]. SAMtools[29] was used for variant calling preprocessing, and single-nucleotide variants, inserts and deletions were called by using LoFreq[30] with the '-call-indels command' and '—no-default-filter command', all other settings were default.

Polykaryon formation assay. HEK293T cells were seeded and grown in 6-well plate format and co-transfected with 2 µg of pCAGGS-GFP and either pCAGGS-EV or pCAGGS-$H18_{WT}$ or pCAGGS-$H18_{K170R,N250S}$. At 24 h after transfection, cells were detached by treating with trypsin, and 100,000 transfected HEK293T cells were then co-seeded together with either 100,000 MDCK-control or MDCK-MHC-II cells in growth medium on glass plates in 24-well format. The next day, cells were treated with trypsin (1 µg ml^{-1} in Opti-MEM) for 30 min at 37 °C to activate H18. Cells were subsequently washed once with PBS, exposed to PBS (pH 5) for 20 min at 37 °C and then incubated in growth medium for 2 h at 37 °C. Finally, the cells were washed twice with PBS, fixed using 4% paraformaldehyde in PBS for 20 min and nuclei were stained for 1 h using 4′,6-diamidino-2-phenylindole (DAPI) at a dilution of 1:10,000 in PBS. Glass slides were mounted and fluorescence images were acquired using a Zeiss Observer.Z1 inverted epifluorescence microscope (Carl Zeiss) equipped with an AxioCamMR3 camera using a ×20 objective.

Cell-culture infections. For consecutive passaging, sub-confluent RIE1495 cells were washed with PBS and treated with 200 mU ml^{-1} of bacterial sialidase (Sigma-Aldrich) diluted in PBS (0.2% BSA) for 1 h at 37 °C or left untreated. Cells were then washed with PBS (0.2% BSA) and infected with passaging supernatant at the indicated MOI in infection medium (DMEM containing 0.2% BSA, 100 U l^{-1} penicillin and 100 mg ml^{-1} streptomycin, and 1 µg ml^{-1} trypsin) for 48 h at 37 °C with 5% CO_2.

For synchronized infection, RIE1495 cells seeded onto glass plates in 24-well plate format were washed once with PBS (0.2% BSA) and subsequently infected with the indicated virus with an input multiplicity of 5 in infection medium on ice. After 1 h, cells were incubated for 15 min at 37 °C, and then washed twice with PBS, incubated in PBS (pH 2) for 30 s, washed with infection medium and further incubated at 37 °C in infection medium. At the indicated time points, cells were fixed, washed three times with PBS and permeabilized using 0.5% Triton X-100 in PBS for 5 min. Viral proteins were stained with monoclonal bat anti-IAV NP antibodies and polyclonal anti-H18 antibodies (1:750) for 1 h at room temperature. Cells were then washed three times with PBS and incubated with corresponding secondary anti-mouse IgG antibodies coupled to AlexaFluor 488 (Jackson ImmunoResearch, 1:500) or anti-rabbit IgG antibodies coupled to Cyanine Cy3 (Jackson ImmunoResearch, 1:500) for 45 min at room temperature. Finally, cells were washed and nuclei were stained for 5 min using DAPI. Glass slides were mounted and fluorescence images were acquired as described above.

To determine whether host cell entry is MHC-II dependent, MDCK-MHC-II and MDCK-control cells were seeded and grown on glass plates in 24-well plate format, washed once with PBS (0.2% BSA) and subsequently infected with the indicated virus at an MOI of 5 in infection medium at room temperature for 1 h. Inoculum was removed and cells were washed twice with PBS and then further incubated in infection medium for 48 h. Viral proteins were visualized as described above.

To analyse the contribution of different H18 and N11 variants to viral replication, viruses encoding $H18_{WT}$ or $H18_{K170R,N250S}$ together with $N11_{WT}$, $N11_{M15}$, $N11_{G107X}$ or $N11_{del}$ were recovered from transfected HEK293T cells, and 500 µl of the respective rescue supernatant in infection medium was used to infect MDCK-MHC-II or MDCK-control cells seeded in 6-well plates. After infection for 48 h at 37 °C, viruses present in the cell supernatant were titrated and infected cells were fixed and H18 antigen was visualized as described above. Next, new MDCK-MHC-II cells seeded in 6-well plate format were washed once with PBS (0.2% BSA) before infection and subsequently infected with the indicated virus at an MOI of 0.001 in infection medium for 60 h. Viral titres were determined over time by titration and cells were finally fixed and viral antigens were visualized.

To determine the expression levels of MHC-II in infected cells, MDCK-MHC-II-expressing cells were seeded onto glass plates in 24-well plate format, washed once with PBS (0.2% BSA) and were then infected with the indicated virus at an MOI of 0.5 in infection medium. At 48 h.p.i., cells were fixed, permeabilized and probed using antibodies against H18 and the human MHC-II molecule HLA-DRα (Santa Cruz, 1:100) for 1 h at room temperature.

Titration. Viral titres were determined using IF on sub-confluent MDCKII cells as described previously[12]. Rabbit polyclonal anti-H18 and secondary anti-rabbit IgG coupled to Cyanine Cy3 (Jackson ImmunoResearch, 1:500) antibodies were used to detect and quantify H18-positive cells.

Bat rectal swab samples were collected in 500 µl brain–heart infusion (BHI) medium and subsequently filtered by adding an additional 500 µl PBS through a 0.45 µm filter. The filtered flow-through was used for virus titration by performing a tenfold dilution series in PBS. Viral titres were determined by IF on sub-confluent MDCKII cells pretreated with 100 mU ml^{-1} sialidase (Sigma-Aldrich) for 1 h and diethylethanolamine for 30 min at 37 °C using rabbit polyclonal anti-NP antibodies (Thermo Fisher Scientific, 1:400) and secondary goat anti-rabbit IgG antibodies coupled to FITC (Thermo Fisher Scientific, 1:400) antibodies.

Western blot analysis. Protein samples from cell lysates were incubated at 95 °C in Laemmli buffer and subsequently separated by SDS–PAGE. Separated protein samples were blotted on a nitrocellulose membrane. Levels of NP, actin or V5 were determined using specific antibodies against NP (Gene Tex, 1:1,000), actin (Sigma-Aldrich, 1:1,000) and V5 (abcam, 1:2,500), respectively. Primary antibodies were detected using peroxidase-conjugated secondary antibodies (Jackson ImmunoResearch, 1:5,000).

Electron microscopy. RIE1495 cells were seeded and grown at 37 °C with 5% CO_2. Cells were washed with PBS (0.2% BSA) and subsequently infected at an MOI of 1 with either WT H18N11 or rP11. At 24 h.p.i., cells were fixed and analysed using electron microscopy as described previously[31] using a Tecnai-G2-Spirit microscope (FEI Company).

Infection of mice. All of the mouse experiments were performed in accordance with the guidelines of the German animal protection law and were approved by the state of Baden-Württemberg (Regierungspräsidium Freiburg; reference number: 35-9185.81/G-17/14). Mouse infection experiments were performed under BSL-3 conditions in line with the local animal care committees. C57BL/6 mice were obtained from Janvier and *Ifnar1*$^{-/-}$ *Ifnlr1*$^{-/-}$ C57BL/6 mice were bred locally in the facility at the Institute of Virology Freiburg and handled in accordance with guidelines of the Federation for Laboratory Animal Science Associations and the national animal welfare body. Virus stocks were diluted in Opti-MEM containing 0.3% BSA. For infection, 6–8-week-old C57BL/6 mice and *Ifnar1*$^{-/-}$ *Ifnlr1*$^{-/-}$ C57BL/6 mice were anaesthetized with a mixture of ketamine (100 mg g^{-1} body weight) and xylazine (5 mg g^{-1} body weight) administered intraperitoneally and were subsequently inoculated intranasally with 40 µl of the indicated virus dose. Throughout the course of the experiment, mice were monitored daily for changes in body weight or severe signs of disease. To determine organ titres, mice were euthanized at the indicated time points after infection and the indicated organs were collected. Organs were homogenized in 1 ml PBS by three subsequent rounds of mechanical treatment for 25 s each at 6.5 m s^{-1}. Tissue debris was removed by centrifuging homogenates for 5 min at 5,000 r.p.m. and 4 °C.

Infection of ferrets. All of the ferret experiments were evaluated by the responsible ethics committee of the State Office of Agriculture, Food Safety, and Fishery in Mecklenburg-Western Pomerania, Germany (LALLF M-V), and gained governmental approval under registration number LVL MV TSD/7221.3-1.1-037/17. The ferrets (*Mustela putorius furo*) were reared at the Friedrich-Loeffler-Institute and housed in groups of two animals per cage. The infection experiments were performed under BSL-3 conditions using a total of 36 animals that were

found to be healthy and negative for influenza virus antibodies. For infection, 3–9-month-old ferrets were anaesthetized by inhalation of 5% isoflurane in O_2 and 12 animals per group were subsequently infected oronasally with either rP11 (10^7 $TCID_{50}$ in 100 µl) or WT H18N11 (10^6 $TCID_{50}$ in 100 µl). Two ferrets received no inoculum and served as control animals. A group of four naive contact ferrets were each paired with infected index ferrets at 1 d.p.i. in a one-to-one setting to monitor viral transmission of rP11 or WT H18N11. Clinical signs of disease (nasal discharge, reduced activity, fever, neurological symptoms and dyspnoea), body temperature and body weight were monitored daily. Nasal-wash samples were collected at 1, 3, 5, 7, 9, 11 and 13 d.p.i. from all of the ferrets under anaesthesia by applying 700 µl PBS to each nostril. To determine viral organ titres and histopathological changes, four animals were euthanized at 4, 7 and 21 d.p.i. and the intestine, trachea, lungs (divided into left and right parts), conchae, heart, kidneys (only WT H18N11 infection), liver (only WT H18N11 infection), olfactory bulb, thigh muscles, cerebellum and cerebrum were collected. Collected organs were homogenized in a 1 ml mixture of equal volumes composed of Hank's balanced salts minimum essential medium (MEM) and Earle's balanced salts MEM containing 2 mM L-glutamine, 850 mg l^{-1} $NaHCO_3$, 120 mg l^{-1} sodium pyruvate and 10% FCS (supplemented with 10% FCS and 1% penicillin–streptomycin) by mechanical treatment for 2 min at 6.5 m s^{-1}. Tissue debris was removed by centrifuging homogenates for 2 min at 13,000 r.p.m.

Infection of bats. All of the work with bats was approved by the Colorado State University (CSU) Institutional Animal Care and Use Committee, protocol 16-6502a. Jamaican fruit bats (*A. jamaicensis*) were sourced from the breeding colony housed at CSU. This colony has been closed for 12 yr and has been determined to be free of influenza virus infection by serology (enzyme-linked immunosorbent assay (ELISA)) and lack of detection of viral RNA (rectal swabs). Bats were housed in bird cages for the duration of the experiments. For inoculation, bats were anaesthetized with 5% isoflurane in O_2 and then oronasally inoculated with 12.5 µl per nostril of either WT H18N11 or rP11 (5×10^5 $TCID_{50}$ in 25 µl). Non-inoculated control bats were included in each experiment. Naive contact bats were co-housed with inoculated index bats 2 d.p.i. or 8 d.p.i to assess transmission. Rectal swabs were collected at 3, 6, 10, 17 and 28 d.p.i. (WT H18N11 infection) or 3, 6, 10, 11, 13, 14, 17 and 20 d.p.i. (rP11 infection) in BHI medium for virus isolation and detection of viral RNA. To perform histopathological analysis, all of the WT H18N11-infected index and contact bats were euthanized at 28 d.p.i. and all of the rP11-infected index and contact bats were euthanized at 27, 31 or 38 d.p.i. by inhalation of isoflurane followed by thoracotomy. Tissues and blood were collected at necropsy and prepared for histopathology, immunohistochemistry and serology.

RT–qPCR analysis. To quantify the levels of viral RNA in the homogenized ferret organs or nasal-wash samples, the samples were first mixed with TRIzol LS Reagent (Thermo Fisher Scientific) and then with chloroform (Thermo Fisher Scientific) to achieve phase separation. The contained RNA was extracted with the NucleoMag VET Kit (Macherey-Nagel) according to the manufacturer's instructions using the BioSprint 96 DNA Plant Kit (Qiagen). RT–qPCR analysis of isolated viral RNA was performed using pan-IAV PB1 primers as described previously[32].

To quantify levels of H18N11 viral RNA in bat rectal swab samples, the respective sample was first mixed with TRIzol reagent for 5 min and chloroform (Thermo Fisher Scientific) was added subsequently, samples were mixed, incubated for a further 3 min at room temperature and then centrifuged at 12,000*g* for 15 min at 4 °C. The aqueous phase was removed and 4 µg of glycogen (Thermo Fisher Scientific) and isopropanol (Thermo Fisher Scientific) was added. Samples were incubated at room temperature for 10 min and then centrifuged at 12,000*g* for 10 min at 4 °C. Supernatant was removed and each RNA pellet was washed once with ethanol (Thermo Fisher Scientific). Samples were then vortexed and centrifuged at 7,500*g* for 5 min at 4 °C. Finally, the supernatant was removed and air-dried before RNA was resuspended in RNase-free water and stored at −80 °C for future use. The isolated viral RNA was then analysed by one-step qPCR using RealTime Ready RNA Virus Master (Roche) to determine $\log_{10}$[$TCID_{50}$ equivalents ml^{-1}] with the NP-specific primers (forward, 5′-AAGAATCACTGACATGAGAACTG-3′; reverse, 5′-CCCTCGTCATTCCCATCCAAAGAA-3′) and probe (FAM/CAACTAACC/ZEN/CGATAGTGCCT/3IABkFQ).

Serology. Ferret serum samples were heat-inactivated at 56 °C for 30 min and analysed using a broad-reactive commercial ELISA for the presence of antibodies to NP using ID Screen Influenza A Nucleoprotein Indirect (IDVet) according to the manufacturer's instructions.

H18N11 neutralizing antibodies against H18 were determined by performing a virus neutralization assay. In brief, 50 µl of medium containing VSV*ΔG-H18 at a concentration of $10^{3.3}$ $TCID_{50}$ was mixed with the same volume of diluted serum. Each serum sample was prepared in triplicate in a 96-well plate and subsequently incubated for 2 h at 37 °C. Each sample was then transferred individually onto RIE1495 cells that were seeded and grown in 96-well format and maintained for 5 d at 37 °C with 5% CO_2. Virus growth was observed by IF.

Bat serum samples were collected from a wing vein. ELISA plates were coated overnight at 4 °C with 1 µg ml^{-1} recombinant H18N11 NP in PBS, blocked with SuperBlock T20 (Thermo Fisher Scientific). Serum was diluted 1:100 in PBS then diluted further ($\log_2$) for endpoint titration. Detection of antibodies was completed with protein-A/G-HRP (Thermo Fisher Scientific) and ABTS substrate (Thermo Fisher Scientific), and absorbance was read at 405 nm. The endpoint was determined as an optical density of 0.200 above the mean of the negative control serum samples.

Histopathology. Specimens of the following organs were sampled from four rP11-infected ferrets euthanized at 4 d.p.i. and fixed in 4% neutral buffered formaldehyde: oral cavity, palatine tonsils, pharyngeal tonsils, lateral retropharyngeal lymph node, trachea, left caudal lung lobe, right cranial and caudal lung lobe, medial bronchial lymph node, heart, spleen, liver, small and large intestines, kidneys, olfactory bulb, cerebrum, cerebellum and bone marrow. The skull was decalcified for 7 d and five standardized coronal sections of one-half of the nasal cavity were prepared (Supplementary Fig. 3b).

Specimens of the following organs were sampled from two WT H18N11-infected bats euthanized at 3 d.p.i. and 6 d.p.i.: oral cavity, palatine tonsils, pharyngeal tonsils, parotid gland, lungs, heart, stomach, small intestine, jejunal Peyer's patches, mesenteric lymph nodes, pancreas, spleen, liver, kidneys, adrenals, testis or uterus, olfactory bulb, cerebrum and bone marrow. At least one coronal section of the complete nasal cavity was prepared after decalcification of the skull for 2 d. Tissues were processed, embedded in paraffin wax and 2–4 µm sections were stained with haematoxylin and eosin. Specimens were evaluated for histopathological lesions using an Axio Imager M2 microscope (Carl Zeiss Microscopy). A semiquantitative severity score was applied for the assessment of inflammatory lesions in the respective organs, ranging from 0 to 3 where 0, no inflammatory lesions; 1, mild inflammatory lesions; 2, moderate inflammatory lesions; and 3, severe inflammatory lesions.

Immunohistochemistry. To visualize IAV matrix protein, immunohistochemistry was performed using the avidin-biotin-peroxidase-complex (ABC) method utilizing the Vectastain Elite ABC Kit Standard (Vector Laboratories) with citric buffer (10 mM, pH 6.0) pretreatment, a monoclonal mouse anti-matrix-protein immunoglobulin G1 containing hybridoma supernatant (ATCC; HB-64[33], 1:200) and 3-amino-9-ethyl-carbazol as a chromogen and haematoxylin counterstain. Archival formalin-fixed and paraffin-embedded tissues of four H7N9-infected ferrets and two uninfected ferrets served as positive and negative controls, respectively. Furthermore, the hybridoma supernatant was replaced by Tris-buffered saline on serial sections as another negative control.

In situ hybridization. In situ hybridization was performed to detect IAV (A/flat-faced bat/Peru/033/2010 (H18N11)) H18-specific RNA using the RNAscope 2.5 HD Reagent Kit-RED (ACDBio) together with the HybEZ II Hybridization System (ACDBio) with a 20ZZ probe (V-Bat-Influenza-H18) that targets base pairs 26–1132 of GenBank accession number CY125945.1; Fast Red was used as a chromogen and haematoxylin counterstain. The distribution of matrix protein and H18N11 H18-specific RNA was semiquantitatively assessed for each organ by scoring on a scale of 0 to 3 where 0, negative; 1, focal or oligofocal; 2, multifocal; and 3, coalescing to diffuse immunoreactive cells.

Representation of three-dimensional protein structures. The three-dimensional structure of the H18 homotrimer (PDB: 4MC5)[7] was obtained from the PDB (https://www.rcsb.org/) and was displayed using the PyMOL software (https://pymol.org/2/).

Reporting Summary. Further information on research design is available in the Nature Research Reporting Summary linked to this article.

Data availability

The data supporting the findings of this study are available within the paper and its Supplementary Information. Any further relevant data are available from the corresponding authors on reasonable request.

Received: 1 April 2019; Accepted: 7 August 2019;
Published online: 16 September 2019

References

1. Webster, R. G., Bean, W. J., Gorman, O. T., Chambers, T. M. & Kawaoka, Y. Evolution and ecology of influenza A viruses. *Microbiol. Rev.* **56**, 152–179 (1992).
2. Desselberger, U. et al. Biochemical evidence that "new" influenza virus strains in nature may arise by recombination (reassortment). *Proc. Natl Acad. Sci. USA* **75**, 3341–3345 (1978).
3. Garten, R. J. et al. Antigenic and genetic characteristics of swine-origin 2009 A(H1N1) influenza viruses circulating in humans. *Science* **325**, 197–201 (2009).
4. Herfst, S. et al. Airborne transmission of influenza A/H5N1 virus between ferrets. *Science* **336**, 1534–1541 (2012).

5. Imai, M. et al. Experimental adaptation of an influenza H5 HA confers respiratory droplet transmission to a reassortant H5 HA/H1N1 virus in ferrets. *Nature* **486**, 420–428 (2012).
6. Tong, S. et al. A distinct lineage of influenza A virus from bats. *Proc. Natl Acad. Sci. USA* **109**, 4269–4274 (2012).
7. Tong, S. et al. New world bats harbor diverse influenza A viruses. *PLoS Pathog.* **9**, e1003657 (2013).
8. Campos, A. C. A. et al. Bat influenza A(HL18NL11) virus in fruit bats, Brazil. *Emerg. Infect. Dis.* **25**, 333–337 (2019).
9. Sun, X. et al. Bat-derived influenza hemagglutinin H17 does not bind canonical avian or human receptors and most likely uses a unique entry mechanism. *Cell Rep.* **3**, 769–778 (2013).
10. Zhu, X. et al. Crystal structures of two subtype N10 neuraminidase-like proteins from bat influenza A viruses reveal a diverged putative active site. *Proc. Natl Acad. Sci. USA* **109**, 18903–18908 (2012).
11. Zhu, X. et al. Hemagglutinin homologue from H17N10 bat influenza virus exhibits divergent receptor-binding and pH-dependent fusion activities. *Proc. Natl Acad. Sci. USA* **110**, 1458–1463 (2013).
12. Li, Q. et al. Structural and functional characterization of neuraminidase-like molecule N10 derived from bat influenza A virus. *Proc. Natl Acad. Sci. USA* **109**, 18897–18902 (2012).
13. Moreira, E. A. et al. Synthetically derived bat influenza A-like viruses reveal a cell type- but not species-specific tropism. *Proc. Natl Acad. Sci. USA* **113**, 12797–12802 (2016).
14. Maruyama, J. et al. Characterization of the glycoproteins of bat-derived influenza viruses. *Virology* **488**, 43–50 (2016).
15. Karakus, U. et al. MHC class II proteins mediate cross-species entry of bat influenza viruses. *Nature* **567**, 109–112 (2019).
16. Maher, J. A. & DeStefano, J. The ferret: an animal model to study influenza virus. *Lab Anim.* **33**, 50–53 (2004).
17. Belser, J. A., Katz, J. M. & Tumpey, T. M. The ferret as a model organism to study influenza A virus infection. *Dis. Model Mech.* **4**, 575–579 (2011).
18. Moore, I. N. et al. Severity of clinical disease and pathology in ferrets experimentally infected with influenza viruses is influenced by inoculum volume. *J. Virol.* **88**, 13879–13891 (2014).
19. Brandtzaeg, P. Food allergy: separating the science from the mythology. *Nat. Rev. Gastroenterol. Hepatol.* **7**, 380–400 (2010).
20. Webster, R. G., Yakhno, M., Hinshaw, V. S., Bean, W. J. & Murti, K. G. Intestinal influenza: replication and characterization of influenza viruses in ducks. *Virology* **84**, 268–278 (1978).
21. Barclay, W. S. Receptor for bat influenza virus uncovers potential risk to humans. *Nature* **567**, 35–36 (2019).
22. Hughes, M. T., Matrosovich, M., Rodgers, M. E., McGregor, M. & Kawaoka, Y. Influenza A viruses lacking sialidase activity can undergo multiple cycles of replication in cell culture, eggs, or mice. *J. Virol.* **74**, 5206–5212 (2000).
23. Kalthoff, D. et al. Truncation and sequence shuffling of segment 6 generate replication-competent neuraminidase-negative influenza H5N1 viruses. *J. Virol.* **87**, 13556–13568 (2013).
24. Samson, M. et al. Characterization of drug-resistant influenza virus A(H1N1) and A(H3N2) variants selected in vitro with laninamivir. *Antimicrob. Agents Chemother.* **58**, 5220–5228 (2014).
25. Ann, J. et al. Impact of a large deletion in the neuraminidase protein identified in a laninamivir-selected influenza A/Brisbane/10/2007 (H3N2) variant on viral fitness in vitro and in ferrets. *Influenza Other Respir. Virus.* **10**, 122–126 (2016).
26. Juozapaitis, M. et al. An infectious bat-derived chimeric influenza virus harbouring the entry machinery of an influenza A virus. *Nat. Commun.* **5**, 4448 (2014).
27. Martin, M. Cutadapt removes adapter sequences from high-throughput sequencing reads. *EMBnet J.* **17**, 10 (2011).
28. Langmead, B. & Salzberg, S. L. Fast gapped-read alignment with Bowtie 2. *Nat. Methods* **9**, 357–359 (2012).
29. Li, H. et al. The Sequence Alignment/Map format and SAMtools. *Bioinformatics* **25**, 2078–2079 (2009).
30. Wilm, A. et al. LoFreq: a sequence-quality aware, ultra-sensitive variant caller for uncovering cell-population heterogeneity from high-throughput sequencing datasets. *Nucleic Acids Res.* **40**, 11189–11201 (2012).
31. Klupp, B. G., Granzow, H. & Mettenleiter, T. C. Primary envelopment of pseudorabies virus at the nuclear membrane requires the UL34 gene product. *J. Virol.* **74**, 10063–10073 (2000).
32. Grund, C. et al. A novel European H5N8 influenza a virus has increased virulence in ducks but low zoonotic potential. *Emerg. Microbes Infect.* **7**, 132 (2018).
33. Yewdell, J., Frank, E. & Gerhard, W. Expression of influenza A virus internal antigens on the surface of infected P815 cells. *J. Immunol.* **126**, 1814–1819 (1981).

Acknowledgements

We thank S. Schuparis and G. Czerwinski for histotechnological support and S. Giese and H. Bolte for reading the manuscript. This work was supported by grants from the DFG to M.S. (SCHW 632/17-2) and M.B. (BE 5187/4-2); the CRIP and the Saint Jude CEIRS, two NIAID-funded CEIRS to A.G.-S. (HHSN272201400008C) and W.M. (HHSN27220140006C), respectively; NIH NIAID grants to G.D.E. (AI067380), R.A.M. (AI134108), W.M. and T.S. (1R01AI134768); the CSU Vice President for Research, College of Veterinary Medicine and Biomedical Sciences, and Department of Microbiology, Immunology and Pathology to T.S.; and the China Scholarships Council (201506170046) to W.R. The funders had no role in study design, data collection and analysis, decision to publish or preparation of the manuscript.

Author contributions

K.C., M.S., M.B., W.M. and T.S. conceived and designed the experiments. K.C. and W.R. performed in vitro and mouse experiments. M.G. and D.H. performed ferret experiments. T.S., A.M., M.E., C.L.C., W.M., J.L. and J.M. performed bat experiments. J.S. and R.U. performed pathology, immunohistochemistry and in situ hybridization. A.P. and R.A.M. performed NGS. K.F. performed electron microscopy. K.C., M.B., T.S., A.G.-S., J.S., R.U., T.A.A., G.D.E., W.M. and M.S. analysed the data. K.C. and M.S. wrote the paper with input from all of the other authors.

Competing interests

The authors declare no competing interests.

Additional information

Supplementary information is available for this paper at https://doi.org/10.1038/s41564-019-0556-9.

Reprints and permissions information is available at www.nature.com/reprints.

Correspondence and requests for materials should be addressed to W.M., T.S., M.B. or M.S.

Publisher's note Springer Nature remains neutral with regard to jurisdictional claims in published maps and institutional affiliations.

nature research

Corresponding author(s): Martin Schwemmle & Martin Beer & Tony Schountz & Wenjun Ma

Last updated by author(s): Jun 19, 2019

Reporting Summary

Nature Research wishes to improve the reproducibility of the work that we publish. This form provides structure for consistency and transparency in reporting. For further information on Nature Research policies, see Authors & Referees and the Editorial Policy Checklist.

Statistics

For all statistical analyses, confirm that the following items are present in the figure legend, table legend, main text, or Methods section.

n/a	Confirmed
☐	☒ The exact sample size (*n*) for each experimental group/condition, given as a discrete number and unit of measurement
☐	☒ A statement on whether measurements were taken from distinct samples or whether the same sample was measured repeatedly
☐	☒ The statistical test(s) used AND whether they are one- or two-sided *Only common tests should be described solely by name; describe more complex techniques in the Methods section.*
☐	☒ A description of all covariates tested
☒	☐ A description of any assumptions or corrections, such as tests of normality and adjustment for multiple comparisons
☐	☒ A full description of the statistical parameters including central tendency (e.g. means) or other basic estimates (e.g. regression coefficient) AND variation (e.g. standard deviation) or associated estimates of uncertainty (e.g. confidence intervals)
☐	☒ For null hypothesis testing, the test statistic (e.g. *F*, *t*, *r*) with confidence intervals, effect sizes, degrees of freedom and *P* value noted *Give P values as exact values whenever suitable.*
☒	☐ For Bayesian analysis, information on the choice of priors and Markov chain Monte Carlo settings
☒	☐ For hierarchical and complex designs, identification of the appropriate level for tests and full reporting of outcomes
☒	☐ Estimates of effect sizes (e.g. Cohen's *d*, Pearson's *r*), indicating how they were calculated

Our web collection on statistics for biologists contains articles on many of the points above.

Software and code

Policy information about availability of computer code

Data collection	GraphPad Prism 7.03,Genome, Sequencer software suite 2.8, Geneious software suite 6.1.6, cutadapt, Bowtie2, SAMtools, LoFreq, AxioVision Rel 4.8, PyMOL 1.3
Data analysis	GraphPad Prism 7.03,Genome, Sequencer software suite 2.8, Geneious software suite 6.1.6, cutadapt, Bowtie2, SAMtools, LoFreq, AxioVision Rel 4.8, PyMOL 1.3

For manuscripts utilizing custom algorithms or software that are central to the research but not yet described in published literature, software must be made available to editors/reviewers. We strongly encourage code deposition in a community repository (e.g. GitHub). See the Nature Research guidelines for submitting code & software for further information.

Data

Policy information about availability of data

All manuscripts must include a data availability statement. This statement should provide the following information, where applicable:

- Accession codes, unique identifiers, or web links for publicly available datasets
- A list of figures that have associated raw data
- A description of any restrictions on data availability

The data that support the findings of this study are available from the corresponding author upon reasonable request.

Field-specific reporting

Please select the one below that is the best fit for your research. If you are not sure, read the appropriate sections before making your selection.

☒ Life sciences ☐ Behavioural & social sciences ☐ Ecological, evolutionary & environmental sciences

Life sciences study design

All studies must disclose on these points even when the disclosure is negative.

Sample size	No sample-size calculations were performed. Sample size was determined to be adequate based on the magnitude and consistency of measurable differences between groups.
Data exclusions	No data were excluded from the analysis.
Replication	For all major experiments at least three independent experiments were done and in all cases results could be reproduced. The number of repeats for each experiment is reported in the figure legends.
Randomization	Allocation of samples and/or mice/ferrets and bats to groups was random.
Blinding	Investigators were not blinded to group allocation in this study.

Reporting for specific materials, systems and methods

We require information from authors about some types of materials, experimental systems and methods used in many studies. Here, indicate whether each material, system or method listed is relevant to your study. If you are not sure if a list item applies to your research, read the appropriate section before selecting a response.

Materials & experimental systems

n/a	Involved in the study
☐	☒ Antibodies
☐	☒ Eukaryotic cell lines
☒	☐ Palaeontology
☐	☒ Animals and other organisms
☒	☐ Human research participants
☒	☐ Clinical data

Methods

n/a	Involved in the study
☒	☐ ChIP-seq
☒	☐ Flow cytometry
☒	☐ MRI-based neuroimaging

Antibodies

Antibodies used	-rabbit polyclonal anti-H18 serum (1:750) and mouse monoclonal anti-NP antibody (supernatant) were described previously (ref. 14) -mouse monoclonal anti IAV-matrix protein IgG1 (ATCC, clone M2-1C6-4R332, 1:200) -rabbit polyclonal anti-IAV-NP (ThermoFisher Scientific, catalog# PA5-32242, 1:400) -rabbit polyclonal anti-IAV-NP (GeneTex, catalog# GTX125989, 1:1000) -mouse monoclonal anti-actin (Sigma-Aldrich, catalog# A3853, 1:1000) -rabbit polyclonal anti-V5 (abcam, catalog# ab9116, 1:2500) -mouse monoclonal anti-HLA-DRa (Santa Cruz, catalog# sc-53499, 1:100) -AlexaFluor 488-labelled anti-mouse IgG (Jackson ImmunoResearch, catalog# 115-546-062, 1:500) -Cy3-labelled anti-rabbit IgG (Jackson ImmunoResearch, catalog# 111-165-003, 1:500) -FITC-labelled anti-rabbit IgG (ThermoFisher Scientific, catalog# 65-6111, 1:400) -Peroxidase-conjugated anti-mouse IgG (Jackson ImmunoResearch, catalog# 315-035-045, 1:5000) -Peroxidase-conjugated anti-rabbit IgG (Jackson ImmunoResearch, catalog# 111-035-045, 1:5000)
Validation	-rabbit polyclonal anti-H18 serum and mouse monoclonal anti-NP antibody were validated on H18N11-infected and mock-infected cells -mouse monoclonal anti IAV-matrix protein antibody was validated on tissue samples from H7N9-infected and mock-infected ferrets -rabbit polyclonal anti-IAV-NP purchased from ThermoFisher Scientific was validated on H18N11-infected and mock-infected cells; see also validation statement on the manufacturer's website (www.thermofisher.com) -rabbit polyclonal anti-IAV-NP purchased from GeneTex was validated on H18N11-infected and mock-infected cell lysates; see also validation statement on the manufacturer's website (www.genetex.com) -mouse monoclonal anti-actin was validated on whole-cell lysates -rabbit polyclonal anti-V5 was validated on cells infected with H18N11 viruses encoding the V5 epitope and mock-infected cells; see also validation statement on the manufacturer's website (www.abcam.com) -mouse monoclonal anti-HLA-DRa was validated on HLA-DR negative cells; see also validation statement in the manufacturer's website and provided datasheet (www.scbt.com) -AlexaFluor 488-labelled anti-mouse IgG was validated by omission of the primary antibody -Cy3-labelled anti-rabbit IgG was validated by omission of the primary antibody -FITC-labelled anti-rabbit IgG was validated by omission of the primary antibody

-Peroxidase-conjugated anti-mouse IgG was validated by omission of the primary antibody
-Peroxidase-conjugated anti-rabbit IgG was validated by omission of the primary antibody

Eukaryotic cell lines

Policy information about cell lines

Cell line source(s)	HEK293T cells were purchased from the American Type Culture Collection (ATCC). RIE1495 and MDCKII cells were obtained from Georg Herrler, University of Veterinary Medicine Hannover, Hannover, Germany and previously described (ref. 12). MDCK cells stably overexpressing human MHC-II (MDCK-MHC-II) and control cells (MDCK-ctrl) were generated and described previously (ref. 14).
Authentication	None of the cell lines used were authenticated.
Mycoplasma contamination	Cell lines used are routinely tested for mycoplasma contamination by sending representative samples for mycoplasma testing. None of the used cell lines ever tested positive for mycoplasma.
Commonly misidentified lines (See ICLAC register)	*Name any commonly misidentified cell lines used in the study and provide a rationale for their use.*

Animals and other organisms

Policy information about studies involving animals; ARRIVE guidelines recommended for reporting animal research

Laboratory animals	-6-8 weeks old B6 (29 females), B6-Ifnar1−/−Ifnlr1−/− mice (28 female) were infected intranasally with the indicated viruses. -3-9 months old ferrets (Mustela putorius furo, 22 female and 14 male) were infected intranasally with the indicated viruses. 1-6 years old old Jamaican fruit bats (Artibeus jamaicensis, 9 female and 17 male) were infected intranasally with the indicated viruses.
Wild animals	This study did not involve wild animals.
Field-collected samples	This study did not involve samples collected in the field.
Ethics oversight	-All mouse experiments were performed in accordance with the guidelines of the German animal protection law and were approved by the state of Baden-Württemberg (Regierungspräsidium Freiburg; reference number: 35-9185.81/G-17/14). -All ferret experiments were evaluated by the responsible ethics committee of the State Office of Agriculture, Food Safety, and Fishery in Mecklenburg-Western Pomerania, Germany (LALLF M-V), and gained governmental approval under registration number LVL MV TSD/7221.3-1.1-037/17. -All work with bats was approved by the Colorado State University (CSU) Institutional Animal Care and Use Committee, protocol 16-6502a.

Note that full information on the approval of the study protocol must also be provided in the manuscript.

nature microbiology

SUPPLEMENTARY INFORMATION

https://doi.org/10.1038/s41564-019-0556-9

In the format provided by the authors and unedited.

Bat influenza viruses transmit among bats but are poorly adapted to non-bat species

Kevin Ciminski[1,2], Wei Ran[1,2,11], Marco Gorka[3,11], Jinhwa Lee[4], Ashley Malmlov[5], Jan Schinköthe[6], Miles Eckley[5], Reyes A. Murrieta[5], Tawfik A. Aboellail[5], Corey L. Campbell[5], Gregory D. Ebel[5], Jingjiao Ma[4], Anne Pohlmann[3], Kati Franzke[7], Reiner Ulrich[6], Donata Hoffmann[3], Adolfo García-Sastre[8,9,10], Wenjun Ma[4]*, Tony Schountz[5]*, Martin Beer[3]* and Martin Schwemmle[1,2]*

[1]Institute of Virology, Medical Center University of Freiburg, Freiburg, Germany. [2]Faculty of Medicine, University of Freiburg, Freiburg, Germany. [3]Institute of Diagnostic Virology, Friedrich-Loeffler-Institut, Greifswald, Germany. [4]Department of Diagnostic Medicine/Pathobiology, College of Veterinary Medicine, Kansas State University, Manhattan, KS, USA. [5]Arthropod Borne and Infectious Diseases Laboratory, Department of Microbiology, Immunology and Pathology, College of Veterinary Medicine and Biomedical Sciences, Colorado State University, Fort Collins, CO, USA. [6]Department of Experimental Animal Facilities and Biorisk Management, Friedrich-Loeffler-Institut, Greifswald, Germany. [7]Institute of Infectology, Friedrich-Loeffler-Institut, Greifswald, Germany. [8]Global Health and Emerging Pathogens Institute, Icahn School of Medicine at Mount Sinai, New York, NY, USA. [9]Department of Microbiology, Icahn School of Medicine at Mount Sinai, New York, NY, USA. [10]Department of Medicine, Division of Infectious Diseases, Icahn School of Medicine at Mount Sinai, New York, NY, USA. [11]These authors contributed equally: Wei Ran, Marco Gorka. *e-mail: wma@vet.k-state.edu; Tony.Schountz@colostate.edu; Martin.Beer@fli.de; martin.schwemmle@uniklinik-freiburg.de

Bat influenza viruses transmit among bats but are poorly adapted to non-bat species

Supplementary Table 1. Sanger sequencing of deleted N11 vRNAs. N11 variants that emerged upon *in vitro* passaging and *in vivo* infection. nt, nucleotides; AA, amino acids.

Variant	Segment length	3' (nt)	5' (nt)	vRNA sequence deletion (%)	Protein length (AA)	Premature stop
1 (*in vitro*)	422	161	261	70.4	48	+
2 (*in vitro*)	305	101	204	78.6	30	+
3 (*in vitro*)	392	133	259	72.5	38	+
4 (*in vitro*)	546	163	383	61.7	52	+
5 (*in vitro*)	600	126	474	57.9	70	+
6 (*in vitro*)	497	128	369	64.2	37	+
7 (*in vivo*)	780	262	518	45.3	130	+
8 (*in vivo*)	546	163	383	61.7	52	+

Supplementary Table 2. Consensus H18N11 genome sequences. Results were obtained by NGS of recombinant and passaged H18N11 variants.

Virus	PB2	PB1	PA	HA	NP	NA	M	NS
wt H18N11	wt	wt	wt	wt	wt	wt	wt	wt
P11	wt	wt	wt	K170R N250S	wt	G107X	wt	wt
rP11	wt	wt	wt	K170R N250S	wt	G107X	wt	wt
rP11$_{\text{N11 G107X,T108X}}$	wt	wt	wt	K170R N250S	wt	G107X T108X	wt	wt

Supplementary Table 3. Results of IHC and ISH in ferret organs. Distribution of the matrix protein antigen and H18-specific RNA signals in the upper and lower respiratory tract of rP11 infected ferrets at 4 dpi as assessed by semiquantitative scoring (1 = focal/oligofocal; 2 = multifocal; 3 = coalescing/diffuse). *, respiratory epithelium; §, transitional epithelium; $, follicle-associated epithelium; #, submucosal; IHC, immunohistochemistry; ISH, in-situ hybridization; nd, not done.

Organ	#9		#10		#11		#12	
	IHC	ISH	IHC	ISH	IHC	ISH	IHC	ISH
Nasal cavity-I	0	0	1^{*}	$1^{*\S}$	1^{*}	1^{*}	0	0
Nasal cavity-II	0	$1^{*\S}$	0	$2^{*\S}$	1^{*}	$1^{*\S}$	0	1^{*}
Nasal cavity-III	0	0	0	1^{*}	0	1^{*}	0	1^{*}
Nasal cavity-IV	0	nd	0	0	0	0	0	0
Nasal cavity-V	0	0	0	0	0	0	0	0
Pharyngeal tonsils	$1^{\$}$	$2^{\$\#}$	0	$1^{\$}$	$1^{\$}$	$2^{\$\#}$	$1^{\$}$	$2^{*\#}$
Palatine tonsils	0	0	0	$1^{\$}$	0	$2^{\$\#}$	0	$1^{\$\#}$
Lateral retropharyngeal lymph node	0	0	0	0	0	0	0	0
Trachea	0	0	0	0	0	0	0	0
Lung, left caudal	0	0	0	0	0	0	0	0
Lung, right cranial	0	1	0	2	0	0	0	0
Lung, right caudal	0	2	0	2	0	0	0	0
Medial bronchial lymph node	0	1	0	1	0	1	0	0

Supplementary Table 4. Viral RT-qPCR titers in various ferret organs. Cq values obtained via RT-qPCR on organ samples harvested from rP11 infected index (#1-#12) and contact ferrets (#1-#4). Positive organs and the respective Cq values are indicated and highlighted in green. N/A, not applicable; nd, not done.

Organ \ Index ferret	#1	#2	#3	#4	#5	#6	#7	#8	#9	#10	#11	#12
Colon	N/A	N/A	N/A	N/A	N/A	N/A	N/A	N/A	N/A	N/A	N/A	N/A
Lung, left	N/A	N/A	N/A	N/A	N/A	N/A	N/A	N/A	32,52	30,19	N/A	N/A
Lung, right	N/A	N/A	N/A	N/A	N/A	N/A	N/A	N/A	N/A	N/A	N/A	N/A
Trachea	N/A	N/A	N/A	N/A	N/A	N/A	N/A	N/A	N/A	29,87	N/A	N/A
Nasal conchae	N/A	N/A	N/A	N/A	N/A	N/A	N/A	N/A	29,07	29,22	33,22	28,17
Cerebrum	N/A	N/A	N/A	N/A	N/A	N/A	N/A	N/A	34,38	35,57	N/A	36,87
Cerebellum	N/A	N/A	N/A	N/A	N/A	N/A	N/A	N/A	N/A	33,08	N/A	34,7
Olfactory bulb	N/A	N/A	N/A	N/A	N/A	N/A	N/A	N/A	N/A	N/A	N/A	35,44
Heart	N/A	N/A	N/A	N/A	N/A	N/A	N/A	N/A	N/A	N/A	N/A	N/A
Thigh muscle	N/A	N/A	N/A	N/A	N/A	N/A	N/A	N/A	N/A	N/A	N/A	N/A
Blood	nd	nd	nd	nd	nd	nd	nd	nd	N/A	N/A	N/A	N/A

Organ \ Contact ferret	#1	#2	#3	#4
Colon	N/A	N/A	N/A	N/A
Lung, left	N/A	N/A	N/A	N/A
Lung, right	N/A	N/A	N/A	N/A
Trachea	N/A	N/A	N/A	N/A
Nasal conchae	N/A	N/A	N/A	N/A
Cerebrum	N/A	N/A	N/A	N/A
Cerebellum	N/A	N/A	N/A	N/A
Olfactory bulb	N/A	N/A	N/A	N/A
Heart	N/A	N/A	N/A	N/A
Thigh muscle	N/A	N/A	N/A	N/A
Blood	nd	nd	nd	nd

Supplementary Table 5. Results of IHC and ISH in bat organs. Distribution of the matrix protein antigen and H18-specific RNA signals in wt H18N11-infected index bats at 3 and 6 dpi as assessed by semiquantitative scoring (1 = focal/oligofocal; 2 = multifocal; 3 = coalescing/diffuse). *, squamos epithelium; §, columnar epithelium (enterocytes); †, lamina propria; $, follicle-associated epithelium; #, submucosal; IHC, immunohistochemistry; ISH, in-situ hybridization; nd, not done.

Organ	3 dpi				6 dpi			
	#9		#10		#7		#8	
	IHC	ISH	IHC	ISH	IHC	ISH	IHC	ISH
Oral cavity	0	0	0	0	0	0	0	0
Pharyngeal tonsils	nd	nd	0	0	0	0	0	0
Palatine tonsils	nd	nd	0	0	1*	2*#	0	1*
Parotid gland	0	0	0	0	0	0	0	0
Stomach	nd	nd	0	0	0	0	0	0
Small intestine	0	1§	0	1§	1§†	2§†	1§†	1§†
Jejunal Peyer's patch	2$#	2$#	0	1$	2$#	2$#	2$#	2$#
Mesenteric lymph nodes	0	0	0	0	0	0	0	0
Pancreas	0	0	0	0	0	0	0	0
Liver	0	0	0	0	0	0	0	0

Supplementary Table 6. N11 sequence variants that emerged upon bat infection. Deep sequencing results for the genomic N11 vRNA sequence isolated from rectal swabs of the rP11 bat infection experiment shown in Fig. 6f-h. N/A, not applicable.

Group	Bat	$N11_{E68K}$	$N11_{G107X}$
Index	#1	12,9%	86,9%
	#2	92,1%	7,8%
	#3	46,1%	53,8%
Contact 1a	#1	99,2%	N/A
	#2	99,9%	N/A
	#3	98,4%	1,5%
Contact 2	#1	99,8%	N/A
	#2	99,9%	N/A
Contact 1b	#1	99,9%	N/A
	#2	99,9%	N/A

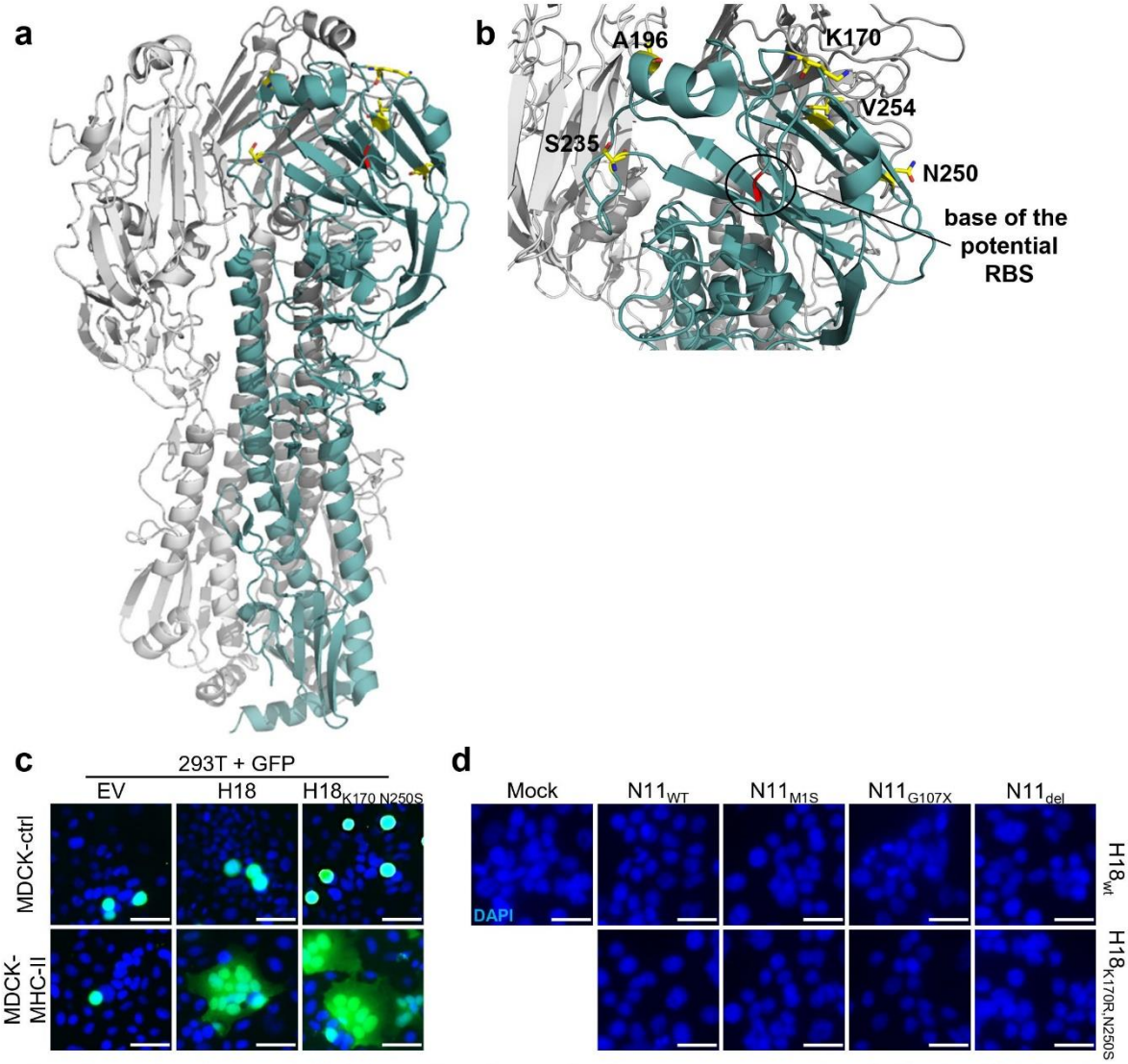

Supplementary Figure 1. Mutations found upon *in vitro* passaging are located in the H18 head domain. a, Cartoon representing the overall structure of the H18 homotrimeric complex. One monomer was colored in cyan for better visibility. Amino acid positions that were found to be substituted upon serial *in vitro* passaging are indicated as sticks colored in yellow. The base of the putative receptor-binding site (RBS) is shown in red. **b,** Magnified depiction of the head domain. Amino acid side chains that were found to mutate are highlighted in yellow. The trimeric H18 complex was created with PyMol based on the available crystal structure (PDB code: 4MC5). **c,** HEK293T cells were co-transfected with pCAGGS expression plasmids coding for GFP and either $H18_{wt}$ or $H18_{K170R,N250S}$. Transfected HEK293T cells were co-seeded with MDCK-MHC-II or MDCK-ctrl and polykaryon formation was examined after trypsin treatment and subsequent exposure of cells to low pH. Representative images of *n*=3 experiments are shown. Cell nuclei were stained by DAPI (blue). Scale bar=20 µm. **d,** MDCK-ctrl cells were infected with rescue supernatant from different H18N11 variants coding for $H18_{wt}$ or $H18_{K170R,N250S}$ together with $N11_{wt}$, $N11_{M1S}$, $N11_{G107X}$ or $N11_{del}$ for 48 h. After infection cells were fixed and H18 antigen was visualized by IF. Representative images of *n*=3 experiments are shown. Scale bar=50 µm.

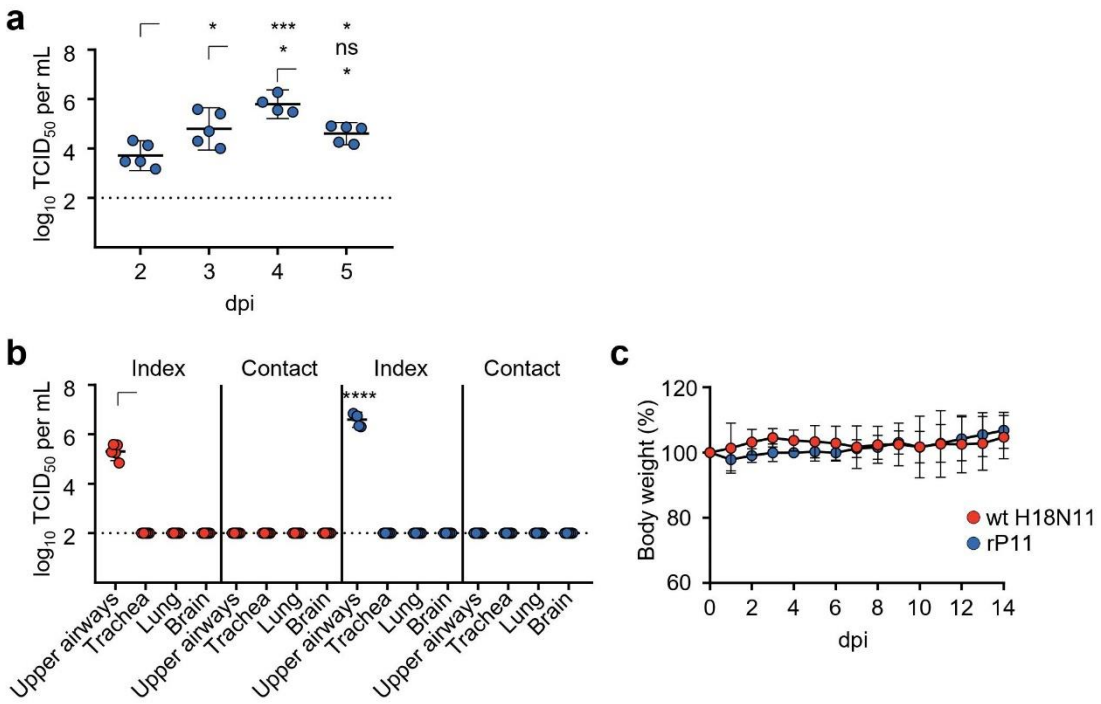

Supplementary Figure 2. H18N11 replicates exclusively in the URT of infected mice without causing weight loss. a, To determine the peaking day of viral replication in the URT of infected mice, four groups of B6 mice, each *n*=5, were intranasally inoculated with rP11 ($1x10^5$ $TCID_{50}$ in 40 µL). At the indicated time points, organs of the URT were harvested and viral titers were determined by endpoint titration on MDCKII cells. Dashed line indicates the detection limit. Data are mean ± 95% confidence interval, statistical significance is indicated; two-tailed *t*-test. **P*=0.04; ****P*=0.001. **b,** Groups of B6-Ifnar1$^{-/-}$Ifnlr1$^{-/-}$ mice (*n*=5) were infected with either wt H18N11 or rP11 intranasally ($1x10^5$ $TCID_{50}$ in 40 µL). At 1 dpi each infected index mouse was separated and co-housed with a naïve contact B6-Ifnar1$^{-/-}$Ifnlr1$^{-/-}$ mouse to determine contact-dependent horizontal transmission. At 4 dpi viral organ titers of the indicated organs were measured by endpoint titration on MDCKII cells. Dashed line indicates the detection limit. Data are mean ± 95% confidence interval, statistical significance is indicated; two-tailed *t*-test. *****P*=0.0001. **c,** Groups of B6-Ifnar1$^{-/-}$Ifnlr1$^{-/-}$ mice each *n*=4 were infected with either wt H18N11 or rP11 ($1x10^5$ $TCID_{50}$ in 40 µL) to monitor changes in body weight for 14 days.

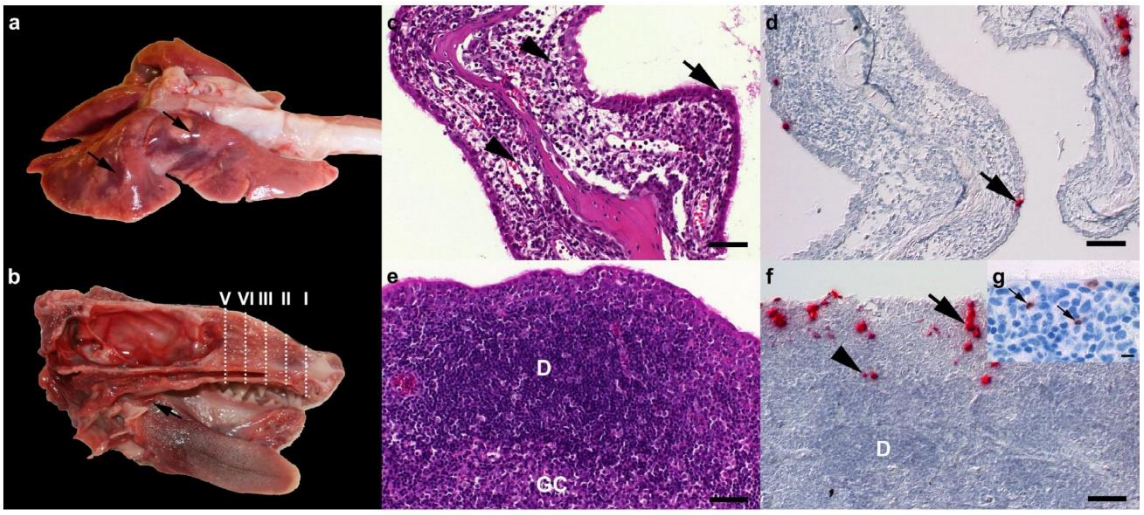

Supplementary Figure 3. Following infection of ferrets with rP11 viral RNA and antigen is detected in the nasal cavity and pharyngeal tonsils. a, Ferret, lung. Moderate, multifocal to coalescing atelectasis (arrows) of the right medial and caudal lobe in ferret #10 at 4 dpi with rP11 (*n*=1). **b,** Ferret, nasal cavity. Depicted is a longitudinal sectioned ferret head with the macroscopically normal appearing palatine tonsils (arrow) and the section planes (white dotted lines I-V) of the nasal coronal sections (*n*=1). **c, d, e, f, g,** Histological findings with detection of viral antigen and RNA in tissues of wt H18N11 infected index ferrets (*n*=4). **c,** Ferret, maxilloturbinalia at nasal coronal section II. Moderate, subacute, focally extensive, suppurative rhinitis with edema, neutrophils (arrowheads) and epithelial flattening (arrow) with loss of cilia and epithelial sloughing. **d,** Ferret, maxilloturbinalia at nasal coronal section II. Multifocal H18-specific RNA positive signals in the respiratory and transitional epithelium (arrow). **e,** Ferret, pharyngeal tonsils. Activated mucosa-associated lymphoid tissue with a prominent follicular dome region (D) adjacent to a germinal center (GC). **f,** Ferret, pharyngeal tonsils. Multifocal H18-specific RNA positive signals predominantly in the follicle-associated epithelium of the respiratory type (arrow) and scattered round cells (arrowhead) in the submucosa near a follicular dome region (D). **g,** Ferret, pharyngeal tonsils. Faintly intracytoplasmic and intranuclear matrix protein immunoreactive cells within the follicle-associated epithelium (arrows). Scale bars, c, d, e, f=50 µm; g=10 µm.

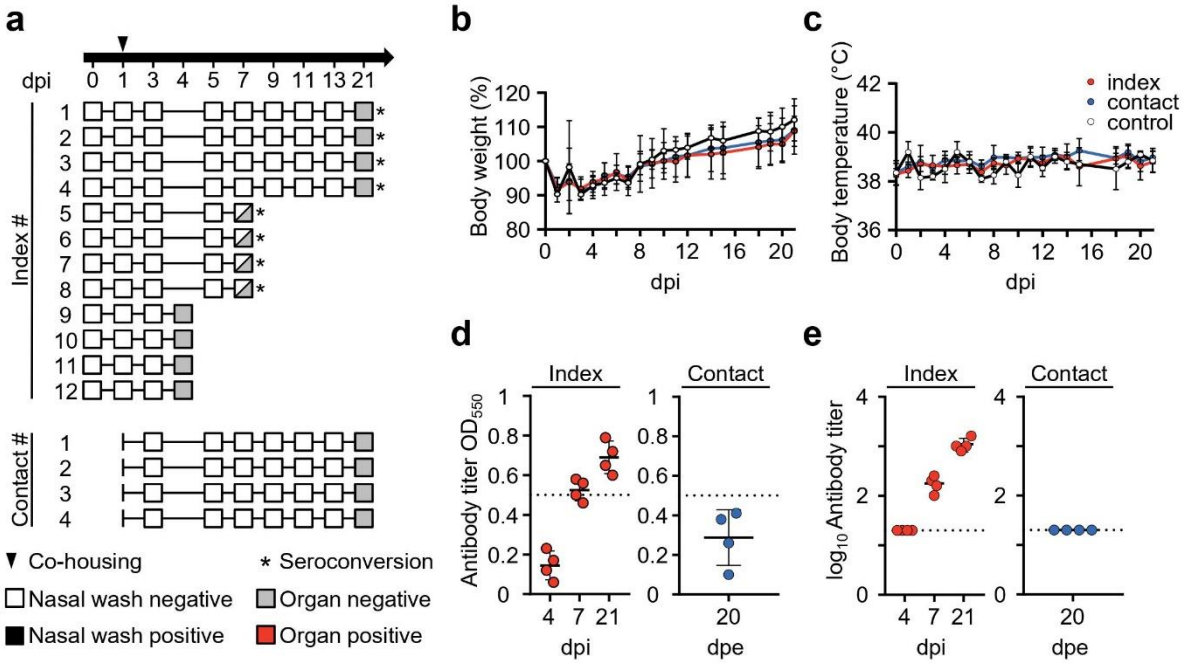

Supplementary Figure 4. wt H18N11 infections in ferrets proceed asymptomatically but induce seroconversion. a, A group of twelve ferrets (#1-#12) was initially infected intranasally with wt H18N11 (10^6 $TCID_{50}$ in 100 µL). At 1 dpi four naïve contact animals (#1-#4) were co-housed to determine viral transmission for further 20 days. White squares indicate absence, black squares presence of viral RNA in nasal washes. Grey squares show absence, red squares presence of H18N11 RNA in at least one organ. Asterisks indicate seroconversion. Two control ferrets were kept separately. Throughout the course of the experiment changes in **b,** body weight and **c,** body temperature of wt H18N11-infected (*n*=12), contact (*n*=4) and control ferrets (*n*=2) were monitored. Data are mean ± SD. **d,** NP-specific antibody titers and **e,** serum neutralizing antibodies to H18 of index (*n*=12) and contact ferrets (*n*=4) were determined. Dashed lines indicate cut-off points. Data are mean ± SD.

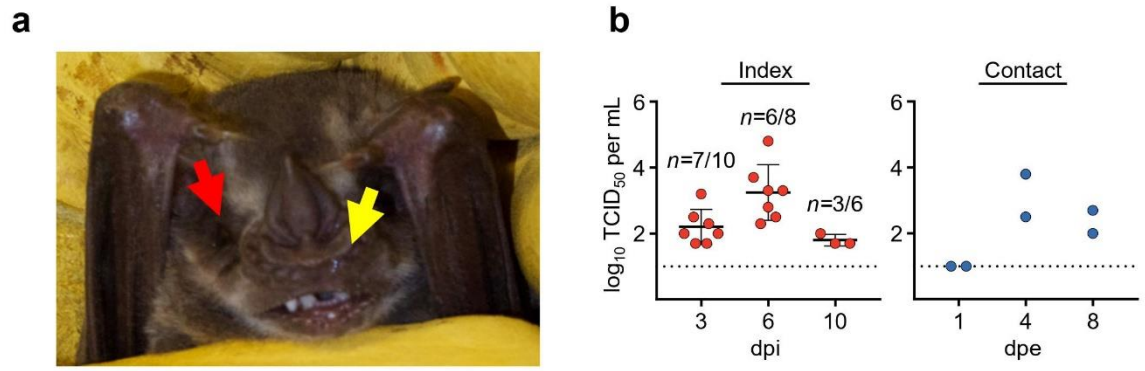

Supplementary Figure 5. Following infection of Neotropical Jamaican fruit bats with wt H18N11 animals develop mild signs of disease and shed infectious virus. a, Signs of disease are characterized by nasal (yellow arrow) and ocular (red arrow) discharge in contact bats (*n*=2) after infection with wt H18N11. These observed clinical signs started in both contact bats at 4 dpe and lasted until 8 dpe. **b,** Rectal swabs containing shed infectious H18N11 virus taken from *n*=10 index (left side) and *n*=2 contact bats (right side) at the indicated time points were titrated by endpoint titration on MDCKII cells. Dashed line indicates the detection limit. Data are mean ± SD.

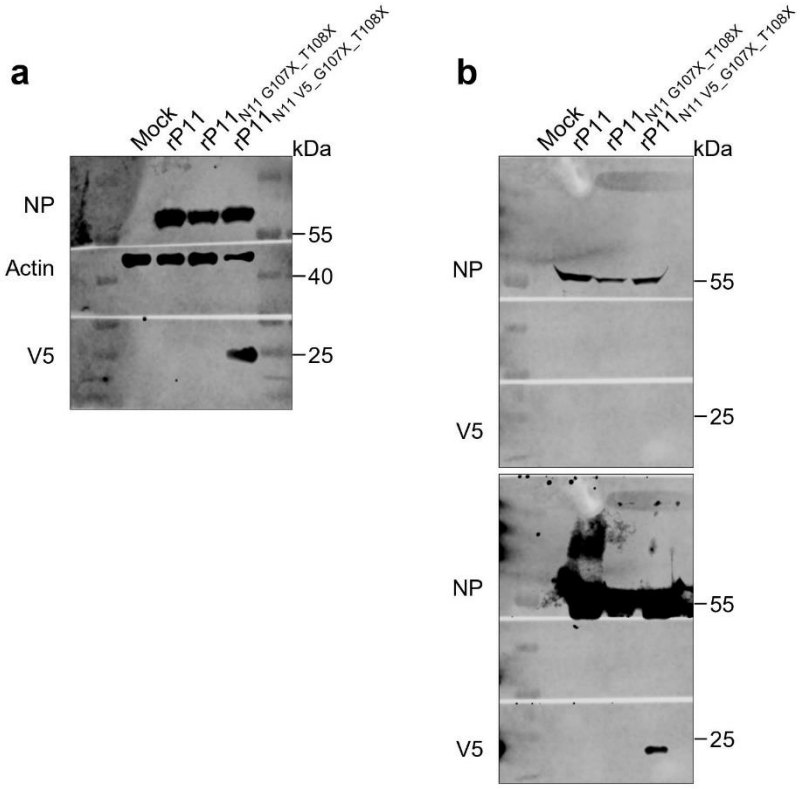

Supplementary Figure 6. Uncropped scans. a, Uncropped scans of Figure 2c upper panel. The membrane was cut and incubated with antibodies against NP, actin and V5 (*n*=1). **b,** Uncropped scans of Figure 2c lower panel. The membrane was cut and incubated with antibodies against NP and V5 (*n*=1). Scan with increased exposure time is shown in the lower panel.

Publication II

IV.2 Characterization of Experimental Oro-Nasal Inoculation of Seba's Short-Tailed Bats (Carollia perspicillata) with Bat Influenza A Virus H18N11

Marco Gorka , Jan Schinköthe, Reiner Ulrich, Kevin Ciminski, Martin Schwemmle , Martin Beer and Donata Hoffmann

Viruses 2020

doi: 10.3390/v12020232

PMID: 32093076

viruses

MDPI

Article

Characterization of Experimental Oro-Nasal Inoculation of Seba's Short-Tailed Bats (*Carollia perspicillata*) with Bat Influenza A Virus H18N11

Marco Gorka [1], Jan Schinköthe [2,3], Reiner Ulrich [2,3], Kevin Ciminski [4,5], Martin Schwemmle [4,5], Martin Beer [1,*] and Donata Hoffmann [1,*]

1 Institute of Diagnostic Virology, Friedrich-Loeffler-Institut, 17493 Greifswald, Insel Riems, Germany; marco.gorka@fli.de
2 Department of Experimental Animal Facilities and Biorisk Management, Friedrich-Loeffler-Institut, 17493 Greifswald, Insel Riems, Germany; Jan.Schinkoethe@vetmed.uni-leipzig.de (J.S.); reiner.ulrich@vetmed.uni-leipzig.de (R.U.)
3 Institute of Veterinary Pathology, Faculty of Veterinary Medicine, Leipzig University, 04109 Leipzig, Germany
4 Institute of Virology, Medical Center, University of Freiburg, 79104 Freiburg, Germany; kevin.ciminski@uniklinik-freiburg.de (K.C.); martin.schwemmle@uniklinik-freiburg.de (M.S.)
5 Faculty of Medicine, University of Freiburg, 79104 Freiburg, Germany
* Correspondence: martin.beer@fli.de (M.B.); donata.hoffmann@fli.de (D.H.)

Received: 4 December 2019; Accepted: 17 February 2020; Published: 19 February 2020

Abstract: In 2012 and 2013, the genomic sequences of two novel influenza A virus (IAV) subtypes, designated H17N10 and H18N11, were identified via next-generation sequencing in the feces of the little yellow-shouldered fruit bat (*Sturnira lilium*) and the flat-faced fruit-eating bat (*Artibeus planirostris*), respectively. The pathogenesis caused by these viruses in their respective host species is currently insufficiently understood, which is primarily due to the inability to obtain and keep these bat species under appropriate environmental and biosafety conditions. Seba's short-tailed bats (*Carollia perspicillata*), in contrast, are close relatives and a natural H18N11 reservoir species, with the advantage of established animal husbandry conditions in academic research. To study viral pathogenesis in more detail, we here oro-nasally inoculated Seba's short-tailed bats with the bat IAV H18N11 subtype. Following inoculation, bats appeared clinically healthy, but the histologic examination of tissues revealed a mild necrotizing rhinitis. Consistently, IAV-matrix protein and H18-RNA positive cells were seen in lesioned respiratory and olfactory nasal epithelia, as well as in intestinal tissues. A RT-qPCR analysis confirmed viral replication in the conchae and intestines as well as the presence of viral RNA in the excreted feces, without horizontal transmission to naïve contact animals. Moreover, all inoculated animals seroconverted with low titers of neutralizing antibodies.

Keywords: bats; virus; bat Influenza A viruses; host species; experimental infection; pathogenesis; transmission

1. Introduction

Influenza A viruses (IAVs) originate from aquatic waterfowl and are important animal pathogens and zoonotic agents, circulating in a broad range of avian and mammalian species [1]. Although spill-over infections from animals to humans are possible, these events are exceedingly rare [2–5]. Bats (order *Chiroptera*) are well known as an important reservoir for various zoonotic pathogens like lyssa-, henipa- or filoviruses; however, until recently they were not considered to harbor IAVs [6,7]. This view changed in 2012 and 2013, when two novel IAVs genomes were identified by next-generation

sequencing in the feces of the little yellow-shouldered fruit bat (*Sturnira lilium*) from Guatemala and the flat-faced fruit-eating bat (*Artibeus planirostris*) from Peru, subsequently designated as H17N10 and H18N11 [8,9]. These bat-derived IAVs exhibited unprecedented characteristics, since both subtypes express hemagglutinin (HA) and neuraminidase (NA) proteins unable to bind sialic acids residues [10–15]. Instead, recent research by Karakus et al. showed that the bat influenza HA proteins H17 and H18 mediate cell entry by utilizing major-histocompatibility-complex class II (MHC-II) molecules [16]. In contrast, the function of the bat IAV NA proteins N10 and N11 remain elusive [11,13,17]. Furthermore, the tropism of H18N11 and the pathogenesis in its natural reservoir is insufficiently understood, as there is currently only one study available focusing on the Neotropical Jamaican fruit bat (*Artibeus jamaicensis*). In this study, viral replication was found to occur in the gastrointestinal tract of infected Jamaican fruit bats, followed by the shedding of wildtype H18N11 via their feces [18]. Intriguingly, seroepidemiological screenings revealed a prevalence of H18-specific antibodies in various Central and South American bat species, including Seba's short-tailed bats (*Carollia perspicillata*) [9]. However, as viral RNA could not be isolated from any Seba's short-tailed bat sample, the relevance of this bat species within the H18N11 ecology remains unknown. We here studied the H18N11-induced pathogenesis in Seba's short-tailed bats, a well established bat infection model [19–21].

2. Materials and Methods

2.1. Ethics Statement

The animal experiments described here were approved by the State Office for Agriculture, Food Safety, and Fishery of Mecklenburg-Western Pomerania under registration number LVL MV TSD/7221.3-1-021/18.

2.2. Virus

Animals were inoculated using recombinant H18N11 virus generated as described [18]. In brief, the eight plasmid pHW2000-based rescue system was used to generate infectious A/flat-faced bat/Peru/033/2010 (H18N11) which could be further passaged on cell culture. In detail, the recombinant bat influenza A virus H18N11 was generated by transfecting HEK293T cells (American Type Culture Collection ATCC, Manassas, VA, USA) seeded in 6-well plates with the eight pHW2000-based rescue plasmids (300 ng of each plasmid per 6-well). Forty-eight hours post transfection, the cell supernatant was collected and concentrated by ultracentrifugation through a sucrose gradient (25000 rpm, 2 h, 8 °C). Stocks were generated by infecting canine RIE1495 cells (canine epithelial cell line, stored in the "Collection of Cell Lines in Veterinary Medicine" (CCLV) at the Friedrich-Loeffler Institute in Greifswald-Insel Riems, Germany with the code CCLV-RIE 1495) at an MOI of 0.1 with concentrated HEK293T rescue supernatant for 48 h. The viral titers were determined by immunofluorescence assay, using H18-specific antibodies.

2.3. Bat Experiment and Sampling

All experiments were conducted following internal standard guidelines under biosafety level 3 conditions at the Friedrich-Loeffler-Institut. Fourteen healthy and influenza-antibody-negative (see serology section below) Seba's short-tailed bats (*Carollia perspicillata*) were enrolled in this study (Figure 1A). These individuals were divided into group A ($n = 4$), B ($n = 8$) and C ($n = 2$). Inoculation of inhalatively anesthetized (5% isoflurane) bats was performed by the oro-nasal route with $10^{5.5}$ tissue culture infectious dose ($TCID_{50}$) of H18N11 in 50 µl in two individuals of group A, and three individuals in group B. The sentinel bats of both groups were housed together with the inoculated ones 24 h after infection, in order to assess virus spread. Clinical signs (nasal discharge, reduced activity, neurological symptoms, dyspnoe), room temperature and relative humidity were monitored daily, as well as collection of pooled fecal samples. All animals in group A were sacrificed at 4 dpi and animals in group

B were sacrificed at 21 dpi, followed by necropsy. Samples from the conchae, trachea, lung (left caudal lung lobe, right cranial lung lobe), heart, kidney, liver, intestine, olfactory bulb, cerebrum, cerebellum and thigh muscles were collected and stored at −80 °C until further processing for virological assays. Blood samples for serology were collected during the terminal bleeding procedure.

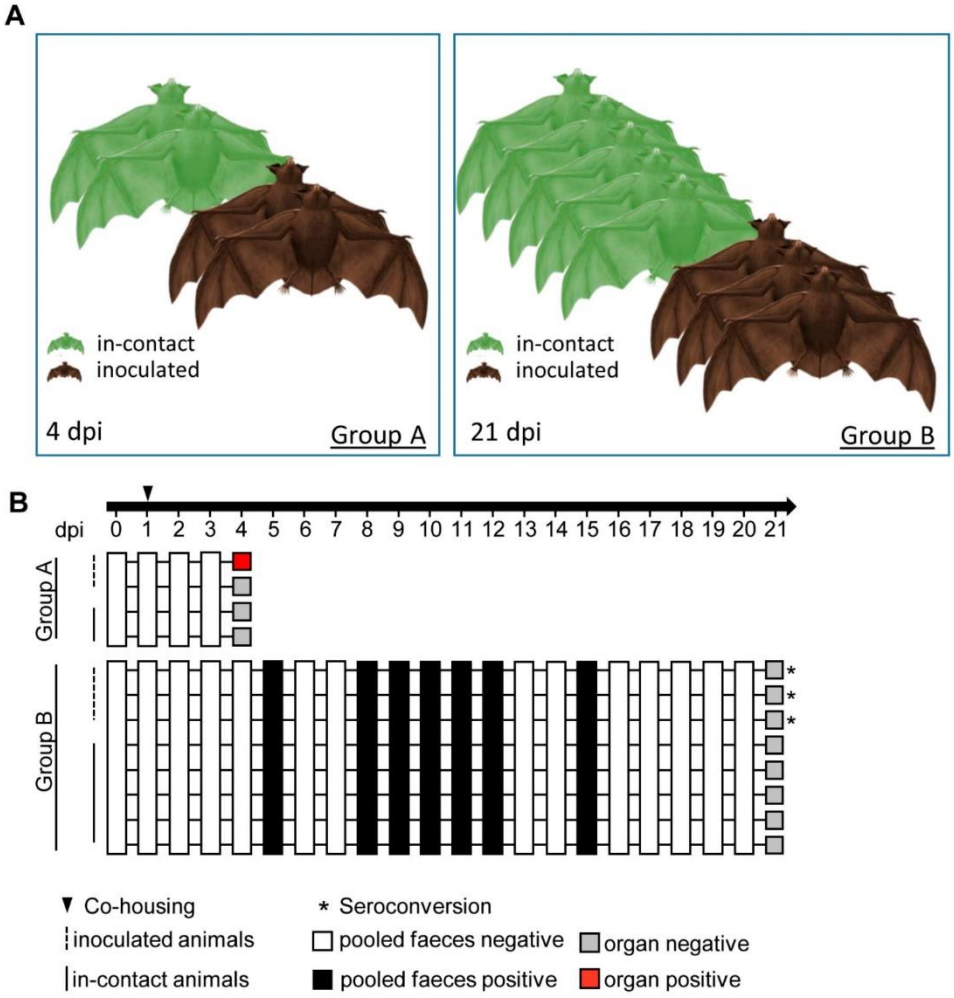

Figure 1. Experimental design. (**A**) Group A consisted of two inoculated bats in direct contact to naïve bats co-housed in one cage. At 4 dpi, the animals were euthanized and the organ material analyzed. Group B involved three inoculated bats co-housed with five naïve animals until 21 dpi. Group C (not presented) included two Seba's short-tailed bats for negative tissue control. (**B**) Index bats were inoculated with $10^{5.5}$ $TCID_{50}$ of H18N11 oronasally. Pooled feces samples were taken at the indicated time points. White squares indicate absence, black squares the presence of viral RNA in feces samples. Grey squares show absence, the red squares presence of H18N11 RNA in at least one organ. Asterisks indicate seroconversion.

2.4. Organ Homogenization

To start with, 2 mL collection tubes were filled with a stainless steel bead (diameter 5 mm, TIS Wälzkörpertechnologie GmbH, Gauting, Germany) and 1 mL of DMEM supplemented with 10%

fetal bovine serum (FBS) and antibiotics (1% penicillin-streptomycin [PenStrep], Biochrom GmbH, Berlin Germany). Homogenization was performed via TissueLyser II (Qiagen, Hilden, Germany) for 2 min. The supernatants, for RNA extractions, were acquired by centrifuging at 13,000 rpm for 2 min.

2.5. RNA Isolation

Organ Samples: Viral RNA extraction was achieved through solubilization of 250 µL of the supernatant of organ homogenates with 750 µl TRIzol LS Reagent (Life Technologies, Carlsbad, CA, USA). After the addition of 200 µL ROTIPURAN (Carl Roth, Karlsruhe, Germany), phase separation was attained. The following steps were completed with the NucleoMag Vet kit (Macherey-Nagel, Düren, Germany) according to the manufacturer's instructions on a Biosprint 96 platform (Qiagen).

Fecal samples: Viral RNA extraction of pooled fecal samples (group A pool and goup B pool) was achieved with the MasterPure™ Complete DNA and RNA Purification Kit (Lucigen, Middleton, WI, USA) according to the manufacturer's instructions, after a dilution of the samples by the factor 1:1000 in PBS.

2.6. RT-qPCR

The real-time RT-PCRs (RT-qPCR) of all organ and fecal samples were performed as described before [22]. In brief, a generic PB1 assay was used to determine the quantification cycle (Cq) using the one-step RT-qPCR Kit qScript™ XLT One-Step RT-qPCR ToughMix® (Quantabio, Beverly, MA USA). The RT-qPCR assay was optimized for using a total volume of 12.5 µl. The reaction was run on a bio-rad cycler Cfx96 machine (Bio-Rad Laboratories, Inc. Hercules, CA, USA). Individual amplification controls on the basis of artificial spiked RNA (fecal samples, [23]) or beta actin (organ samples modified [24]) were used to evaluate inhibitory effects.

2.7. Virus Isolation

Virus isolation attempts were performed using RIE1495 cells and homogenized organ samples, which scored positive for viral RNA. Briefly, 50µL supernatant from the homogenized organ was applied onto 12.5 cm^2 cell culture flask (Corning, Corning, NY, USA). Afterwards four blind passages of potential infected cells were done, followed by a RT-qPCR based analysis.

2.8. Serology

Serum samples from all animals were heat inactivated at 56°C for 30 min and analyzed using an indirect immunofluorescence test and a virus neutralization assay. After fixation of RIE1495 cells and RIE1495 cells infected with A/flat-faced bat/Peru/033/2010 (H18N11) using aceton methanol (1:1 vol%), the cells were incubated for one hour with the bat sera. After three washing steps using PBS, goat anti-bat IgG (H+L) secondary antibody (Novus Biologicals, Littleton, CO, USA) was applied for one hour at room temperature. After an additional three washing steps with PBS, chicken anti-goat Alexa 488 (ThermoFisher scientific, Waltham, MA, USA) was added and incubated for one hour at room temperature.

Briefly, the neutralization assay was performed with 50 µl of medium containing VSV*ΔG-H18 [25] at a concentration of $10^{3.3}$ $TCID_{50}$ that was mixed with the same volume of diluted serum. Each serum was prepared in triplicate in a 96-well plate. After incubation of 2 h at 37 °C the dilution was transferred on 100 µL medium and 24 h grown in RIE 1495 cells. The viral replication was assessed after an incubation of 5 days (37 °C, 5% CO_2) via visualization of GFP expression. Validation was achieved by titration of the virus dilutions.

2.9. Necropsy and Histologic Examination

A complete necropsy with macroscopic evaluation of tissues was done for all animals of this study. Histopathologic, immunohistologic and in situ hybridization workup was performed for

all animals necropsied at 4 dpi (group A) and two non-inocluated bats (group C). A specimen of parenchymal organs and the skull were fixed in 4% neutral buffered formaldehyde. The skulls were decalcified (Formical 2000, Quartett Immundiagnostika und Biotechnologie Vertriebs GmbH, Berlin, Germany) and the following organs were processed to formalin fixed, paraffin embedded (FFPE) tissue blocks: four standardized coronal nasal sections with minimal adjustment to size ratios of *Carollia perspicillata* skulls as described elsewhere [16,18], the middle and inner ear, parotis, eye, oral cavity, esophagus, trachea, thyroidea, left caudal lung lobe, right cranial lung lobe, heart, liver, pancreas, stomach, small intestine with jejunal Peyer's patches, mesenteric lymph nodes, kidney, adrenal glands, bulbus olfactorius, cerebrum, cerebellum and bone marrow. Two to four micron-thick sections were cut and stained with hematoxylin and eosin. All specimens were evaluated for histopathologic lesions using an Axio Imager M2 microscope equipped with 10×, 20×, and 40× Plan Neofluar objectives and an AxioCam ICc3 3.3-megapixel digital camera (Carl Zeiss Microscopy GmbH, Jena, Germany).

2.10. Immunohistochemistry

To visualize IAV-matrix protein, immunohistochemistry (IHC) was performed using the avidin-biotin-peroxidase-complex (ABC) method (Vectastain® Elite ABC Kit Standard, Vector Laboratories, Burlingame, CA, USA) with citric buffer (10 mM, pH 6,0) pre-treatment, a monoclonal mouse anti-IAV-matrix protein immunoglobulin G1 containing hybridoma supernatant (dilution 1:10, clone M2-1C6-4R3 [26]), with 3-amino-9-ethyl-carbazol as chromogen and hematoxylin counterstain. Archival formalin-fixed and paraffin embedded (FFPE) tissues of one H18N11-infected Jamaican fruit bat [18], as well as H18N11-infected and mock-inoculated RIE1495 cell pellets served as positive and negative controls, respectively. Furthermore, the primary antibody was replaced by Tris-buffered saline on a following section as a second negative control for each evaluated tissue section.

2.11. In Situ Hybridization

In situ hybridization (ISH) was performed for the detection of IAV (A/flat-faced bat/Peru/033/2010 (H18N11)) H18-specific RNA using a RNAscope® 2.5 assay (ACDbio, Newark, CA, USA) with target retrieval and protease pretreatment, RNAscope® 2.5 HD Reagent Kit—RED, the HybEZ™ hybridization system with a 20ZZ probe named V-Bat-Influenza-HA targeting base pairs 26-1132 of gene bank accession number CY125945.1 and Fast Red as chromogen and hematoxylin counterstain, as described previously [16,18].

3. Results

A recent study reported that H18N11 replicates especially in the lamina propria of the small intestine and the follicle-associated epithelium of the jejunal Peyer's patches of infected Jamaican fruit bats [18]. Although these acutely infected animals shed high viral loads via the rectal route, no inflammatory lesions were observed. To determine tissue tropism and pathogenesis in the related Seba's short-tailed bats (*Carollia perspicillata*) at different time points after infection, animals were split into three groups: Group A consisted of four bats sacrificed at 4 dpi, from which two were initially inoculated and two others that remained naïve in order to monitor viral transmission (Figure 1A). Group B comprised three inoculated bats and five co-housed naïve contact animals that were sacrificed at 21 dpi. Two naïve bats were kept as controls in group C.

Following oro-nasal inoculation of the group A bats, none of the inoculated index or naïve contact animals exhibited clinical signs of disease and viral RNA was not present in the feces (Figure 1B). One of two H18N11-inoculated group A individuals was found viral RNA-positive in the nasal conchae (quantification cycle value (Cq) 33.62) and in the colon (Cq 34.72) (Table 1), whereas all other tested organ samples were PCR-negative. However, despite detection of viral RNA in some tissue samples, all attempts to isolate the infectious virus from these organs failed.

Table 1. Distribution of viral RNA and matrix protein antigen signals in H18N11-infected bats at 4 dpi.

Animal No.	**1**			**2**		
Method	**PCR**	**ISH**	**IHC**	**PCR**	**ISH**	**IHC**
Conchae	**33.6**	**1** [#]	**1**	-	0	0
Trachea	-	0	0	-	0	0
Lung	-	2	2	-	0	0
Heart	-	0	0	-	0	0
Kidney	-	0	0	-	0	0
Liver	-	0	0	-	0	0
Intestine	**34.7** [†]	**2** [*]	**2** [*]	-	**2** [*]	**1** [*]
Olfactory bulb	-	0	0	-	0	0
Cerebrum	-	0	0	-	0	0
Cerebellum	-	0	0	-	0	0
Muscle	-	nd	nd	-	nd	nd

PCR, quantitative real-time polymerase chain reaction; ISH, in situ hybridization; IHC, immunohistochemistry; -, no Cq; nd, not done; [#] semiquantitative scoring (1 = focal/oligofocal; 2 = multifocal; 3 = coalescing/diffuse); [*] in jejunal Peyer's patches, score 1 in jejunum, [†] in colon.

No gross lesions were observed in infected and naïve contact bats at 4 dpi, however, histopathologic examination revealed a mild, oligofocal, acute, necrotizing rhinitis in the rostral and caudal coronal sections of the nasal cavity, characterized by erosive alterations of the respiratory epithelium with pyknotic and karyorrhectic cells in the PCR-positive index bat (Figure 2A). Correspondingly, oligofocal H18-specific RNA in luminal debris (Figure 2B) and oligofocal strong IAV-matrix protein positive cells were seen (Figure 2C, Table 1). Erosive alterations were also present in the olfactory epithelium with mild infiltration of neutrophils in the lamina propria (Figure 2D). Oligofocal H18-specific RNA (Figure 2E) and oligofocal strong IAV-matrix protein positive reactions (Figure 2F) were mainly seen in cells interpreted as sustentacular cells. In the lower respiratory tract, multifocal H18-specific RNA signals and IAV-matrix protein immunoreactive cells were seen in clusters and in single cells mostly confined to alveoli closely associated with respiratory bronchioles interpreted as alveolar macrophages and/or pneumocytes type 2 (Figure 2I), despite a lack of unequivocal histopathologic lesions (Figure 2G). Small intestinal villi and jejunal Peyer's patches (JPP, Figure 2J) showed no alterations. However, multifocal H18-specific RNA signals predominantly in follicle-associated epithelium (FAE) and subepithelial dome regions (Figure 2K), and oligofocal in enteroyctes of small intestinal villi were seen in both infected bats (Table 1). A similar distribution of strong IAV-matrix protein immunoreactive cells was seen in the FAE (Figure 2L) of JPPs and oligofocal within enterocytes and round cells in the lamina propria, interpreted as macrophages or dendritic cells (Figure 2M). No comparable lesions, no H18-specific RNA and no IAV matrix proteins were detectable in the organs of either naïve contact animals.

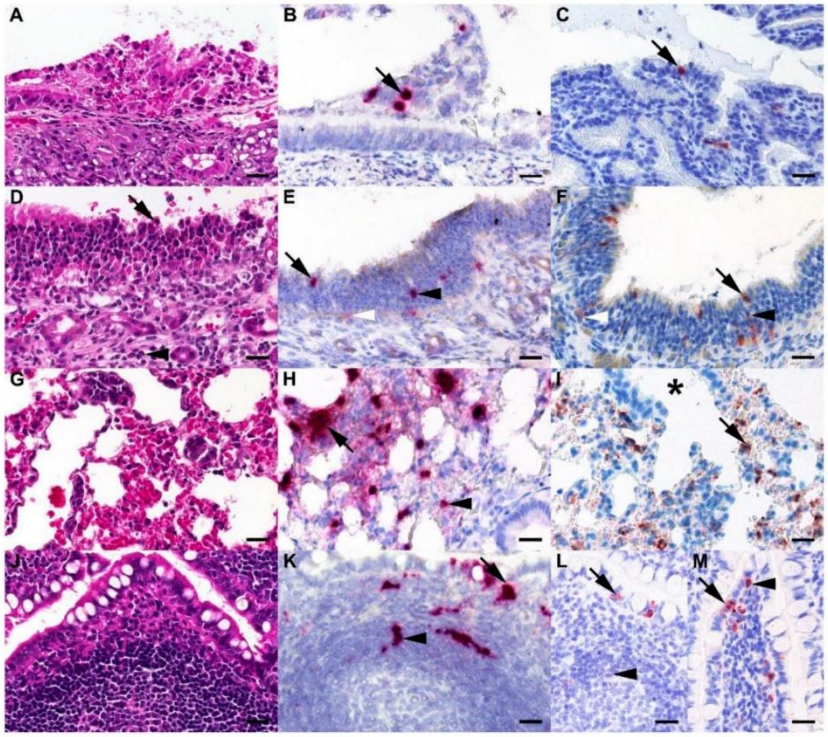

Figure 2. Histologic lesions exhibit H18-specific RNA signals and IAV-matrix protein immunoreactivity in the upper and lower respiratory tract of H18N11-infected Seba's short-tailed bat (*Carollia perspicillata*) at 4 dpi. (**A**) Bat, rostral nose. Mild, focal, acute, necrotizing rhinitis with erosion of the respiratory epithelium and sloughing of cells. (**B**) Bat, rostral nose. Oligofocal single H18-specific RNA signals in luminal debris (arrow). (**C**) Bat, rostral nose. Oligofocal strong intracytoplasmic and intranuclear IAV-matrix protein immunoreactive respiratory epithelial cells (arrow). (**D**) Bat, caudal nose. Mild, focal, acute, necrotizing rhinitis with pyknotic cells (arrow) and mild multifocal infiltration of neutrophils (arrowhead) in the Bowman's glands rich lamina propria. (**E**,**F**) Bat, caudal nose. Oligofocal H18-specific RNA signals and strong intracytoplasmic and intranuclear IAV-matrix protein immunoreactive cells interpreted as sustentecular cells (black arrow), olfactory receptor neurons (black arrowhead) and basal cells (white arrowhead). (**G**) Bat, right cranial lung lobe. Normal appearing lung tissue with alveolar spaces. (**H**) Bat, right cranial lung lobe. Multifocal H18-specific RNA signals in intra-alveolar cellular clusters (arrow) and in single cells (arrowhead). (**I**) Multifocal strong IAV-matrix protein reactive cells (arrow) in areas associated with respiratory bronchioles (asterisk). (**J**) Bat, jejunal Peyer's patch (JPP). Follicle-associated epithelium (FAE) and a lymphocyte-rich subepithelial dome region of a normal appearing JPP is depicted. (**K**) Bat, JPP. Multifocal H18-specific RNA signals are seen in FAE (arrow) and in the subepithelial dome regions (arrowhead). (**L**) Bat, JPP. Oligofocal strong intracytoplasmic IAV-matrix protein immunoreactive cells are seen in the FAE (arrow) and faintly intracytoplasmic reactive cells next to a germinal center (arrowhead). (**M**) Bat, jujunal villus. Oligofocal strong intracytoplasmic and intranuclear IAV-matrix protein immunoreactive enterocytes (arrow) and lamina propria associated round cells interpreted as macrophages or dendritic cells (arrowhead) were evident. A, D, G, J, Hematoxylin eosin stain; B, E, H, K, in situ hybridization, target retrival and protease pretreatment, RNAscope® 2.5 assay H18-specific RNA, Fast Red chromogen (red), hematoxylin counterstain (blue), C, F, I, L, M IAV-matrix protein immunohistochemistry, avidin-biotin-peroxidase complex method with 3-amino-9-ethyl-carbazol as chromogen and hematoxylin counterstain; bars, A–M = 20 μm.

While the bats of group A appeared clinically healthy and shed no infectious virus until 4 dpi, two bats of group B developed a green-colored diarrhea between 9 and 21 dpi. Although we could not obtain individual rectal swabs of healthy and diseased bats without compromising their health status due to the stressful catching procedure, a RT-qPCR analysis of pooled fecal samples revealed the presence of viral RNA at 5, between 8 and 12 and 15 dpi (Figures 1B and 3).

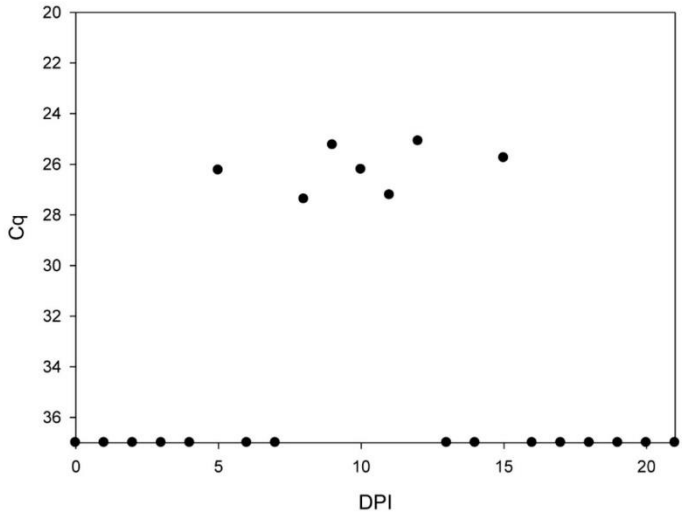

Figure 3. Quantification of IAV RNA loads by RT-qPCR in pooled fecal samples. The amounts of viral genome load were measured by RT-qPCR at the indicated time points. Prior to extraction the guano samples were diluted 1:1000. Calculated values are presented.

At necropsy, an untypical green to grey-colored and softened ingesta was seen in the colon and rectum in two of the eight bats from group B. Consistent with the observation that viral RNA was shed in the feces only until 15 dpi, the examined tissues of inoculated index and contact bats were found RT-qPCR-negative at 21 dpi. Furthermore, a histopathological analysis and immunohistochemistry of all tissues collected from animals with diarrhea (n = 2) found lesion-free, IAV-matrix protein antigen negative reactions. Importantly, aside from the green-colored softened feces, no further symptoms of disease were monitored throughout the course of the experiment.

Serum samples were taken from all group B bats after euthanasia and tested for the presence of neutralizing antibodies. The sera obtained from all three inoculated index bats revealed a low-titer seroconversion with a 50% neutralization dose (ND50) of 1:20, 1:253 and 1:16, whereas all naïve contact bats were tested seronegative (Figure 1B).

4. Discussion

Here, we show that the Seba's short-tailed bat—a species showing positive seroreactivities against H18N11 in nature [9]—is susceptible to experimental oro-nasal infection with H18N11. The detection of viral RNA in tissues of the upper respiratory tract and the intestines in one of the inoculated bats at 4 dpi might indicate a productive oro-nasal and intestinal infection, although we cannot entirely exclude the possibility of detecting residual inoculum in these animals. Upon histopathological analysis, the PCR-positive bats exhibited mild necrotizing alterations confined to respiratory and olfactory epithelium. Moreover, H18-specific RNA signals and IAV-matrix protein immunoreactive cells were present in the nose and gut-associated-lymphoid-tissue (GALT) at early time points (4 dpi), and viral RNA was detected in fecal samples at later time points, which altogether corresponds to the previously suggested gastro-intestinal tissue tropism of H18N11 in Jamaican fruit bats and its spread

by the rectal route [18]. Our findings further support the idea of viral replication in MHC-II-positive antigen-presenting cells, such as macrophages and dendritic cells [16,18], which are present in high frequencies at the FAE of Peyer's patches and other inductive sites of the mucosal immunity [27].

During experimentation, some bats—presumably the index animals—developed a mild exsiccosis and catarrhal enteritis, characterized by green-colored diarrhea, and two bats additionally exhibited abnormal softened ingesta at the time of necropsy at 21 dpi. It is open to discussion whether the mild enteritis is a sequela of the IAV infection or a result of animal handling or simply an independent background lesion.

In contrast to the previous H18N11 infection study performed in Jamaican fruit bats [18], no horizontal transmission occurred among Seba's short-tailed bats. A generally unlikely, yet possible explanation for this finding could be that the contact bats were exposed to bat IAV before, but their antibody titers dropped below the detection threshold. Continuous re-exposure could have triggered a rapidly spiking and thereafter declining antibody response sufficient to prevent an infection. Such rapidly waning antibody responses after an infection—resulting in seronegativity—have been described before for Marburg virus infections in Egyptian fruit bats [28]. Another possibility could be the advanced age of the bats used in this study. Older bats mount a more efficient antiviral immune response which makes the transmission of viruses between individuals a more challenging task [29]. In this context, the previously described constitutively "always on" type I IFN activity in bat cells [30] might also interfere with viral replication and could hence restrict virus transmission among a group of bats, compared to other mammalian species. Alternatively, the lack of transmission could also be attributed to an *Artibeus* species specificity of H18N11. Although various South American fruit bat species have been found seropositive for H17 and H18 [9], until now full H18N11 genomic sequences or infectious viruses have been only isolated from *Artibeus planirostris* and *Artibeus lituratus* or *Artibeus jamaicensis*, respectively [9,18,31]. Considering this, it is tempting to speculate that species-specific differences in the immunity or the adaptation of H18 to MHC-II molecules of *Artibeus* spp. have influenced the infection outcome.

In summary, Seba's short-tailed bats are susceptible to, and develop, mild upper respiratory tract lesions after experimental infection with the bat-derived H18N11 subtype, but transmission to contact bats was not evident. Therefore, Seba's short-tailed bats most likely do not contribute to transmission cycles of H18N11 in nature.

Author Contributions: Conceptualization: D.H., M.S. and M.B. Methodology: M.G., J.S., K.C. D.H. Validation: D.H., R.U., M.B. Formal Analysis: M.G., J.S., K.C. Writing—original draft preparation: M.G. Writing—review and editing: D.H., J.S., R.U., K.C., M.S. M.B. Supervision: D.H. M.B. Funding acquisition: M.S. and M.B. All authors have read and agreed to the published version of the manuscript.

Funding: This work was supported by grants from the Deutsche Forschungsgemeinschaft (DFG) to MS (SCHW 632/17-2) and MB (BE 5187/4-2).

Acknowledgments: The authors thank Silvia Schuparis and Gabriele Czerwinski for histotechnological support.

Conflicts of Interest: The authors declare that they have no conflict of interest.

References

1. Webster, R.G.; Bean, W.J.; Gorman, O.T.; Chambers, T.M.; Kawaoka, Y. Evolution and ecology of influenza A viruses. *Microbiol. Rev.* **1992**, *56*, 152–179. [CrossRef] [PubMed]
2. Garten, R.J.; Davis, C.T.; Russell, C.A.; Shu, B.; Lindstrom, S.; Balish, A.; Sessions, W.M.; Xu, X.; Skepner, E.; Deyde, V.; et al. Antigenic and Genetic Characteristics of Swine-Origin 2009 A(H1N1) Influenza Viruses Circulating in Humans. *Science* **2009**, *325*, 197–201. [CrossRef]
3. Imai, M.; Watanabe, T.; Hatta, M.; Das, S.C.; Ozawa, M.; Shinya, K.; Zhong, G.; Hanson, A.; Katsura, H.; Watanabe, S.; et al. Experimental adaptation of an influenza H5 HA confers respiratory droplet transmission to a reassortant H5 HA/H1N1 virus in ferrets. *Nature* **2012**, *486*, 420–428. [CrossRef]

4. Desselberger, U.; Nakajima, K.; Alfino, P.; Pedersen, F.S.; Haseltine, W.A.; Hannoun, C.; Palese, P. Biochemical evidence that "new" influenza virus strains in nature may arise by recombination (reassortment). *Proc. Natl. Acad. Sci. USA* **1978**, *75*, 3341–3345. [CrossRef] [PubMed]
5. Herfst, S.; Schrauwen, E.J.A.; Linster, M.; Chutinimitkul, S.; De Wit, E.; Munster, V.J.; Sorrell, E.M.; Bestebroer, T.M.; Burke, D.; Smith, D.J.; et al. Airborne Transmission of Influenza A/H5N1 Virus Between Ferrets. *Science* **2012**, *336*, 1534–1541. [CrossRef] [PubMed]
6. Calisher, C.H.; Childs, J.E.; Field, H.E.; Holmes, K.V.; Schountz, T. Bats: Important Reservoir Hosts of Emerging Viruses. *Clin. Microbiol. Rev.* **2006**, *19*, 531–545. [CrossRef]
7. Wynne, J.W.; Wang, L.F. Bats and viruses: Friend or foe? *PLoS Pathog.* **2013**, *9*. [CrossRef]
8. Tong, S.; Li, Y.; Rivailler, P.; Conrardy, C.; Castillo, D.A.A.; Chen, L.-M.; Recuenco-Cabrera, S.; Ellison, J.A.; Davis, C.T.; York, I.; et al. A distinct lineage of influenza A virus from bats. *Proc. Natl. Acad. Sci. USA* **2012**, *109*, 4269–4274. [CrossRef]
9. Tong, S.; Zhu, X.; Li, Y.; Shi, M.; Zhang, J.; Bourgeois, M.; Yang, H.; Chen, X.; Recuenco-Cabrera, S.; Gómez, J.; et al. New World Bats Harbor Diverse Influenza A Viruses. *PLOS Pathog.* **2013**, *9*. [CrossRef]
10. Sun, X.; Shi, Y.; Lu, X.; He, J.; Gao, G.F.; Yan, J.; Qi, J.; Gao, G.F. Bat-Derived Influenza Hemagglutinin H17 Does Not Bind Canonical Avian or Human Receptors and Most Likely Uses a Unique Entry Mechanism. *Cell Rep.* **2013**, *3*, 769–778. [CrossRef]
11. Li, Q.; Sun, X.; Li, Z.; Liu, Y.; Vavricka, C.J.; Qi, J.; Gao, G.F. Structural and functional characterization of neuraminidase-like molecule n10 derived from bat influenza a virus. *Proc. Natl. Acad. Sci. USA* **2012**, *109*, 18897–18902. [CrossRef] [PubMed]
12. Zhu, X.; Yu, W.; McBride, R.; Li, Y.; Chen, L.-M.; Donis, R.O.; Tong, S.; Paulson, J.C.; Wilson, I.A. Hemagglutinin homologue from H17N10 bat influenza virus exhibits divergent receptor-binding and pH-dependent fusion activities. *Proc. Natl. Acad. Sci. USA* **2013**, *110*, 1458–1463. [CrossRef]
13. Zhu, X.; Yang, H.; Guo, Z.; Yu, W.; Carney, P.J.; Li, Y.; Chen, L.-M.; Paulson, J.C.; Donis, R.O.; Tong, S.; et al. Crystal structures of two subtype N10 neuraminidase-like proteins from bat influenza A viruses reveal a diverged putative active site. *Proc. Natl. Acad. Sci. USA* **2012**, *109*, 18903–18908. [CrossRef] [PubMed]
14. Gambaryan, A.; Tuzikov, A.; Piskarev, V.; Yamnikova, S.S.; Lvov, D.K.; Robertson, J.; Bovin, N.V.; Matrosovich, M. Specification of Receptor-Binding Phenotypes of Influenza Virus Isolates from Different Hosts Using Synthetic Sialylglycopolymers: Non-Egg-Adapted Human H1 and H3 Influenza A and Influenza B Viruses Share a Common High Binding Affinity for 6?-Sialyl(N-acetyllactosamine). *Virology* **1997**, *232*, 345–350. [PubMed]
15. Sauter, N.K.; Bednarski, M.D.; Wurzburg, B.A.; Hanson, J.E.; Whitesides, G.M.; Skehel, J.J.; Wiley, N.C. Hemagglutinins from two influenza virus variants bind to sialic acid derivatives with millimolar dissociation constants: A 500-MHz proton nuclear magnetic resonance study. *Biochemistry* **1989**, *28*, 8388–8396. [CrossRef] [PubMed]
16. Karakus, U.; Thamamongood, T.; Ciminski, K.; Ran, W.; Günther, S.C.; Pohl, M.; Eletto, D.; Jeney, C.; Hoffmann, D.; Reiche, S.; et al. MHC class II proteins mediate cross-species entry of bat influenza viruses. *Nature* **2019**, *567*, 109–112. [CrossRef]
17. Juozapaitis, M.; Moreira, É.A.; Mena, I.; Giese, S.; Riegger, D.; Pohlmann, A.; Höper, D.; Zimmer, G.; Beer, M.; García-Sastre, A.; et al. An infectious bat-derived chimeric influenza virus harbouring the entry machinery of an influenza A virus. *Nat. Commun.* **2014**, *5*. [CrossRef]
18. Ciminski, K.; Ran, W.; Gorka, M.; Lee, J.; Malmlov, A.; Schinköthe, J.; Eckley, M.; Murrieta, R.A.; Aboellail, T.A.; Campbell, C.L.; et al. Bat influenza viruses transmit among bats but are poorly adapted to non-bat species. *Nat. Microbiol.* **2019**, *4*, 2298–2309. [CrossRef]
19. Rasweiler, J.; Badwaik, N.K. Improved procedures for maintaining and breeding the short-tailed fruit bat (Carollia perspicillata) in a laboratory setting. *Lab. Anim.* **1996**, *30*, 171–181. [CrossRef]
20. Rasweiler, J.J.; Cretekos, C.J.; Behringer, R.R. The Short-Tailed Fruit Bat Carollia perspicillata: A Model for Studies in Reproduction and Development. *Cold Spring Harb. Protoc.* **2009**, *2009*. [CrossRef]
21. Rasweiler, J.J.; Cretekos, C.J.; Behringer, R.R. Feeding Short-Tailed Fruit Bats (Carollia perspicillata). *Cold Spring Harb. Protoc.* **2009**, *2009*. [CrossRef] [PubMed]
22. Grund, C.; Hoffmann, D.; Ulrich, R.; Naguib, M.; Schinköthe, J.; Hoffmann, B.; Harder, T.; Saenger, S.; Zscheppang, K.; Tönnies, M.; et al. A novel European H5N8 influenza A virus has increased virulence in ducks but low zoonotic potential. *Emerg. Microbes Infect.* **2018**, *7*. [CrossRef] [PubMed]

23. Hoffmann, B.; Depner, K.; Schirrmeier, H.; Beer, M. A universal heterologous internal control system for duplex real-time RT-PCR assays used in a detection system for pestiviruses. *J. Virol. Methods* **2006**, *136*, 200–209. [CrossRef] [PubMed]
24. Toussaint, J.F.; Sailleau, C.; Breard, E.; Zientara, S.; De Clercq, K. Bluetongue virus detection by two real-time rt-qpcrs targeting two different genomic segments. *J. Virol. Methods* **2007**, *140*, 115–123. [CrossRef]
25. Moreira, É.A.; Locher, S.; Kolesnikova, L.; Bolte, H.; Aydillo, T.; García-Sastre, A.; Schwemmle, M.; Zimmer, G. Synthetically derived bat influenza A-like viruses reveal a cell type- but not species-specific tropism. *Proc. Natl. Acad. Sci. USA* **2016**, *113*, 12797–12802. [CrossRef]
26. Yewdell, J.W.; Frank, E.; Gerhard, W. Expression of influenza A virus internal antigens on the surface of infected P815 cells. *J. Immunol.* **1981**, *126*, 1814–1819.
27. Brandtzaeg, P.; Kiyono, H.; Pabst, R.; Russell, M.W. Terminology: Nomenclature of mucosa-associated lymphoid tissue. *Mucosal Immunol.* **2008**, *1*, 31–37. [CrossRef]
28. Schuh, A.J.; Amman, B.R.; Sealy, T.K.; Spengler, J.R.; Nichol, S.T.; Towner, J.S. Egyptian rousette bats maintain long-term protective immunity against Marburg virus infection despite diminished antibody levels. *Sci. Rep.* **2017**, *7*, 8763. [CrossRef]
29. Baker, M.L.; Schountz, T.; Wang, L.F. Antiviral immune responses of bats: A review. *Zoonoses Public Health* **2013**, *60*, 104–116. [CrossRef]
30. Schountz, T.; Baker, M.; Butler, J.; Munster, V.J. Immunological Control of Viral Infections in Bats and the Emergence of Viruses Highly Pathogenic to Humans. *Front. Immunol.* **2017**, *8*. [CrossRef]
31. Campos, A.C.A.; Góes, L.G.B.; Moreira-Soto, A.; De Carvalho, C.; Ambar, G.; Sander, A.-L.; Fischer, C.; Da Rosa, A.R.; De Oliveira, D.C.; Kataoka, A.P.G.; et al. Bat Influenza A(HL18NL11) Virus in Fruit Bats, Brazil. *Emerg. Infect. Dis.* **2019**, *25*, 333–337. [CrossRef] [PubMed]

CHAPTER V: DISCUSSION

Ebola virus, the cause of a devastating outbreak in 2014, which lead to 11310 deaths in Guinea, Sierra Leone and Liberia, Severe acute respiratory syndrome coronavirus (SARS-CoV) in China 2003, pandemic IAV H1N1 2009, but also Rabies, are examples of zoonotic viruses, which were able to cross the species barrier between bats, other mammals and humans.[141-144] The most recent example is the ongoing SARS-CoV-2 pandemia, with more than 500 000 infected people worldwide and more than 20 000 deaths (26th of March 2020). The combination of significant rises in EIDs, bats being able to harbor a wide range of zoonotic viruses and the intensive contact and harassment of wildlife, especially concerning the numerous bat species worldwide, led to multiple questions regarding the newly discovered batIAV. Therefore, the main goal of the present study was to fathom the ability of the H18N11 batIAV to transmit among bats and to non-bat animals, and evaluate their potential zoonotic risk and further put the main focus on the characterization of H18N11 in the bat model.

V.1 Transmission experiments – Characterizing H18N11 and its variant rP11

(Chapter IV.1; publication I)

In the majority of cases, IAV are connected to outbreaks among poultry and swine, potentially leading to the death of thousands of individual animals, either through the consequence of the disease itself or the necessity of major culling events in order to prevent further virus spreading.[145] Apart from the fact, that these outbreaks are able to cause major economic consequences, a significant amount of work force might be required for the sake of curbing. By all means, the ability of IAV to cross the barrier from their animal host species to humans takes the center of attention. Just the imagination of a connection between IAV and the order of Chiroptera, which are described to represent one of the main sources and risks of zoonotic diseases, automatically raises several important and mandatory to answer issues. Therefore, the discovery and publication of H17N10 and H18N11 from bats in Guatemala and Peru [12, 13], respectively, immediately mounted concerns about their pathogenesis, capability to spread among bats and especially the possibility of spillover infections to humans, among other things.

In this present study, we investigated important properties of H18N11 corresponding to the pathogenesis, transmission and cell-tropism in vitro and in mice, ferrets and Neotropical Jamaican fruit bats. In 2016, Moreira et al. investigated the susceptibility of different cell-lines towards the newly discovered batIAV by using a recombinant vesicular stomatitis virus (VSV) model. Among more than 30 screened cell-lines, “Rie1495” cells of canine origin appeared to be one of the most potent candidates for future in vitro passaging experiments.[146] With the objective of unraveling the enigma of replication features and put the genetic stability to the touch, a series of in vitro passaging with wild type (wt) virus $H18N11_{WT}$ was conducted. Besides consecutively increasing viral titers, our studies showed two dominant mutations within the H18 and the inclusion of a premature stop codon in the N11 at G107X (publication I). Based on the number of passages, the final H18N11 virus variant was designated as “rP11”, encoding the mutations $H18_{K170N250S}$ and $N11_{G107X}$.

In order to get insights about the also observed rising titers and the potential properties of variant rP11 in comparison to $H18N11_{WT}$ upon passaging, recombinant viruses encoding different combinations of $H18_{WT}$, $H18_{K170N250S}$, $N11_{WT}$ and $N11_{G107X}$ among others. All viruses encoding the single amino acid mutation $H18_{K170N250S}$ were infectious and could be further propagated in vitro, regardless of which kind of neuramindase they were paired with. However, virus variants encoding $H18_{WT}$ were only infectious, if mated with a full-length $N11_{WT.}$ The in vitro infection experiments further demonstrated, that the higher viral titers achieved during the passaging on the Rie1495 cell-line are coherent with a higher infectivity, which is most likely connected with the two amino acid substitutions in the H18. This also indicates that NA independent virus variants (stop codon variants) are functional as long as the virus is also encoding the hemagglutinin variant $H18_{K170N250S}$. Similar NA-negative, but attenuated, virus mutants were already described before e.g. for HPAIV H5N1 or IAV H1N1, using either cell or in ovo passaging methods.[147-150]

The fact that N11-impaired virus variants containing the $H18_{WT}$ could not generate infectious and replicating virus particles demonstrates the necessity of a collaborating pair of $H18_{wt}$ and $NA11_{wt}$, in a similar style compared to conventional IAV. Vice versa, NA-deletion requires the observed HA-mutations. The NAs of batIAV lack conserved amino acids responsible for binding to and cleaving from sialic acid residues, resulting in a non-existing sialidase activity.[134-136] (Chapter II.3)

However, there is evidence suggesting a similar function of batIAV NAs compared with their conventional IAV NA companions. Since batIAV use MHC-II molecules for cell-entry purposes, the function of the NAs is different, but in some general principles comparable. The study of Weininger et al. revealed structural conformity between the NA of H17N10 and the staphylococcal enterotoxin I (SEI), which is able to bind to the β-chain of human MHC-II molecules.[151] Together with the information of full-length NA11 being able to downregulate the expression of MHC-II molecules (publication I), these evidences indicate an important interaction between the cell-entry mediator MHC-II and the NAs of batIAV. The detailed function of batIAV NAs however remains unclear and should be one of the main focuses of upcoming studies.

In a next step, the analyses switched from a pure in vitro system of serial passaging on Rie1495 cells to in vivo experiments in mice, ferrets and Neotropical Jamaican fruit bats (*Artibeus jamaicensis,* family Phyllostomidae). Based on the previous discovery of MHC- II molecules representing the major cell-entry mediator of H17N10 and H18N11[139], additional concerns rose about the epizootic and zoonotic potential of these batIAV. The previously mentioned genetic variability of $H18_{WT}$ and $NA11_{WT}$, which both quickly adapted upon passaging in the in vitro cell system, equally lit the same discussion of H17N10 or H18N11 being able to potentially infect and pose a serious and yet unknown threat to humans.

In order to examine replication properties and genetic stability in an in vivo model, we first inoculated C57BL/6 mice intranasally with a 10^5 50% tissue culture infective dose ($TCID_{50}$) with either WT-H18N11 or variant virus rP11, respectively. Interestingly, the results of the mice experiments matched the in vitro passaging in equal measure. While viral replication in both of the test series only appeared in the upper respiratory tract, viral titers showed up to be significant higher in the rP11 experiments compared to the WT-infected mice. Furthermore, rP11 was genetically stable in contrast to WT-H18N11. Therefore, these results could be interpreted in a similar vein to the in vitro experiments, namely that an efficient replication requires two mutations in the head domain of $H18_{WT}$. In the ensuing experiments, an intranasal inoculation of immunodeficient C57BL/6 mice, which lack the functional type I and III interferon receptors, with either WT-H18N11 or rP11, should reveal the possibility of transmission to naïve contact mice or at least highlight the necessities to do so successfully.

However, viral replication was again strictly limited to the upper respiratory tract again for both viruses and we could not detect any transmission to contact animals, both foregrounding, that the mouse model might not be suitable for transmission experiments of bat-borne influenza A-like viruses without any further adaption.

Two major factors influenced the decision to take the in vivo experiments a step further and inoculate ferrets as well as Jamaican neotropical fruit bats with both WT-H18N11 and rP11, respectively. The first reason was that MHC-II molecules appeared to be one of the major parameters in the cell entry process of H18N11 bat influenza a-like viruses. In fact, these molecules are omnipresent in the world of mammals, including mice, bats, ferrets and, of course, humans.

The second factor summarizes the in vitro passaging on Rie1495 and the series of experiments regarding the C57BL/6 mice. Both trials indicated rP11 being able to also replicate in a non-bat mammal.

Ferrets are the main animal model for research purposes of non-adapted human IAV. They mirror humans in characteristics regarding susceptibility, clinical signs and transmission features and are therefore well suited in order to investigate the zoonotic potential of rP11 and WT-H18N11.[152-154] Since the mutant variant already demonstrated its potential in the mouse model, ferrets were inoculated using rP11 with a $TCID_{50}$ of 10^7. Four naïve contact ferrets were put into contact with the original 12 index ferrets after one day with the ultimate goal to observe successful transmission between the animals. Though only moderate levels of RNA could be measured with the help of RT-qPCR in the lungs, trachea and even brain of some of the index animals, it still demonstrated a general susceptibility of ferrets towards batIAV. However, there was no detectable amount of RNA in any organ of the contact individuals and no seroconversion, a fact that led to the conclusion of a general low potential zoonotic risk. Additionally, we could not observe any clinical signs among the ferrets emphasizing this interpretation likewise. Surprisingly, sequencing data revealed a mutation in the neuraminidase back to the original open reading frame of $N11_{WT}$, suggesting a species dependent necessity of adaption regarding H18N11. Yet, another animal experiment with the same basic setup, but inoculation with the original WT-H18N11 demonstrated even lower replication levels, insinuating that batIAV are poorly adapted to ferrets or even non-bat mammals in general.

With both mice and ferrets showing very clear restrictions concerning replication and spread of H18N11, still data about replication in the natural bat host was missing. Therefore, with the goal to further examine transmission properties, we inoculated Jamaican neotropical bats with either WT-H18N11 or rP11 in a similar setup compared to the ferret experiments. Here, a different behavior could be observed. High loads of viral RNA in rectal swabs and actually infectious virus in feces samples indicated a distribution among bats through contaminated feces. It is definitely not the first time, an IAV tends to prefer the gastrointestinal route, as a similar way of infection was already described by Webster at al. in ducks in the year of 1978. [155]

This theory was further supported as not only viral loads could be detected in the feces of naïve contact bats, but they also developed mild clinical signs in the shape of nasal and ocular discharge. And the genetic plasticity of H18N11 surprised once again, as in the bat model, the variant rP11 reverted into its original genetic shape, comparable to changes seen in the ferret trials. It can be therefore finally concluded that rP11 appears to be a species-specific adaption rather than representing a mutant with basic advantages over the wild-type virus, and wild type H18N11 is best adapted for replication and spread in its natural bat host.

Histopathological analyses regarding the ferrets and the bat experiments support the previous discovery of MHC-II molecules representing the major cell-entry mediator likewise. Viral antigen could be found in the follicle-associated epithelium (FAE) of the palatine and pharyngeal tonsils for ferrets and in the FAE of Peyer's patches of Jamaican neotropical bats, all areas densely equipped with MHC-II molecules.

In summary, the studies described in publication I demonstrate that H18N11 is only poorly adapted to non-bat species, especially ferrets, and therefore does most likely only pose a minor risk of a zoonotic spill-over to humans. However, the ability of WT-H18N11 to quickly adapt to new circumstances by generating an N11-negative variant advice to keep these newly discovered IAV under observation. In contrast, we could show a gastrointestinal pathway of the virus and further spread among Jamaican neotropical bats, a relative species of the flat-faced fruit-eating bat (*Artibeus planirostris*) of which H18N11 originated from, a case that has to be further examined and confirmed in future studies.

Especially other bat infection experiments were necessary to allow a better understanding of host range and natural infection cycles. Therefore, Seba's short-tailed bats (*Carollia perspicillata*) were inoculated with H18N11 in a first follow up study.

V.2 Inoculation of Carollia perspicillata with H18N11

(Chapter IV.2, publication II)

Seba's short-tailed bat (*Carollia perspicillata*) represents a common, relatively small and frugivorous bat species from Central- and South America.[156] Similar to the Flat-faced fruit-eating bat (*Artibeus planirostris*) and the Jamaican fruit bat (*Artibeus jamaicensis*) they appertain to the family of the Leaf-nosed bats (*Phyllostomidae*) and further share their habitats.[156] Even though H18N11 was only detected and successfully sequenced from *Artibeus planirostris*, *Artibeus jamaicensis* and the Great fruit-eating bat (*Artibeus lituratus*), there is serological evidence for viral contact to batIAV of various species, including Seba's short-tailed bats (*Carollia perspicillata)*. Despite their biological and geographic connection to the original host species of H18N11, Seba's short-tailed bats provide researchers all around the world with different advantages regarding potential animal experiments. They comprise the simplicity of obtainment, housing conditions like feeding, temperature and air moisture requirements in relation to other bat candidates. In addition, several publications about approaching these obstacles are accessible, mainly due to their history in reproductive research.[157-162] Interestingly, numerous publications covering up laboratory methods concerning *Carollia perspicillata* are available as well.[163-166]

In my study, I could demonstrate that Seba's short-tailed bats are in principal susceptible to an oronasal inoculation with WT-H18N11. Viral RNA could be detected in the upper respiratory tract and the intestine of the inoculated index animals (publication II). Further histopathological analysis revealed mild necrotizing alterations at the olfactory and respiratory epithelium, overall corresponding results compared to the already discussed inoculation of the Jamaican neotropical fruit bats.

Parallel findings of H18-specific RNA and IAV-matrixprotein immunoreactive cells in the nose and gut-associated-lymphoid-tissue (GALT) support the theory of an oronasal and gastrointestinal infection route. And it again backs up the findings of MHC-II molecules representing the major cell-entry mediator of batIAV.

Since viral RNA was also detectable in pooled feces samples, we assumed that a transmission via rectal spreading might be possible, but no viral RNA could be detected in any of the tissues of the naïve contact bats, and there was no seroconversion. The first and most likely explanation for a failed transmission among the bats appears to be a potential species-dependency or even dependency towards the genus of Neotropical fruit bats (*Artibeus)* in general.

As mentioned in chapter II.2, 20% of mammals are bats of the order Chiroptera, which are also one of the main contributing factor of EIDs.[118, 119] There are more than 1300 different species known, making it one of the most diverse orders just behind rodents.[112, 113] Therefore, it does not come as a surprise that differences among bat species regarding virus transmission, susceptibility or pathogenicity occur on a regular basis. Concerning North American bat species, these evolutionary distinctions arose about a time frame of 3 to 60 million years.[167, 168] The huge divergences between different bat species can also be observed regarding the surveillance, incidence and cross species transmission (CST) of lyssaviruses in North America.[167, 169] Though the most common colonial bat species of North America are the Big big brown bat (*Epetesicus fuscus*), Little brown bat (*Myotis lucifugus*) and the Mexican free-tailed bat (*Tadarida brasiliensis*), human cases of rabies are often associated with the more rare Silver-haired bat (*Lasionycteris noctivagans*).[169] This could provide another example of huge divergences in CST, especially between bats and humans or virus shedding. Further phylogenetic analysis of rabies viruses in North America revealed a strong species association and probably rare CSTs, even among bats, which also supports the theory of a species dependency of batIAV.[167, 168, 170, 171]
We are also not able to exclude the improbable scenario of an already established, not detectable adaptive immunity against other, yet undetected, novel IAV.

During the animal trial, some of the bats developed a mild exsiccosis and catarrhal enteritis. Latter occurred between 9 and 20 dpi and peaked in the showcasing of green colored diarrhea. The late point in time excludes dietary reasoning but no other potential non infection-based causes. A further explanation for a failed transmission might be the superior antiviral response of bats of a higher age, as were used in this study.

In conclusion, Seba's short-tailed bats seem to be in general susceptible to WT-H18N11, but transmission to other individual bats failed, despite lesions in the upper respiratory tract and gastrointestinal clinical signs. We therefore assume, that these bats might not play a major role in the distribution and spreading of H18N11, despite positive antibody reactions.[13] Finally, Seba's short tailed bats represent a rather poor overall model for investigation of not only H18N11 but also other viruses in the future. In comparison to the Neotropical Jamaican Fruit bats (publication I), they not only lack in terms viral transmission or showing of clinical signs, but are also much more difficult to handle, mainly because of their smaller size and the sensitivity towards anesthesia.

Final conclusion

The main goal was to investigate characteristics of batIAV, especially of H18N11 with the help of in vitro as well as different in vivo experiments. In doing so, we mainly focused on features regarding the genetic plasticity, intraspecies transmission, finding a suitable animal model and evaluation of the zoonotic potential. In the latter case, our findings suggest an overall low zoonotic risk. Ferrets, which also mirror the human α2,6-linked SAR, usually represent an established animal model for zoonotic IAV research. However, batIAV appear to be poorly adapted to non-bat mammals, especially ferrets, as both tested viruses, WT-H18N11 and rP11 featured a weak replication and no transmission to contact animals at all. A potential zoonotic hazard can't be excluded completely, mainly due to the fact of batIAV utilizing MHC-II molecules for a successful cell entry. Therefore, ferrets might not represent the best animal model for a proper risk assessment in all cases. H18N11 tends to adapt rapidly upon in vitro propagating, leading to a virus variant harboring mutations in the HA and NA. Though the variant rP11 was able to infect and replicate well in the mouse model, it failed using ferrets or bats, leading to the conclusion of a more species dependent adaptability.

The in vivo experiments in both publications revealed, that Neotropical Jamaican fruit bats, a close relative to the original host species, the Flat-faced Fruit-eating bat, is by far the best model for further batIAV investigations. While batIAV appear to be poorly adapted to non-bat mammals like mice or ferrets in general, there was also a reduced replication and shedding efficiency of batIAV H18N11 in Seba's short-tailed bats.

Overall, the ongoing SARS-CoV 2 pandemia, with 500000 infected people and 20000 deaths (26th March 2020), once more proves, how important an early investigation of potential zoonotic EIDs is. The necessity of further studies concerning batIAV is therefore inevitable.

CHAPTER VI: SUMMARY

In times of the ongoing SARS-CoV2 pandemic, which currently controls the whole world, they are suddenly back on everyone's lips again: bats. The main focus is on the diseases that these animals can carry and which so often cause serious and even deadly infections in humans. For scientists, on the other hand, research into zoonotic diseases that originate in bats is an omnipresent topic. Nevertheless, the world of virology was taken by surprise when the sequences of two novel influenza A viruses, known as H17N10 and H18N11, were discovered in two South American bat species in 2013. The combination of potentially zoonotic influenza viruses with the order of bats is both fascinating and frightening, as it is well known that lyssa-, corona- and ebolaviruses share this common reservoir hosts. The two publications listed in this dissertation aim to analyse and discuss the properties of bat influenza viruses H17N10 and H18N11. The main points are the analysis of the zoonotic potential, the genetic stability and also the finding of a suitable animal model for future animal experiments. In trials with ferrets, which are an excellent model animal for research on the human risk of influenza viruses, only a very low zoonotic risk was found. However, the fact that bat influenza viruses use MHC-II molecules as cell-entry mediators does not allow the complete exclusion of a zoonosis. Passages on the cell line Rie1495 led to rapidly occurring mutations in HA and NA, and a virus variant that is well adapted to the mouse model but could not replicate these results in ferrets and the Neotropical Jamaican fruit bat. From this we conclude that there is a strong but species-specific genetic plasticity. With the help of Seba's short-tailed bats, which on paper have particularly advantageous properties for future animal experiments, we wanted to create an animal model for the future as well as testing the infection route, pathogenesis and viral shedding in a related bat species. While our results indicate oral uptake and gastrointestinal passage and excretion, Seba's short-tailed bats, due to their difficult handling and lack of transmission of H18N11 to naive animals, were classified as less suitable for future animal experiments in comparison to the Neotropical Jamaica fruit bat. The results of the here described studies should also lead to further research on these highly interesting viruses, e.g. to further investigate and understand the role of bats in the spread and transmission of potentially zoonotic viruses by using the here established bat flu model.

CHAPTER VII: ZUSAMMENFASSUNG

In Zeiten der SARS-CoV2 Pandemie, welche im Moment die ganze Welt in Atem hält, sind sie plötzlich wieder in aller Munde: Fledermäuse. Dabei liegt das Hauptaugenmerk vor allem auf den Krankheitserregern, die diese Tiere in sich tragen können und welche so häufig ernste und sogar tödliche Infektionen beim Menschen hervorrufen können. Für Wissenschaftler dagegen, ist die Erforschung zoonotischer Krankheiten, bei denen der Ursprung oft in Fledermäusen zu finden ist, ein allgegenwärtiges Thema. Dennoch wurde die Welt der Virologie ordentlich durcheinandergewirbelt, als im Jahr 2013 die Sequenzen zweier neuartiger Influenza A Viren, welche als H17N10 und H18N11 bezeichnet werden, in zwei südamerikanischen Fledermausarten entdeckt worden sind. Die Kombination von potenziell zoonotischen Influenzaviren mit der Ordnung von Fledertieren, ist dabei zugleich faszinierend aber ebenso beängstigend, ist es doch weitreichend bekannt, dass auch Tollwut-, Corona- oder Ebolaviren diesen gemeinsamen Ursprung teilen.

Die beiden in dieser Dissertation aufgeführten Publikationen zielen darauf ab, die Eigenschaften dieser Fledermausinfluenzaviren zu erörtern. Der Fokus liegt dabei auf der Analyse des zoonotischen Potentials, der genetischen Stabilität aber auch dem Finden eines passenden Tiermodells für zukünftige Tierversuche.

In Versuchen mit Frettchen, welche normalerweise ein hervorragendes Modelltier für die Erforschung von humanpathogenen Influenzaviren darstellen, zeigte sich glücklicherweise nur ein sehr geringes zoonotisches Risiko. Die Tatsache, dass Fledermausinfluenzaviren jedoch MHC-II Moleküle als Rezeptoren für das Eindringen in Zellen verwenden, lässt jedoch keinen vollständigen Ausschluss einer Zoonose zu. So führten Passagen auf der Zelllinie Rie1495 zu schnell auftretenden Mutationen im HA und NA und einer Virusvariante, welche gut an das Mausmodell angepasst war. Jedoch konnten diese Ergebnisse in Frettchen und der Jamaika-Fruchtfledermaus nicht wiederholt werden. Daraus schließen wir auf eine starke, aber dennoch speziesspezifische genetische Plastizität.

Mit Hilfe der Brillenblattnase, welche auf dem Papier besonders vorteilhafte Eigenschaften für zukünftige Tierversuche mitbringt, wollten wir zum einen ein Tiermodell für die Zukunft schaffen, als auch Infektionsroute, Pathogenese und Ausscheidung des Virus in einer verwandten Fledermausart testen.

Während unsere Ergebnisse auf eine orale Aufnahme und gastrointestinale Passage und Ausscheidung hindeuteten, erwiesen sich die Brillenblattnasen insgesamt aufgrund ihres schwierigen Handlings und einer nicht vorhandenen Transmission zu naiven Tieren im Vergleich mit der Jamaica-Fruchtfledermaus als weniger geeignet für zukünftige in vivo Studien.

Die Ergebnisse dieser hier vorgestellten Arbeiten sollen auch dazu führen, diese interessanten Viren weiter zu erforschen, um z.B. die Rolle von Fledertieren bei der Verbreitung und Übertragung von Zoonosen an diesem Modell weiter zu ergründen.

CHAPTER VIII: REFERENCES

1. World Health Organization, *Fact sheet - Seasonal influenza* 2019.
2. World Health Organization, *Fact sheet - influenza (avian and other zoonotic).* 2019.
3. Hause, B.M., et al., *Isolation of a novel swine influenza virus from Oklahoma in 2011 which is distantly related to human influenza C viruses.* PLoS Pathog, 2013. **9**(2): p. e1003176.
4. Mostafa, A., et al., *Zoonotic Potential of Influenza A Viruses: A Comprehensive Overview.* Viruses, 2018. **10**(9).
5. ICTV, I.C.o.T.o.V., *Virus Taxonomy* 2018.
6. Shaw, M. and P. Palese, *Fields virology, p 1151–1185.* Fields virology, 6th ed. Lippincott Williams & Wilkins, Philadelphia, PA, 2013.
7. Kuno, G., et al., *Phylogeny of Thogoto virus.* Virus Genes, 2001. **23**(2): p. 211-4.
8. Presti, R.M., et al., *Quaranfil, Johnston Atoll, and Lake Chad viruses are novel members of the family Orthomyxoviridae.* J Virol, 2009. **83**(22): p. 11599-606.
9. Cottet, L., et al., *Infectious salmon anemia virus--genetics and pathogenesis.* Virus Res, 2011. **155**(1): p. 10-9.
10. Webster, R.G., et al., *Evolution and ecology of influenza A viruses.* Microbiol Rev, 1992. **56**(1): p. 152-79.
11. Gatherer, D., *The 2009 H1N1 influenza outbreak in its historical context.* J Clin Virol, 2009. **45**(3): p. 174-8.
12. Tong, S., et al., *A distinct lineage of influenza A virus from bats.* Proc Natl Acad Sci U S A, 2012. **109**(11): p. 4269-74.
13. Tong, S., et al., *New world bats harbor diverse influenza A viruses.* PLoS Pathog, 2013. **9**(10): p. e1003657.
14. Wille, M., N. Latorre-Margalef, and J. Waldenström, *Of Ducks and Men: Ecology and Evolution of a Zoonotic Pathogen in a Wild Reservoir Host*, in *Modeling the Transmission and Prevention of Infectious Disease*. 2017, Springer. p. 247-286.
15. Yang, J.R., et al., *Phylogenetic and evolutionary history of influenza B viruses, which caused a large epidemic in 2011-2012, Taiwan.* PLoS One, 2012. **7**(10): p. e47179.
16. McCullers, J.A., T. Saito, and A.R. Iverson, *Multiple genotypes of influenza B virus circulated between 1979 and 2003.* J Virol, 2004. **78**(23): p. 12817-28.
17. Li, W.C., et al., *Clinical and genetic characterization of severe influenza B-associated diseases during an outbreak in Taiwan.* J Clin Virol, 2008. **42**(1): p. 45-51.
18. Gouarin, S., et al., *Study of influenza C virus infection in France.* J Med Virol, 2008. **80**(8): p. 1441-6.
19. Matsuzaki, Y., et al., *Clinical features of influenza C virus infection in children.* J Infect Dis, 2006. **193**(9): p. 1229-35.
20. Yuanji, G. and U. Desselberger, *Genome analysis of influenza C viruses isolated in 1981/82 from pigs in China.* J Gen Virol, 1984. **65 (Pt 11)**: p. 1857-72.
21. Guo, Y.J., et al., *Isolation of influenza C virus from pigs and experimental infection of pigs with influenza C virus.* J Gen Virol, 1983. **64 (Pt 1)**: p. 177-82.
22. Hause, B.M., et al., *Characterization of a novel influenza virus in cattle and Swine: proposal for a new genus in the Orthomyxoviridae family.* MBio, 2014. **5**(2): p. e00031-14.
23. Chiapponi, C., et al., *Detection of Influenza D Virus among Swine and Cattle, Italy.* Emerg Infect Dis, 2016. **22**(2): p. 352-4.
24. Fujiyoshi, Y., et al., *Fine structure of influenza A virus observed by electron cryo-microscopy.* EMBO J, 1994. **13**(2): p. 318-26.
25. Harris, A., et al., *Influenza virus pleiomorphy characterized by cryoelectron tomography.* Proc Natl Acad Sci U S A, 2006. **103**(50): p. 19123-7.
26. Noda, T., et al., *Architecture of ribonucleoprotein complexes in influenza A virus particles.* Nature, 2006. **439**(7075): p. 490-2.

27. Fields, B., D. Knipe, and P. Howley, *Fields virology. 5th ed2007*. Philadelphia: Wolters Kluwer Health/Lippincott Williams & Wilkins.
28. Mair, C.M., et al., *Receptor binding and pH stability - how influenza A virus hemagglutinin affects host-specific virus infection.* Biochim Biophys Acta, 2014. **1838**(4): p. 1153-68.
29. Godefroy, C., et al., *Mimicking influenza virus fusion using supported lipid bilayers.* Langmuir, 2014. **30**(38): p. 11394-400.
30. Horimoto, T. and Y. Kawaoka, *Influenza: lessons from past pandemics, warnings from current incidents.* Nature Reviews Microbiology, 2005. **3**(8): p. 591-600.
31. Barrowclough, G.F., et al., *How Many Kinds of Birds Are There and Why Does It Matter?* PLoS One, 2016. **11**(11): p. e0166307.
32. Reid, A.H., J.K. Taubenberger, and T.G. Fanning, *Evidence of an absence: the genetic origins of the 1918 pandemic influenza virus.* Nat Rev Microbiol, 2004. **2**(11): p. 909-14.
33. Taubenberger, J.K. and J.C. Kash, *Influenza virus evolution, host adaptation, and pandemic formation.* Cell Host Microbe, 2010. **7**(6): p. 440-51.
34. Boni, M.F., *Vaccination and antigenic drift in influenza.* Vaccine, 2008. **26 Suppl 3**: p. C8-14.
35. Lu, L., S.J. Lycett, and A.J. Leigh Brown, *Reassortment patterns of avian influenza virus internal segments among different subtypes.* BMC Evol Biol, 2014. **14**: p. 16.
36. Nelson, M.I. and E.C. Holmes, *The evolution of epidemic influenza.* Nat Rev Genet, 2007. **8**(3): p. 196-205.
37. Urbaniak, K. and I. Markowska-Daniel, *In vivo reassortment of influenza viruses.* Acta Biochim Pol, 2014. **61**(3): p. 427-31.
38. Liu, J., et al., *Highly pathogenic H5N1 influenza virus infection in migratory birds.* Science, 2005. **309**(5738): p. 1206.
39. Webby, R.J. and R.G. Webster, *Are we ready for pandemic influenza?* Science, 2003. **302**(5650): p. 1519-22.
40. Schrauwen, E.J., et al., *Determinants of virulence of influenza A virus.* Eur J Clin Microbiol Infect Dis, 2014. **33**(4): p. 479-90.
41. Bertram, S., et al., *Novel insights into proteolytic cleavage of influenza virus hemagglutinin.* Rev Med Virol, 2010. **20**(5): p. 298-310.
42. Garten, W., et al., *Proteolytic activation of the influenza virus hemagglutinin: The structure of the cleavage site and the enzymes involved in cleavage.* Virology, 1981. **115**(2): p. 361-74.
43. World Health Organization, *INFECTION WITH AVIAN INFLUENZA VIRUSES.* 2019.
44. Ozawa, M. and Y. Kawaoka, *Cross talk between animal and human influenza viruses.* Annu Rev Anim Biosci, 2013. **1**: p. 21-42.
45. Claas, E.C., et al., *Human influenza A H5N1 virus related to a highly pathogenic avian influenza virus.* Lancet, 1998. **351**(9101): p. 472-7.
46. Yuen, K.Y., et al., *Clinical features and rapid viral diagnosis of human disease associated with avian influenza A H5N1 virus.* Lancet, 1998. **351**(9101): p. 467-71.
47. Claas, E.C., et al., *Human influenza virus A/HongKong/156/97 (H5N1) infection.* Vaccine, 1998. **16**(9-10): p. 977-8.
48. Subbarao, K., et al., *Characterization of an avian influenza A (H5N1) virus isolated from a child with a fatal respiratory illness.* Science, 1998. **279**(5349): p. 393-6.
49. World Health Organization, *Cumulative Number of Confirmed Human Cases of Avian Influenza A(H5N1) Reported to WHO.* 2020.
50. Gu, J., et al., *H5N1 infection of the respiratory tract and beyond: a molecular pathology study.* Lancet, 2007. **370**(9593): p. 1137-45.
51. Uiprasertkul, M., et al., *Influenza A H5N1 replication sites in humans.* Emerg Infect Dis, 2005. **11**(7): p. 1036-41.
52. Uiprasertkul, M., et al., *Apoptosis and pathogenesis of avian influenza A (H5N1) virus in humans.* Emerg Infect Dis, 2007. **13**(5): p. 708-12.
53. de Jong, M.D., et al., *Fatal outcome of human influenza A (H5N1) is associated with high viral load and hypercytokinemia.* Nat Med, 2006. **12**(10): p. 1203-7.

54. de Jong, M.D., et al., *Fatal avian influenza A (H5N1) in a child presenting with diarrhea followed by coma.* N Engl J Med, 2005. **352**(7): p. 686-91.
55. Chen, H., et al., *Avian flu: H5N1 virus outbreak in migratory waterfowl.* Nature, 2005. **436**(7048): p. 191-2.
56. Kurtz, J., R.J. Manvell, and J. Banks, *Avian influenza virus isolated from a woman with conjunctivitis.* Lancet, 1996. **348**(9031): p. 901-2.
57. Belser, J.A., et al., *Past, present, and possible future human infection with influenza virus A subtype H7.* Emerg Infect Dis, 2009. **15**(6): p. 859-65.
58. Fouchier, R.A., et al., *Avian influenza A virus (H7N7) associated with human conjunctivitis and a fatal case of acute respiratory distress syndrome.* Proc Natl Acad Sci U S A, 2004. **101**(5): p. 1356-61.
59. Koopmans, M., et al., *Transmission of H7N7 avian influenza A virus to human beings during a large outbreak in commercial poultry farms in the Netherlands.* Lancet, 2004. **363**(9409): p. 587-93.
60. Puzelli, S., et al., *Human infection with highly pathogenic A(H7N7) avian influenza virus, Italy, 2013.* Emerg Infect Dis, 2014. **20**(10): p. 1745-9.
61. Gao, R., et al., *Human infection with a novel avian-origin influenza A (H7N9) virus.* N Engl J Med, 2013. **368**(20): p. 1888-97.
62. World Health Organization, *Analysis of recent scientific information on avian influenza A(H7N9) virus.* 2017.
63. Zhu, H., et al., *Infectivity, transmission, and pathology of human-isolated H7N9 influenza virus in ferrets and pigs.* Science, 2013. **341**(6142): p. 183-6.
64. Belser, J.A., et al., *Pathogenesis and transmission of avian influenza A (H7N9) virus in ferrets and mice.* Nature, 2013. **501**(7468): p. 556-9.
65. Food and Agriculture Organization of the United Nations, *H7N9 situation update.* 2019.
66. Zeng, X., et al., *Vaccination of poultry successfully eliminated human infection with H7N9 virus in China.* Sci China Life Sci, 2018. **61**(12): p. 1465-1473.
67. Li, X., et al., *Genetics, receptor binding property, and transmissibility in mammals of naturally isolated H9N2 Avian Influenza viruses.* PLoS Pathog, 2014. **10**(11): p. e1004508.
68. Li, C., et al., *Genetic evolution of influenza H9N2 viruses isolated from various hosts in China from 1994 to 2013.* Emerg Microbes Infect, 2017. **6**(11): p. e106.
69. Homme, P.J., B.C. Easterday, and D.P. Anderson, *Avian influenza virus infections. II. Experimental epizootiology of influenza A-turkey-Wisconsin-1966 virus in turkeys.* Avian Dis, 1970. **14**(2): p. 240-7.
70. Xu, K.M., et al., *Evolution and molecular epidemiology of H9N2 influenza A viruses from quail in southern China, 2000 to 2005.* J Virol, 2007. **81**(6): p. 2635-45.
71. Smietanka, K., et al., *Avian influenza H9N2 subtype in Poland--characterization of the isolates and evidence of concomitant infections.* Avian Pathol, 2014. **43**(5): p. 427-36.
72. Zecchin, B., et al., *Influenza A(H9N2) Virus, Burkina Faso.* Emerg Infect Dis, 2017. **23**(12): p. 2118-2119.
73. Kammon, A., et al., *Characterization of Avian Influenza and Newcastle Disease Viruses from Poultry in Libya.* Avian Dis, 2015. **59**(3): p. 422-30.
74. El Houadfi, M., et al., *First outbreaks and phylogenetic analyses of avian influenza H9N2 viruses isolated from poultry flocks in Morocco.* Virol J, 2016. **13**(1): p. 140.
75. Kandeil, A., et al., *Genetic and antigenic evolution of H9N2 avian influenza viruses circulating in Egypt between 2011 and 2013.* Arch Virol, 2014. **159**(11): p. 2861-76.
76. Peacock, T.H.P., et al., *A Global Perspective on H9N2 Avian Influenza Virus.* Viruses, 2019. **11**(7).
77. Abdel-Moneim, A.S., M.A. Afifi, and M.F. El-Kady, *Isolation and mutation trend analysis of influenza A virus subtype H9N2 in Egypt.* Virol J, 2012. **9**: p. 173.
78. Pan, Y., et al., *Human infection with H9N2 avian influenza in northern China.* Clin Microbiol Infect, 2018. **24**(3): p. 321-323.

79. Liu, D., et al., *Origin and diversity of novel avian influenza A H7N9 viruses causing human infection: phylogenetic, structural, and coalescent analyses.* Lancet, 2013. **381**(9881): p. 1926-32.
80. Lam, T.T., et al., *The genesis and source of the H7N9 influenza viruses causing human infections in China.* Nature, 2013. **502**(7470): p. 241-4.
81. Peiris, M., et al., *Human infection with influenza H9N2.* Lancet, 1999. **354**(9182): p. 916-7.
82. World Health Organization, *Human infection with avian influenza A(H9N2) in China.* 2019.
83. Aamir, U.B., et al., *Characterization of avian H9N2 influenza viruses from United Arab Emirates 2000 to 2003.* Virology, 2007. **361**(1): p. 45-55.
84. Chen, H., et al., *Clinical and epidemiological characteristics of a fatal case of avian influenza A H10N8 virus infection: a descriptive study.* Lancet, 2014. **383**(9918): p. 714-21.
85. To, K.K., et al., *Emergence in China of human disease due to avian influenza A(H10N8)--cause for concern?* J Infect, 2014. **68**(3): p. 205-15.
86. Yang, L., et al., *Genesis and Dissemination of Highly Pathogenic H5N6 Avian Influenza Viruses.* J Virol, 2017. **91**(5).
87. Ma, W., R.E. Kahn, and J.A. Richt, *The pig as a mixing vessel for influenza viruses: Human and veterinary implications.* J Mol Genet Med, 2008. **3**(1): p. 158-66.
88. Scholtissek, C., et al., *The nucleoprotein as a possible major factor in determining host specificity of influenza H3N2 viruses.* Virology, 1985. **147**(2): p. 287-94.
89. Rogers, G.N. and J.C. Paulson, *Receptor determinants of human and animal influenza virus isolates: differences in receptor specificity of the H3 hemagglutinin based on species of origin.* Virology, 1983. **127**(2): p. 361-73.
90. Rogers, G.N. and B.L. D'Souza, *Receptor binding properties of human and animal H1 influenza virus isolates.* Virology, 1989. **173**(1): p. 317-22.
91. Ito, T., et al., *Molecular basis for the generation in pigs of influenza A viruses with pandemic potential.* J Virol, 1998. **72**(9): p. 7367-73.
92. Kida, H., et al., *Potential for transmission of avian influenza viruses to pigs.* J Gen Virol, 1994. **75 (Pt 9)**: p. 2183-8.
93. Webster, R.G., C.H. Campbell, and A. Granoff, *The "in vivo" production of "new" influenza A viruses. I. Genetic recombination between avian and mammalian influenza viruses.* Virology, 1971. **44**(2): p. 317-28.
94. Webster, R.G. and C.H. Campbell, *The in vivo production of "new" influenza A viruses. II. In vivo isolation of "new" viruses.* Virology, 1972. **48**(2): p. 528-36.
95. Webster, R.G., C.H. Campbell, and A. Granoff, *The "in vivo" production of "new" influenza viruses. 3. Isolation of recombinant influenza viruses under simulated conditions of natural transmission.* Virology, 1973. **51**(1): p. 149-62.
96. Smith, G.J., et al., *Origins and evolutionary genomics of the 2009 swine-origin H1N1 influenza A epidemic.* Nature, 2009. **459**(7250): p. 1122-5.
97. Joseph, U., et al., *The ecology and adaptive evolution of influenza A interspecies transmission.* Influenza Other Respir Viruses, 2017. **11**(1): p. 74-84.
98. Garten, R.J., et al., *Antigenic and genetic characteristics of swine-origin 2009 A(H1N1) influenza viruses circulating in humans.* Science, 2009. **325**(5937): p. 197-201.
99. Guo, Y.J., X.Y. Xu, and N.J. Cox, *Human influenza A (H1N2) viruses isolated from China.* J Gen Virol, 1992. **73 (Pt 2)**: p. 383-7.
100. Castrucci, M.R., et al., *Genetic reassortment between avian and human influenza A viruses in Italian pigs.* Virology, 1993. **193**(1): p. 503-6.
101. Shu, B., et al., *Genetic analysis and antigenic characterization of swine origin influenza viruses isolated from humans in the United States, 1990-2010.* Virology, 2012. **422**(1): p. 151-60.
102. Bowman, A.S., et al., *Swine-to-human transmission of influenza A(H3N2) virus at agricultural fairs, Ohio, USA, 2012.* Emerg Infect Dis, 2014. **20**(9): p. 1472-80.
103. Myers, K.P., C.W. Olsen, and G.C. Gray, *Cases of swine influenza in humans: a review of the literature.* Clin Infect Dis, 2007. **44**(8): p. 1084-8.

104. Saenz, R.A., H.W. Hethcote, and G.C. Gray, *Confined animal feeding operations as amplifiers of influenza.* Vector Borne Zoonotic Dis, 2006. **6**(4): p. 338-46.
105. Hayden, F. and A. Croisier, *Transmission of avian influenza viruses to and between humans.* J Infect Dis, 2005. **192**(8): p. 1311-4.
106. Belser, J.A., et al., *The eyes have it: influenza virus infection beyond the respiratory tract.* Lancet Infect Dis, 2018. **18**(7): p. e220-e227.
107. Kandeel, A., et al., *Zoonotic transmission of avian influenza virus (H5N1), Egypt, 2006-2009.* Emerg Infect Dis, 2010. **16**(7): p. 1101-7.
108. Van Kerkhove, M.D., et al., *Frequency and patterns of contact with domestic poultry and potential risk of H5N1 transmission to humans living in rural Cambodia.* Influenza Other Respir Viruses, 2008. **2**(5): p. 155-63.
109. Areechokchai, D., et al., *Investigation of avian influenza (H5N1) outbreak in humans--Thailand, 2004.* MMWR Suppl, 2006. **55**(1): p. 3-6.
110. Dinh, P.N., et al., *Risk factors for human infection with avian influenza A H5N1, Vietnam, 2004.* Emerg Infect Dis, 2006. **12**(12): p. 1841-7.
111. Greiner, M., et al., *Expert opinion based modelling of the risk of human infection with H5N1 through the consumption of poultry meat in Germany.* Berl Munch Tierarztl Wochenschr, 2007. **120**(3-4): p. 98-107.
112. Fenton, M.B. and N.B. Simmons, *Bats: a world of science and mystery*. 2015: University of Chicago Press.
113. International Union for Conservation and Nature, *IUCN SSC Bat Specialist Group.* 2019.
114. International Union for Conservation and Nature, *IUCN Redlist of Threatened Species.* 2019.
115. Calisher, C.H., et al., *Bats: important reservoir hosts of emerging viruses.* Clin Microbiol Rev, 2006. **19**(3): p. 531-45.
116. Hayman, D.T., *Bats as Viral Reservoirs.* Annu Rev Virol, 2016. **3**(1): p. 77-99.
117. Kohl, C. and A. Kurth, *European bats as carriers of viruses with zoonotic potential.* Viruses, 2014. **6**(8): p. 3110-28.
118. Jones, K.E., et al., *Global trends in emerging infectious diseases.* Nature, 2008. **451**(7181): p. 990-3.
119. Morens, D.M. and A.S. Fauci, *Emerging infectious diseases: threats to human health and global stability.* PLoS Pathog, 2013. **9**(7): p. e1003467.
120. Luis, A.D., et al., *A comparison of bats and rodents as reservoirs of zoonotic viruses: are bats special?* Proc Biol Sci, 2013. **280**(1756): p. 20122753.
121. Wynne, J.W. and L.F. Wang, *Bats and viruses: friend or foe?* PLoS Pathog, 2013. **9**(10): p. e1003651.
122. Kuzmin, I.V., et al., *Innate Immune Responses of Bat and Human Cells to Filoviruses: Commonalities and Distinctions.* J Virol, 2017. **91**(8).
123. Banerjee, A., et al., *Novel Insights Into Immune Systems of Bats.* Front Immunol, 2020. **11**: p. 26.
124. Paweska, J.T., et al., *Experimental Inoculation of Egyptian Fruit Bats (Rousettus aegyptiacus) with Ebola Virus.* Viruses, 2016. **8**(2).
125. Schuh, A.J., et al., *Egyptian rousette bats maintain long-term protective immunity against Marburg virus infection despite diminished antibody levels.* Sci Rep, 2017. **7**(1): p. 8763.
126. Munster, V.J., et al., *Replication and shedding of MERS-CoV in Jamaican fruit bats (Artibeus jamaicensis).* Sci Rep, 2016. **6**: p. 21878.
127. Middleton, D.J., et al., *Experimental Nipah virus infection in pteropid bats (Pteropus poliocephalus).* J Comp Pathol, 2007. **136**(4): p. 266-72.
128. Halpin, K., et al., *Pteropid bats are confirmed as the reservoir hosts of henipaviruses: a comprehensive experimental study of virus transmission.* Am J Trop Med Hyg, 2011. **85**(5): p. 946-51.
129. Kandeil, A., et al., *Isolation and Characterization of a Distinct Influenza A Virus from Egyptian Bats.* J Virol, 2019. **93**(2).

130. Freidl, G.S., et al., *Serological evidence of influenza A viruses in frugivorous bats from Africa.* PLoS One, 2015. **10**(5): p. e0127035.
131. Hoffmann, M., et al., *The Hemagglutinin of Bat-Associated Influenza Viruses Is Activated by TMPRSS2 for pH-Dependent Entry into Bat but Not Human Cells.* PLoS One, 2016. **11**(3): p. e0152134.
132. Maruyama, J., et al., *Characterization of the glycoproteins of bat-derived influenza viruses.* Virology, 2016. **488**: p. 43-50.
133. Juozapaitis, M., et al., *An infectious bat-derived chimeric influenza virus harbouring the entry machinery of an influenza A virus.* Nat Commun, 2014. **5**: p. 4448.
134. Zhu, X., et al., *Crystal structures of two subtype N10 neuraminidase-like proteins from bat influenza A viruses reveal a diverged putative active site.* Proc Natl Acad Sci U S A, 2012. **109**(46): p. 18903-8.
135. Li, Q., et al., *Structural and functional characterization of neuraminidase-like molecule N10 derived from bat influenza A virus.* Proc Natl Acad Sci U S A, 2012. **109**(46): p. 18897-902.
136. Garcia-Sastre, A., *The neuraminidase of bat influenza viruses is not a neuraminidase.* Proc Natl Acad Sci U S A, 2012. **109**(46): p. 18635-6.
137. Zhu, X., et al., *Hemagglutinin homologue from H17N10 bat influenza virus exhibits divergent receptor-binding and pH-dependent fusion activities.* Proc Natl Acad Sci U S A, 2013. **110**(4): p. 1458-63.
138. Sun, X., et al., *Bat-derived influenza hemagglutinin H17 does not bind canonical avian or human receptors and most likely uses a unique entry mechanism.* Cell Rep, 2013. **3**(3): p. 769-78.
139. Karakus, U., et al., *MHC class II proteins mediate cross-species entry of bat influenza viruses.* Nature, 2019. **567**(7746): p. 109-112.
140. Barclay, W.S., *Receptor for bat influenza virus uncovers potential risk to humans.* Nature, 2019. **567**(7746): p. 35-36.
141. Murray, K., et al., *A morbillivirus that caused fatal disease in horses and humans.* Science, 1995. **268**(5207): p. 94-7.
142. World Health Organization, *Ebola outbreak 2014-2016.* 2016.
143. Peiris, J.S., Y. Guan, and K.Y. Yuen, *Severe acute respiratory syndrome.* Nat Med, 2004. **10**(12 Suppl): p. S88-97.
144. Badrane, H. and N. Tordo, *Host switching in Lyssavirus history from the Chiroptera to the Carnivora orders.* J Virol, 2001. **75**(17): p. 8096-104.
145. World Organisation for Animal Health, *Avian Influenza Portal: Prevention & control.*
146. Moreira, E.A., et al., *Synthetically derived bat influenza A-like viruses reveal a cell type- but not species-specific tropism.* Proc Natl Acad Sci U S A, 2016. **113**(45): p. 12797-12802.
147. Kalthoff, D., et al., *Truncation and sequence shuffling of segment 6 generate replication-competent neuraminidase-negative influenza H5N1 viruses.* J Virol, 2013. **87**(24): p. 13556-68.
148. Ann, J., et al., *Impact of a large deletion in the neuraminidase protein identified in a laninamivir-selected influenza A/Brisbane/10/2007 (H3N2) variant on viral fitness in vitro and in ferrets.* Influenza Other Respir Viruses, 2016. **10**(2): p. 122-6.
149. Samson, M., et al., *Characterization of drug-resistant influenza virus A(H1N1) and A(H3N2) variants selected in vitro with laninamivir.* Antimicrob Agents Chemother, 2014. **58**(9): p. 5220-8.
150. Hughes, M.T., et al., *Influenza A viruses lacking sialidase activity can undergo multiple cycles of replication in cell culture, eggs, or mice.* J Virol, 2000. **74**(11): p. 5206-12.
151. Weininger, A. and S. Weininger, *Using common spatial distributions of atoms to relate functionally divergent influenza virus N10 and N11 protein structures to functionally characterized neuraminidase structures, toxin cell entry domains, and non-influenza virus cell entry domains.* PLoS One, 2015. **10**(2): p. e0117499.
152. Thangavel, R.R. and N.M. Bouvier, *Animal models for influenza virus pathogenesis, transmission, and immunology.* J Immunol Methods, 2014. **410**: p. 60-79.

153. Bouvier, N.M. and A.C. Lowen, *Animal Models for Influenza Virus Pathogenesis and Transmission.* Viruses, 2010. **2**(8): p. 1530-1563.
154. Matsuoka, Y., E.W. Lamirande, and K. Subbarao, *The ferret model for influenza.* Curr Protoc Microbiol, 2009. **Chapter 15**: p. Unit 15G 2.
155. Webster, R.G., et al., *Intestinal influenza: replication and characterization of influenza viruses in ducks.* Virology, 1978. **84**(2): p. 268-78.
156. Cloutier, D. and D.W. Thomas, *Carollia perspicillata.* Mammalian species, 1992(417): p. 1-9.
157. De Bonilla, H. and J.J.t. Rasweiler, *Breeding activity, preimplantation development, and oviduct histology of the short-tailed fruit bat, Carollia, in captivity.* Anat Rec, 1974. **179**(3): p. 385-403.
158. Rasweiler, J.J.t. and H. de Bonilla, *Menstruation in short-tailed fruit bats (Carollia spp.).* J Reprod Fertil, 1992. **95**(1): p. 231-48.
159. Rasweiler, J.J.t. and N.K. Badwaik, *Improved procedures for maintaining and breeding the short-tailed fruit bat (Carollia perspicillata) in a laboratory setting.* Lab Anim, 1996. **30**(2): p. 171-81.
160. Rasweiler, J.J.t., C.J. Cretekos, and R.R. Behringer, *Feeding short-tailed fruit bats (Carollia perspicillata).* Cold Spring Harb Protoc, 2009. **2009**(3): p. pdb prot5159.
161. Rasweiler, J.J.t., C.J. Cretekos, and R.R. Behringer, *The short-tailed fruit bat Carollia perspicillata: a model for studies in reproduction and development.* Cold Spring Harb Protoc, 2009. **2009**(3): p. pdb emo118.
162. Rasweiler, J.J.t., C.J. Cretekos, and R.R. Behringer, *Collection of short-tailed fruit bats (Carollia perspicillata) from the wild.* Cold Spring Harb Protoc, 2009. **2009**(3): p. pdb prot5161.
163. Rasweiler, J.J.t., C.J. Cretekos, and R.R. Behringer, *Whole-mount in situ hybridization of short-tailed fruit bat (Carollia perspicillata) embryos with RNA probes.* Cold Spring Harb Protoc, 2009. **2009**(3): p. pdb prot5164.
164. Rasweiler, J.J.t., C.J. Cretekos, and R.R. Behringer, *Alcian blue staining of cartilage of short-tailed fruit bat (Carollia perspicillata).* Cold Spring Harb Protoc, 2009. **2009**(3): p. pdb prot5165.
165. Rasweiler, J.J.t., C.J. Cretekos, and R.R. Behringer, *Alcian blue/alizarin red staining of cartilage and bone of short-tailed fruit bat (Carollia perspicillata).* Cold Spring Harb Protoc, 2009. **2009**(3): p. pdb prot5166.
166. Rasweiler, J.J.t., C.J. Cretekos, and R.R. Behringer, *Whole-mount immunohistochemistry of short-tailed fruit bat (Carollia perspicillata).* Cold Spring Harb Protoc, 2009. **2009**(3): p. pdb prot5167.
167. Streicker, D.G., et al., *Host phylogeny constrains cross-species emergence and establishment of rabies virus in bats.* Science, 2010. **329**(5992): p. 676-9.
168. Bininda-Emonds, O.R., et al., *The delayed rise of present-day mammals.* Nature, 2007. **446**(7135): p. 507-512.
169. Davis, A.D., et al., *Susceptibility and pathogenesis of little brown bats (Myotis lucifugus) to heterologous and homologous rabies viruses.* J Virol, 2013. **87**(16): p. 9008-15.
170. Blanton, J.D., et al., *Rabies surveillance in the United States during 2008.* J Am Vet Med Assoc, 2009. **235**(6): p. 676-89.
171. Hughes, G.J., L.A. Orciari, and C.E. Rupprecht, *Evolutionary timescale of rabies virus adaptation to North American bats inferred from the substitution rate of the nucleoprotein gene.* J Gen Virol, 2005. **86**(Pt 5): p. 1467-1474.

CHAPTER IX: SUPPLEMENTS

IX.1 Abbreviations

Aa	Amino acid
AIV	Avian influenza viruses
CST	Cross species transmission
EID	Emerging Infectious Diseases
ELISA	Enzyme-linked immunosorbent assay
FAE	Follicle-associated epithelium
FAO	Food and Agriculture Organization of the United Nations
GALT	Gut-associated-lymphoid-tissue
HA	Hemagglutinin
HLA-DR	Human leukocyte antigen DR isotypes
HP	High pathogenic
IALV	Influenza A-like virus
IAV	Influenza A virus
IBV	Influenza B virus
ICV	Influenza C virus
IDV	Influenza D virus
IV	Influenza virus
IVPI	Intravenous pathogenicity index
LBM	Live bird markets
LP	Low pathogenic
MBCS	Multibasic cleavage site
MHC-II	Major histocompatibility complex class II
NA	Neuraminidase
NP	Nucleoprotein
NS2	Non-structural protein 2
NT	Nucleotide
OIE	World Organisation for Animal Health

PA	Polymerase acidic protein
PB1	Polymerase basic protein 1
PB2	Polymerase basic protein 2
PCR	Polymerase chain reaction
RdRp	RNA dependent RNA polymerase
RNA	Ribonucleic acid
RNP	Ribonucleocomplexes
RT-qPCR	Quantitative reverse transcription PCR
SARS-CoV	Severe acute respiratory syndrome coronavirus
SEI	Staphylococcal enterotoxin I
SRA	Sialic acid receptor
TCID	Tissue culture infectious dose
TMPRSS2	Transmembrane protease serine 2
VSV	Vesicular stomatitis virus
WHO	World Health Organization
WT	Wild type

IX.2 List of figures

IX.3 Permissions for reproduction

Figure 1. Permission for reproduction was granted by the Copyright Clearance Center's RightsLink® service.

Figure 2. Permission for reproduction was granted by the Copyright Clearance Center's RightsLink® service.

Figure 3. Permission for reproduction was granted by the Copyright Clearance Center's RightsLink® service.

CHAPTER X: ACKNOWLEDGEMENT

DANKSAGUNG

Herrn Prof. Dr. Gerd Sutter und den Gutachtern möchte ich für die Beurteilung dieser Arbeit danken.

Ein besonderer Dank gebührt meinem Mentor Prof. Dr. Martin Beer, der mir nicht nur ermöglicht hat, meine Dissertation am Friedrich-Loeffler-Institut anzufertigen, sondern auch immer mit Rat und Tat zur Seite stand.

Herzlich bedanken möchte ich mich auch bei PD Dr. Donata Hoffmann, die in guten wie in schlechten Zeiten stets einen kühlen Kopf bewahrt hat und durch ihr hervorragendes Fachwissen, konstruktive Kritik und unzählige Stunden Korrekturlesen einen wesentlichen Beitrag zu dieser Arbeit beisteuerte.

Natürlich gebührt mein Dank auch allen anderen Mitarbeitern des NRL für Affenpocken, bei denen neben der hervorragenden wissenschaftlichen und labortechnischen Unterstützung auch immer das notwendige Quäntchen Spaß nie zu kurz kam. Deshalb ein großes Dankeschön an Doris Junghans, Mareen Lange, Dr. Annika Franke, Saskia Weber, Dr. Kore Schlottau und natürlich Dr. Jacob Schön.

Besonders bedanken möchte ich mich auch bei allen Tierpflegern des FLI, da sie mich zu jedem Zeitpunkt unterstützt haben, insbesondere bei den aufwendigen und anspruchsvollen Fledermausversuchen.

Außerdem möchte ich mich bei allen Ko-Autoren dieser Arbeit bedanken.

Last but not least gebührt ein unendlich großes Dankeschön meinen Eltern und meinen Geschwistern, die immer an mich geglaubt haben, auch wenn ich bereits am Boden war. Danke für eure Unterstützung. Man könnte sich keine bessere Familie wünschen!